1-1-1989

Stress and deformation coupled moisture transport in polymers/

Makarand H. Chipalkatti
University of Massachusetts Amherst

STRESS AND DEFORMATION COUPLED MOISTURE TRANSPORT IN POLYMERS

A Dissertation Presented

by

MAKARAND H. CHIPALKATTI

Submitted to the Graduate School of the
University of Massachusetts in partial fulfillment
of the requirements for the degree of
DOCTOR OF PHILOSOPHY

February 1989

Polymer Science and Engineering

Materials Research Laboratory

Contract No: NSF DMR 86-00340

STRESS AND DEFORMATION COUPLED MOISTURE TRANSPORT IN POLYMERS

Dissertation Presented

By

MAKARAND H. CHIPALKATTI

Approved as to style and content by:

Richard J. Farris, Chairman

Julio M. Ottino, Co-chairman

Michael F. Malone, Member

James E. Donovan, Member

William J. MacKnight, Department Head
Polymer Science and Engineering

To my parents Shanta and Hanmanta:

Who taught me that knowledge is the ultimate pursuit,

Without whom this work would never have been conceived.

To my wife Renu:

Who taught me to smile in the midst of adversity,

Without whom this work would never have been consummated.

ACKNOWLEDGEMENTS

To all my teachers past and present, I thank you for your wisdom, guidance and for recognizing in me the potential for better, and for urging me to strive for more than I may have on my own. My deepest gratitude goes to Professor Richard J. Farris whose encouragement and faith in me was a constant inspiration. Our association has left me greatly enriched. My warmest thanks extend to Professor Julio M. Ottino, who also guided me and urged me to strive for my fullest potential. I will always endeavour to live up to the standards that both of them have taught me to uphold. My sincere thanks also to Professors James E Donovan and Michael F. Malone for their participation, comments and suggestions. I would like to express my gratitude to the Department of Polymer Science and Engineering and the University of Massachusetts for the unique opportunity extended to me.

There are a veritable host of colleagues and friends who have helped me along my way. I would like to extend my thanks to the elves of the Electronic shop and the Machine shop particularly John Domian, Norman Page and Richard Zinck. Also my thanks to the departmental staff Sophia Kinney, Carol Moro, Marylin Cummings, Eleanor Thorpe and Jan Kari who have efficiently smoothed the way all these years. My fellow group members and comrades-in-arms who have made these years most enjoyable and rewarding. In particular, Scott Sackinger, Robin Hwang and Siu-Ki Chang for all their kind words and support. Dearest friend Gary William Adams, whose companionship, encouraging words and technical discussions have truly enriched me Many thanks for all the cups of *chai* and great conversation that we shared. Indeed it was not the cup but the company that cheered.

I would like to thank all those who over the past year at GTE Laboratories, helped me along with their unreserved support and implicit faith in my abilities. The staff at Technical Publications who put up with my frequent demands, and in particular my managers and colleagues, Drs. J. Tom Smith, Han Kim, Gus Bandyopadhyay and last but not least Dan Sandman and Jim Staark. Thank you for your confidence in me and the constant encouragement.

Finally, words cannot adequately express my feelings towards my family who have stood by me always, even when I may not have been the best son, brother or husband. My parents, who unselfishly put up with my absence for all these years and instead encouraged me to follow my dreams. My parents-in-law, who urged me on with their kindness and gentle words. My brother, who put up with his crazy sibling and egged him on with pep talks and admonishments. Last and certainly not the least, my dearest friend, constant companion and spouse Renu, who has paved my way with her love and selfless efforts. It is impossible to conceive that I would be writing this without all her cajoling, caring and sacrifice of all these years. For putting up with my usually unreasonable demands, the endless proofreading and drawing of figures while always retaining her gentle sweetness, I unconditionally designate her as my co-author.

ABSTRACT

STRESS AND DEFORMATION COUPLED

MOISTURE TRANSPORT IN POLYMERS

FEBRUARY 1989

MAKARAND H. CHIPALKATTI

B.TECH., INDIAN INSTITUTE OF TECHNOLOGY

M.S., MICHIGAN TECHNOLOGICAL UNIVERSITY

PH.D., UNIVERSITY OF MASSACHUSETTS

Directed by: PROFESSOR RICHARD J. FARRIS

Co-directed by: PROFESSOR JULIO M. OTTINO

The main theme of this dissertation is the effect of stress and deformation on the sorption of moisture in polymers. A major finding of this study is the existence of a coupled interaction between stress or strain and transport in a permeant-polymer system. The effect of applied stress and deformation on the equilibrium solubility, diffusion and swelling coefficients is also established experimentally. A novel experimental technique has been developed which enables the study of sorption and diffusion on samples under constant stress or strain. Sample mass, in fiber or ribbon samples, is determined from the propagation velocity of transverse vibrational pulses and the applied tension. The technique, referred to as "The Vibrational Time Delay

Method", measures the velocities and tension during the course of sorption or desorption experiments.

In this study, it is shown that the apparent equilibrium solubility of moisture in various engineering polymers (polycarbonate, polyimide, polyaramid, polyamides and poly-m-phenylene-bis-benzimidazole) is a function of the applied stress or strain. The equilibrium solubility in a polymer is found to be a function of not only the relative humidity but also the applied stress. It is seen that a sample at equilibrium at a given stress absorbs additional moisture on increasing the stress. The new solubility may even be twice as much as the "stress-free" value. Furthermore, diffusion and swelling coefficients are typically found to increase with applied tension. Usually, stress enhancement of the equilibrium solubilities and diffusion coefficients is observed as long as sample deformation remains within elastic limits. Beyond the linear elastic region, the effect of applied stress is seen to be less consistent and may even lower the solubility and diffusion coefficients.

Transport characteristics exhibit history dependence and vary over repeated cycles of stress-coupled sorption and desorption. The effect of history is found to be reversible by heating the materials under low tension at temperatures below their glass transition temperatures (polycarbonate, polyimide). History dependent behavior is modified by the application of stresses and is often dominated by sufficiently large stresses.

TABLE OF CONTENTS

LIST OF TABLES

LIST OF FIGURES

CHAPTER 1

STRESS COUPLED TRANSPORT

1.1 Purpose

The newly emerging applications for polymeric materials have triggered a renewed examination of their transport properties. Until a few years ago, research had primarily been motivated because of their use in containers and as barrier materials in packaging. However, more recently, the deployment of a new generation of engineering and high performance polymers in structural applications has created a new set of issues. Polymers are now used in circuit boards, interconnects, and also as multi-layered aerospace composites. In such applications, performance specifications are very stringent and the tolerances in properties and dimensions far more demanding. Factors affecting the performance of such materials that were previously neglected have become the subject of closer scrutiny. One of the most critical factors is the coupling of mechanical stress and transport processes.

The objective of this dissertation is to present an experimental study of stress or strain coupled sorption and transport in glassy polymers. Such coupling is anticipated based on theoretical analyses as well as physical intuition based on a variety of indirect experimental evidence. Analyses such as those based on equilibrium thermodynamics of swollen gels and rubbers, indicate that the value of the equilibrium solubility results from a balance

between the osmotic pressure of the permeant and the elastic response of the rubber. Some mechanisms of diffusion that have been proposed postulate that applied stresses and deformation also alter the kinetics of transport. This effect has been attributed to changes in chain mobility, the volume or number of diffusion sites or the activation energy for intermediate steps during diffusion.

Until recently, the number of studies addressing stress-coupling interactions has been rather small. This is partly because the effects were considered inconsequential and also because of the inherent limitations of the experimental techniques employed. Indeed, traditional techniques are unable to measure permeant penetration or sample weight gain and concurrently control and measure the state of stress or deformation. Such simultaneous measurements are an indispensable feature in the study of coupled diffusion and provide the ability to perform controlled experiments as functions of stress or strain. Thus, one of the major objectives of this dissertation is to discuss a novel experimental technique designed to study stress or strain-coupled diffusion.

1.2 Outline of the Dissertation

The concept of stress-coupled transport is introduced in section 1.3.0. The literature related to the study of the effect of stresses and strains on transport phenomena is reviewed; the two main analytical approaches are outlined and their primary differences pointed out, especially with reference

to equilibrium and transient transport. The literature review largely focuses on previous experimental techniques and their inherent limitations as related to the study of coupled transport.

In Chapter 2 the physical basis of the experimental technique, along with the principal assumptions that are implicit in the technique are discussed. The design and construction of the "vibrational time delay" measurement apparatus are described along with the experimental procedures employed. A description of the verification and calibration procedures and the accuracy and precision of the technique are also reported. In addition, the classes of experiments conducted along with their analyses and calculation procedures are discussed.

The main focus of this dissertation, specifically the coupling between the sorption and diffusion of permeants with mechanical fields, is addressed in Chapter 3. This chapter also outlines the scheme of experiments and describes sorption in samples under constant stress or strain. In addition, the results of experiments where diffusion is induced in samples at equilibrium by changing their state of stress or strain are presented. Chapter 3 also discusses the overall conclusions with a view towards providing a rationale for the effects observed.

Typically, polymers are non-equilibrium materials with internal rearrangements continuously progressing towards an equilibrium state. This dynamic situation gives rise to time dependent behavior in many of their properties. The time or history dependent aspect of stress coupled diffusion is addressed in Chapter 4. The literature related to the history dependence of

transport phenomena in polymers is first briefly reviewed. Experiments demonstrating history dependenee in stress-eoupled diffusion are then reported with the main eonelusions made.

The broad conclusions of this work as well as reeommendations for future work are diseussed in Chapter 5. The suggestions made are mainly directed towards further developing the capabilities of the experimental teehnique. Also additional features of stress-eoupling interaetions are highlighted as potential targets of further study.

1.3 Backround

In many high modulus materials, the diffusion of permeants often generates stresses of the same or greater magnitude than externally applied stresses. In faet, the deformations that sometimes result from the presence of permeants may even exceed engineering toleranees. Conversely, external stresses and strains may influenee the equilibrium solubility of permeants as well as transient diffusion and often give rise to non-Fiekian diffusion. Thus, in the transient case, the coupling of stress and diffusion is manifest via two modes of interaction; stresses induced by diffusion and diffusion modified by internal and external stresses. At equilibrium, both the time-varying internal stresses as well as transport proeesses are at steady state. Sinee there are no internal stress gradients at equilibrium, only the solubility of the permeant in the material is affeeted by the stresses.

A comparison of typical thermal and swelling coefficients of common materials demonstrates the order of magnitude of stresses generated by the diffusion of molecules through polymers. In the case of common epoxies, the moisture swelling coefficient ($\approx 5.4 \times 10^{-3}$/% moisture) is about 100 times as large as the linear coefficient of thermal expansion for a typical epoxy ($\approx 5.2 \times 10^{-5}$/°C). Consequently, the strain resulting from a 1% moisture gain is equal to that due to a 100 °C rise in temperature! Alternatively, in dimensionally constrained samples, the stresses generated are of equal magnitude. The contribution of deformations to the internal energy is significant. Thus, stress and strain effects cannot always be ignored in transport analyses, as implied by Fick's and Fourier's laws. Recognition of the role played by internal and external stresses associated with the diffusion processes resulted in substantial theoretical effort examining transient and equilibrium behavior. The effect of stress and strain on polymers as well as the impact on diffusion is extensively reviewed by Haward (1973) and Morton and Hearle (1975).

Treloar's study of water sorption by hair and cellulose, was one of the earliest to address the issue of coupling and to use thermodynamic principles to model moisture sorption and anisotropic swelling in samples under tension (Treloar 1952, 1953). A straightforward approach to stress-diffusion interactions in gels and rubbers was provided, and constitutes a "limiting" equilibrium thermodynamic example of stress-coupled sorption. Treloar analytically demonstrated that a material with a positive swelling coefficient experienced an increase in moisture content due to the effect of a tensile stress. The increase in equilibrium moisture due to the applied tensile stress was found to be reversed on removing the stress. Further, equations

based on thermodynamic theory were derived to describe the influence of tensile stress on the moisture content, for the case of anisotropic swelling. Treloar also described experiments demonstrating that progressively increasing local orientations in a polymer result in a diminishing influence of stress on sorption. This result has also been observed during this investigation and is discussed in Chapter 4.

In the case of constrained swelling or differential swelling within a material, one approach assumed that swelling and dimensional constraint were mutually independent (Alfrey, Gurney and Lloyd 1966). Hence, the material was considered to swell freely due to solvent sorption and then the stresses required to restore the sample to its original (unswollen) dimension were calculated by assuming the deformation to be elastic. The procedure described is essentially equivalent to the "method of strain suppression" for the calculation of thermal stresses discussed by Timoshenko and Goodier (1970). The technique is inherently limited in that it does not explicitly deal with coupling interactions, assumes only elastic behavior and does not account for the effect of temperature and permeants on material properties.

The equilibrium swelling analyses for solvent-rubber systems, represent a direct attempt to describe the counterbalancing of the osmotic pressure (thermodynamic driving force for diffusion) with the elastic restraints (internal or external) offered by the material. This approach successfully applies reversible thermodynamics to the equilibrium sorption of polymers under stress. It is also considered to be a limiting case analysis for

the general problem of stress coupled-sorption (Barkas 1940, 1942a, b; Treloar 1952, 1953; Hearle 1957 and Sternstein 1972).

Barkas discussed swelling stresses in gels by using the analogy between swelling and osmotic phenomena in gels. He then applied this analysis to the swelling of wood by water sorption. In swelling, as in osmosis, solvent migrates into the region of lower concentration (the matrix). The elastic response of the swollen material then opposes further sorption until the elastic pressure due to the deformation of the matrix is sufficient to balance the osmotic pressure (Rosen 1962). Consequently, sorption is expected to be dependent on the stresses within the material. The application of volume constraints on a swollen material resulted in stresses that acted in conjunction with the natural elastic response of the material. An "abnormal solute absorptivity" was observed in volumetrically constrained swollen polymers. Rosen further extended the above analysis to viscoelastic materials with retarded elastic response thus incorporating time-dependent behavior.

Morton and Hearle (1975) generated sorption isotherms by applying the approach developed by Barkas (1942a, b) referred to above. They examined moisture sorption by a block of wood under: 1) no constraint (free swelling), 2) constant applied compressive stress, 3) compressive stress proportional to the swelling strain, 4) constant volume or totally constrained sample. The results seen in Figure 1.1 are qualitative illustrations of sorption characteristics of polymers under key modes of applied *compressive* stress or strain. While they cannot be compared directly with the data presented here, they provide theoretical results based on equilibrium thermodynamics which are qualitatively consistent with experimental observations. The zero

constraint case resembles the typical stress-free case of diffusion in polymers while the volumetrically constrained sample is at the other extreme. The condition of constant applied stress is most similar to the constant stress experiments conducted during this work. The case where the stress is proportional to swelling is more suited to situations where no external stress is applied or when the local internal swelling stresses dominate during the transient process. In reality, the stress-coupled case may be considered to result from a combination of cases 2 and 3.

Sternstein (1972) applied a similar approach to the case of the inhomogeneous swelling of an elastomer internally constrained by a spherical inclusion. A state of swelling equilibrium was assumed within the network. The matrix was assumed to be incompressible and the swollen volume considered to be the sum of the volumes of the matrix and the solvent. Sternstein employed the thermodynamic results for homogeneously swollen networks (Flory 1953; Treloar 1958); specifically, the free energy of swelling was considered to be composed of the free energy of mixing and the work of network deformation.

The above analyses of sorption under stress described the interaction of stresses and internal constraints with sorption at equilibrium. Prior to equilibrium, an increase in the level of permeant within the material reduces internal concentration gradients and hence the diffusional or osmotic driving force. At the same time, the increasing solvent concentration results in local differential swelling increases the elastic counter-pressure exerted by the network or gel. Equilibrium is therefore the result of a balance of forces: the diffusional driving force opposed by the elastic restoring force of the

deformed nctwork.

The above description of the stress dependent sorption of solvents suggests that at equilibrium the gradient of the chemical potentials, concentrations and stresses throughout the material is zero; hence further diffusion of solvcnt ceases. If an external stress were to be applied under such conditions, thc elastic pressure would no longer be balanced by the osmotic pressurc, and diffusion of the solvent would proceed till a new equilibrium is rcachcd between the osmotic pressure and the stress statc. Thus, an additional tcnsile strcss would result in further sorption whereas a compressive stress is likely to reduce the solubility. The enhancement of solubility by applied tcnsion has bcen expcrimentally dcmonstrated by Chipalkatti et al. (1986a). Clcarly, thc qualitative modcl of counterbalancing forces discussed in the earlicr paragraph is restricted to matcrials having ideal network structures, and is not applicable in an identical form to the case of glassy and non-equilibrium matcrials.

A succcssful approach applicd to the analysis of problems of strcss-couplcd diffusion has evolvcd from the continuum theories of interstitial diffusion in metals (Larche and Cahn 1982) and was recently extended to polymer network systems by Kim and Neogi (1984). Isotropic linearly elastic materials subject to small strains were studied, with their chemical potential considered to depend on the total strain expericnced by the material. The total strain was defined as the sum of the mechanically applied strain and the strain resulting from internal changes in permeant concentration. The gradient in the potential was then considered to generate thc driving force for transport. The authors demonstrated that the local

diffusion flux in solids depended on stresses induced by concentration gradients, and thus focussed on a limitation of Fick's law. Kim and Neogi (1984) incorporated the coupling of stress and strain with the diffusion flux in their analysis by amending the transport law to include local stresses or strains.

Diffusion has also been treated as a purely mechanical process in various works (Adkins 1964; Crochet and Naghdi 1966; Aifantis 1980). Equations of motion are formulated for each of the diffusing species. The diffusing species is considered to be continuously distributed throughout the medium and assumed to sustain as well as generate stress. Local momentum exchanges between the inter-diffusing materials are manifested as a diffusive drag that acts as a body force in the equation of motion. Equations for the stress and the diffusive force are expressed as functions of concentration and its gradients. This analysis can be specialized for various cases of diffusion and in the simplest stress-free case, results in Fick's law. Also, for a statically stressed linear elastic solid, the diffusive flux is found to be a linear function of the hydrostatic stress (in addition to the concentration gradient).

A slightly different approach is provided by the the Theory of Interacting Continua (Bowen 1976). This approach is also referred to as the Theory of Mixtures, and it treats the interpenetration of solvent and matrix as a process of mixing of the two (or more) species. Unlike the earlier purely mechanical analyses, it also includes thermodynamic condition based on the Second Law along with the conservation laws of mass, momentum and energy. Shi et al. (1981) applied the theory of mixtures to the case of diffusion of an ideal fluid through a stretched layer of crosslinked polymer and compared it to the experimental results of Paul and Ebra-Lima (1970). Good agreement was

achieved with experimental results, particularly in the low to intermediate range of concentrations. In fact, the agreement was considerably better than that obtained by means of Fick's law.

In conclusion, the equilibrium analysis developed by Sternstein offers a thermo-mechanical description of stress-coupled solubility. It provides flexibility in the choice of models for the free energy of mixing and deformation, thus making it applicable to a wide range of polymer-solvent systems. Of the analyses of the transient transport processes, that of Kim and Neogi (1984), treating the chemical potential as a function of the total strain, is a relatively direct approach and has recently seen greater acceptance. The direct, albeit *ad hoc*, modifications of the diffusion coefficient such as those proposed by Smith and Adam (1980), have also been successfully applied as an alternative in some simple cases.

1.4 Earlier Experimental Techniques

Numerous experimental techniques have been employed in the study of diffusion under applied stress or strain. Crank and Park (1968) have reviewed some of the traditional techniques for diffusion in stress-free samples. In these works, stresses were typically applied by stretching or bending samples while diffusion was measured via gas permeation, light transmission, solvent weight gain or even by the use of radioactive tracers. A classification of these methods along with their salient features are discussed below. Also, the results of some of the prominent experimental investigations

are summarized in Table 1.1.

A study of the influence of stresses on permeant levels within polymer samples was performed by Marshall et al. (1983). Vinyl ester laminates were subjected to three point bending while immersed in tritiated water. After a fixed time interval, the radiation from thin sections of each sample was measured. As the radiation count varied in direct proportion to the amount of tritiated water in the region, the concentration profiles of water through the samples were then determined. It was seen that the convex surface (under tension) exhibited a higher diffusion coefficient perpendicular to the surface, whereas the concave surface (the compressed side) did not show any substantial change in diffusion characteristics.

Other beam bending experiments, conducted by Fahmy and Hurt (1980), compared the curvature of wet pre-flexed bars of epoxy with that of dry bars under identical initial curvatures. The internal stress, estimated from the radius of curvature, was found to be larger in the wet bars. Berry and Pritchet (1984) employed moisture induced bending of bi-layered strips of polymer and impervious substrate to measure the stress generated due to sorption and differential swelling. Marom and Broutman (1981) also discussed the moisture pick-up of fiber reinforced epoxy composites under external tensile loading.

Rosen (1960), discussed a study of the permeability of gases in circumferentially clamped polymer films, while Yasuda and Peterlin (1974) examined the effect of strain (over a wide range of deformation) on the permeability of crystalline polyethylene held in a similar fashion. Analogous

experiments on polyimide and polycarbonate films were also reported by Smith and Adam (1980). In all these cases, the diffusion and permeability coefficients were found to increase with the applied stress. Semicrystalline polyethylene was the only exception; the diffusion coefficients increased with strain for small deformations (≤ 2.5 % tensile strain), and then decreased with any additional strain.

A study of the stresses generated during the constrained swelling of rubber was presented by Edelenyi et al. (1984). This work correlated the calculated value of stress associated with free swelling and the experimentally determined value of swelling pressure. The authors proposed that the free energy changes associated with free swelling consisted of two components. One component originating from the flexible shape change of the rubber counterbalancing the free energy changes due to the swelling. In the case of constrained swelling the contribution of the swelling pressure was added to the free energy of deformation and dominated in the case of small deformations. Rubber samples enclosed in perforated brass sleeves were immersed in a variety of solvents. The pressure, which monitored at one end of the cylindrical sample by a force transducer, was then considered to be a measure of the swelling pressure. A direct linear correlation was found between the equilibrium swelling pressure and the calculated stress due to free swelling.

All of the above investigators reported the continuous measurement of one quantity: such as mass, applied stress or strain. Typically, if the applied deformation was kept constant, then gas permeation was measured continuously. Alternatively, when stress was monitored during

diffusion, weight pick-up was measured only intermittently or at equilibrium. In some cases, deformation and weight gain were both measured at equilibrium and the experiments performed over extended periods of time, often many days or weeks. The experience from previous works suggests that while the coupled interaction of stress and diffusion is undoubtedly of immense theoretical and practical significance, it is a very elusive phenomenon to study experimentally. In fact, in most cases of coupled diffusion, the application of stress alters the diffusion coefficients in addition to the equilibrium solubility. Further, the process of diffusion itself generates local stresses and influences local transport which in turn modify localized stress distributions. No doubt, the solubility at equilibrium is solely dependent on the externally applied stress as all the local gradients tend to zero. However, an understanding of the mechanism of coupling also requires an examination of the transient process. Hence, the study of the coupling interaction is only feasible when the entire transport process is monitored and not only at initial and equilibrium states.

A coupled interaction may imply that the solubility of a material is altered and permeant transport driven by a change in the state of stress alone. A system specifically designed to study the coupling between stress and diffusion, developed by Chipalkatti, Farris and Hutchinson (1987), has been employed during the course of this study. The experimental technique directly measures applied tension and strain while it conveniently determines the linear density of fibers or thin films. The technique is uniquely qualified for the experimental study of coupled transport, since the primary variable is the uniaxially applied stress or strain and the sample density is experimentally determined.

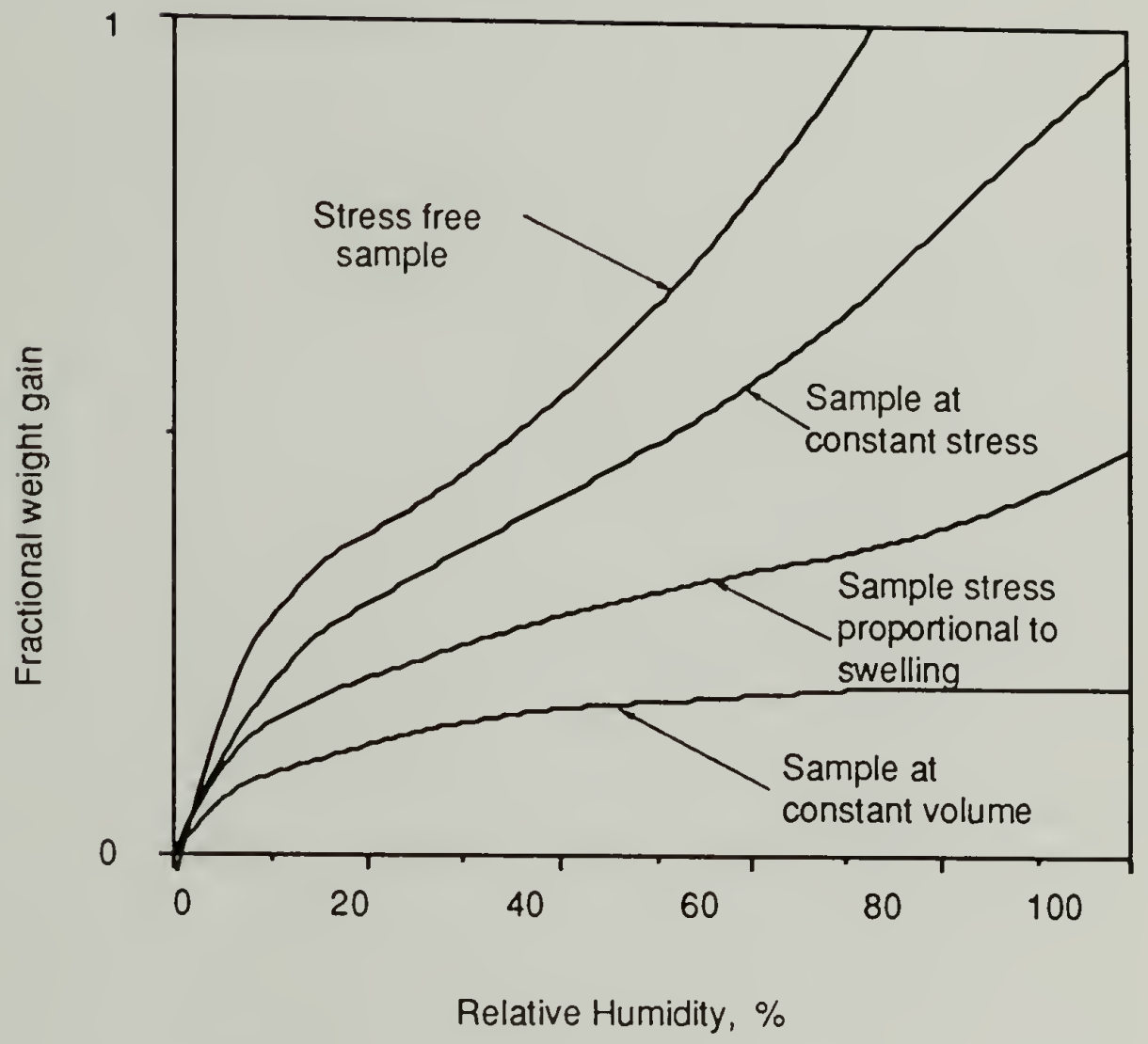

Figure 1.1 Theoretical sorption isotherms developed by Barkas (1942a, b) and Morton and Hearle (1975) for a block of wood subject to various applied stress and strain conditions. The applied stress referred to here is compressive.

Table 1.1 Summary of the experimental literature related to stress enhanced transport in polymers. (This is not a complete review but presents some of the key examples)

Investigator	Approach	Technique/Materials	Type of Data	Analysis/Conclusions	Comments
Treloar (1952, 1963)	Fibers under tension	Weighing of fibers held in tension in environments of varying humidity. (Cellulose, hair)	Weight gain of moisture versus time.	Effect of stress on sorption, reversibility demonstrated. Thermodynamic rationale discussed. Stress effect related to the effect of orientation.	Samples held under fixed tension. Prior conditioning of samples. Effect of anisotropy discussed.
Rosen (1960)	Gas permeability in biaxially stretched films	Helium, nitrogen permeation through supported and unsupported films (P-Styrene, PMMA, PET)	Downstream pressure of permeating gas, time-lag measurements.	Enhanced diffusion coefficients due to tension, sample extension.	Only linear elastic region examined. Equilibrium solubility and stress effects not examined.
Yasuda Stannett Frisch Peterlin (1974)	Gas permeability in stretched rubber	Permeation of oxygen, nitrogen, helium in biaxially oriented membranes (Vulcanized rubber)	Downstream pressure of permeating gas, time-lag measurements.	No effect of extension on the diffusion coefficients.	No volume effect due to extension (Poisson's ratio = 0.5) hence no effect on P. D.
Yasuda Peterlin (1974)	Gas permeability in stretched membranes	Carbon dioxide permeation through films drawn in the elastic and plastic regions. (Semi-crystalline, crystalline P-ethylene)	Downstream pressure of permeating gas, time-lag measurements.	P, D increase in elastic regime decrease in plastic regime maxima in the transition region	Equilibrium solubility and stress effects not considered.
Smith Adam (1980)	Gas permeability in stretched films	Hydrogen, nitrogen, carbon dioxide permeation in stretched films. (P-imide, P-carbonate)	Downstream pressure of permeating gas, time-lag measurements.	P, D Maxima observed in dependence on applied strain.	Equilibrium solubility not discussed. Elastic limits not identified.
Marshall Marshall Pinzelli (1983)	Epoxy-vinyl ester laminates. Effect of tension and compression.	Diffusion of tritiated water in laminates subject to 3-point bending under water. (Epoxy-vinyl ester)	Sectional radiation count as a measure of concentration. Weight gain by integration of c v/s distance.	Enhanced diffusion coefficients under tension (convex side). Inconclusive for effect of compression (concave side).	Interfacial sorption/ defects ignored. Equilibrium effects not discussed.

CHAPTER 2

THE VIBRATIONAL TIME DELAY METHOD

2.1 Principle

The experimental technique is based on the simple principle that the propagation velocity of transverse and longitudinal vibrations depends on the density of the medium of travel. Furthermore, in a thin stretched material such as an elastic fiber, the velocity of transverse wave propagation varies in proportion to the square root of the ratio of tension to linear density and is independent of the material's elastic properties. The velocity of a transverse wave in a stretched fiber can be monitored precisely and simultaneously with the sample tension, thus enabling the calculation of the linear density as a function of the applied stress or strain. When such measurements are carried out while diffusion occurs, the effect of applied stress or elongation can be systematically examined.

An instrument called a "vibroscope", was developed by Gonzalvez (1947) to measure the denier of fibers. It is based on the relationship between the frequency of transverse vibrations on the fiber tension and the square root of the linear density. Measurements of the resonance frequency of fibers were made by Downes and Mackay (1955) in a modified version of the basic instrument which yielded a plot of the vibration frequency versus tension. They initiated mass transfer by passing air of different humidities over the

sample. However, this technique has remained almost exclusively a method for fiber denier estimation. A system uniquely designed to study the coupling between stress and diffusion and related in principle to the "vibroscope", was developed by the authors (Chipalkatti et al. 1987). This experimental technique is discussed in the current section.

This new apparatus for fiber denier measurement, monitors axial tension via a force transducer during vibrational velocity measurements. Two basic types of experiments are thus conducted:

1) By stretching the fiber to a constant elongation, it is possible to determine the change in tension and diffusion under constant applied strain.

2) Conversely, by maintaining a constant tension on the fiber, it is possible to monitor changes in sample length during sorption or desorption.

The sample has been treated as a string under tension and hence some basic assumptions about the wave propagation velocity follow from this assumption. It has been experimentally demonstrated that the assumptions made are very realistic, particularly since the technique is designed with them in mind. These assumptions form the basis of the vibroscope type of instrument and are listed below:

- The string is "ideal" (flexible) and the tension provides the restoring force to the vibrations.
- Displacements from the mean (stationary) position are extremely small.

- The mass per unit length is constant through the length of the string, and it is otherwise homogeneous.

- All vibrations are assumed to take place in a single plane.

Under these conditions the transverse displacement of the fiber obeys the equation:

$$\frac{\partial^2 v}{\partial x^2} = \frac{\rho}{T}\frac{\partial^2 v}{\partial t^2}, \tag{2.1}$$

where:

x = direction of wave motion

v = is the transverse displacement, $v = v(x,t)$

t = is the time

ρ = is the mass per unit length

T = is the tension

The general solution of equation (2.1) can be expressed in the form:

$$v(x,t) = f(x-vt) + g(x+vt) \tag{2.2}$$

such that,

$$v = \frac{L}{\Delta T} = \left\{\frac{T}{\rho}\right\}^{\frac{1}{2}} \tag{2.3}$$

where:

L = the fiber length

Δt = the time required for the wave to traverse the length L

The above relations are purely kinematical in nature. As a result, no constitutive description of the material is required and the experimental results are not affected by the changes in material properties. In fact, the same equations govern the techniques used to determine fiber denier and have proven to be quite effective in the case of high modulus fibers.

2.2 Design of the Experimental Apparatus

The fiber to be studied is stretched between a force transducer at one end and a fixed vertical post at the other. Both of these are mounted on a heavy steel base with the force transducer attached by means of a movable assembly and a vernier gauge. The vernier gauge measures the displacement of the moving end with an accuracy of 0.01 mm. The major portion of the fiber, except at the ends, is enclosed in a horizontal tubular glass sorption chamber held horizontally by means of clamps. Another external glass tube is mounted concentrically and houses the heating element. This is used when temperatures higher than ambient are required. The force transducer output is periodically recorded from a digital readout. The schematic diagram of the equipment is presented in Figure 2.1 and a photograph of the entire assembly is shown in Figure 2.2.

Specially developed vibration sensors (Figure 2.3) are mounted at either end of the sorption chamber, for the purpose of detecting the

transverse waves. Two types of sensors have been designed to enable use on a wide range of samples:

(1) Contact Wire Sensors (For ribbons and thick fibers, dia.>0.8mm): These are on-off switches consisting of very fine gauge nickel wire attached to a flat brass plate (Figure 2.4). The wire is clamped at the upper end and the entire surface except at the contact tip is covered with an insulating film. These sensors are attached to transversely mounted screw gauge mechanisms, such that their distance from the fiber can be precisely adjusted. A simple RC circuit is connected, with a 9V DC power supply to the sensors, as shown in Figure 2.4. The fiber sample is threaded between the wire and the brass plate. While the fiber is motionless the wire and brass surface make contact, resulting in closed circuit. When a vibrational pulse passes through the sensor, the contact wire is lifted by the sample and the connection is momentarily broken. The resulting voltage discontinuity is indicated and stored on a recording digital oscilloscope (Nicolet Explorer III). A movable cursor on the oscilloscope enables the measurement of the time delay between the traces due to the voltage drops in the two sensors A photograph of typical signals is shown in Figure 2.5.

(2) Laser Sensing System (for very fine fibers): A single-mode laser transmitter-receiver pair is used in a "beam breaker" type of vibration sensor (Figure 2.6). The light beam is conducted via fiber-optic cables (100μm dia.) whose ends are fitted axially opposed to each other, on either side of a transverse slot in a metal sleeve. The fiber sample is threaded through a 1 mm slot. The sensor assembly is mounted on a movable stage with a screw gauge type micro-positioner. A 5V DC power supply and the required amounts biasing circuit (Hewlett Packard Optoelectronics Users Catalog) are connected

to the laser diode and receiver pair. When the beam circuit is complete, the receiver generates a voltage output that is a function of the beam intensity and is registered on the oscilloscope. The beam intensity across the gap can be controlled by adjusting the transmitter biasing voltage (hardware adjustment) or by changing the gap width (local adjustment). In the stationary state, both the sensors are carefully positioned such that the light beam is exactly intercepted by the fiber sample. The slightest vibration of the sample allows the beam to complete the optical circuit, and registers as a voltage pulse on the oscilloscope. The complete blockage of the beam during the vibration of very fine samples, such as Kevlar monofilaments (12 μm dia.), is ensured by reducing the beam intensity as well as increasing the sensor gap.

Desorption is performed by exposing the sample to a stream of dry nitrogen (≤5% relative humidity) while sorption is carried out in humidified nitrogen (≥96% relative humidity). A "dry" sample thus contains a base level of absorbed nitrogen. Estimates of the mass transfer resistances involved show the fiber resistance to be orders of magnitude larger than the outside resistance. This makes the technique a viable means for the study of diffusion within the fiber in addition to making mass-uptake and equilibrium solubility determinations.

2.3 Calibration and Validation of the Technique

The load cell used for tension measurement has a maximum capacity of 550.0 gm (Toyo Measuring Instruments Co. #TI-550-430), and is

sensitive to changes in tension as low as 0.085 gm (.002V). The load cell is calibrated periodically prior to a series of experiments in order to check for linearity and zero error. In addition, the zero of the load cell-readout system is adjusted by first shorting the two output wires (green and red) and setting the amplifier offset to zero. Then the amplifier balance is zeroed with the sample held slack. A cotton thread is stretched between the load cell at one end and a frictionless pulley at the other end. An amplifier gain of 1000 is typically used. Weights ranging from to 5 gm to 550 gm are hung at the free end of the thread and the corresponding voltages noted. The thread and weights are shielded from extraneous vibrations throughout the calibration procedures. The results of a sample calibration are shown in Figure 2.7 for future use and comparison.

The validity of the assumptions made earlier as well as the ability of the technique to make mass measurements is confirmed independently by comparing the results with weight measurements performed on a sensitive balance (resolution 0.001 g). The difference in the two sets of values, when corrected for the changes in length resulting from the applied tension, range from 0.2% for the polyaramid monofilament to about 2% for commercial cotton thread. Another test for the validity of the technique is the verification of equation 2.3 which states that for a constant mass system, the square of the velocity is proportional to the tension in the sample. Clearly, this remains true for small deformations of the sample as the linear mass will change only negligibly in such cases. Figure 2.8 is a plot of the sample tension in a monofilament of Kevlar 49® (PPTA) plotted against the square of the wave propagation velocity. Figure 2.8 demonstrates that Equation 2.3 holds for this system. Such independent verifications of the accuracy of the technique are

recommended over the entire range of sample tensions intended to be used. This procedure ascertains the reliability of the technique and also defines the lower limits of tension that may used with an acceptable level of error.

2.4 Design of Experiments

The Vibrational Time Delay Technique enables the measurement of the linear density of uniaxial samples under tension. However, it is important to elucidate the relative significance of applied stress or applied strain on transport for any system being considered. This makes it necessary to conduct diffusion experiments with samples under constant tension and constant elongation respectively. The technique developed has the ability to examine these cases and two such experimental schemes have been implemented during the course of this research.

2.4.1 Constant Tension Experiments

Samples under constant elongation undergo stress relaxation as well as swelling or shrinkage during sorption-desorption cycles and during heat-treatment. The sample tension, which has to be kept constant, is adjusted by changing the sample length by appropriate amounts. In a typical constant tension experiment, a fiber or ribbon sample was threaded through the tubular environmental chamber. Rectangular metal tabs bonded at either end

of the sample were used to grip the sample, one end secured to the fixed post and the other end attached to the force transducer.

The sample was conditioned by drying it in a controlled flow (volumetric flow rate ≈ 0.0018 m^3/s at 1 atmosphere pressure and 25 °C) of dehumidified nitrogen (relative humidity ≤ 5 %). The sample was held under near zero tension during the drying phase. After approximately 3 hours of conditioning, the sample tension was adjusted to the level necessary for the constant stress experiment. Periodic linear mass measurements were made thereafter to ensure that the sample was completely dry and to establish the lowest constant value as the sample's dry mass prior to exposing it to moisture. This value was then used as the basis for the calculation of the moisture gain for that sample, through all the cycles of sorption and desorption. Changes in the value of tension during the experiment were compensated for by altering the sample length by steady adjustments of the screw gauge on which the load cell is mounted. These adjustments were made manually as often as necessary to keep the tension always within 0.1-0.2 % (≈2-6 mV on the readout) of the desired value.

2.4.1.1 Precautions

1) During constant tension experiments, care was taken to always maintain sufficiently large tensions in the sample. Only then does the tension act as the restoring force in the vibrations and Equation 2.3 remains valid. It can be shown that for very low tensions, the elastic modulus enters the

calculation and introduces errors in the linear density determinations. This was avoided by using long samples with at least a moderate to high tension in the sample.

2) Care was taken to avoid the application of tensions too close to the breaking tension for the sample or the maximum capacity of the force transducer used.

3) A wave was initiated in the sample by striking a vertical wire held adjacent to the sample and close to one of the sensors. The vibrations of the vertical wire generated travelling wave pulses in the horizontally held sample. When striking the vertical strike wire, care was taken to ensure that only light strikes involving small displacements from the mean were made and damage to the sample was at a minimum. However such strikes needed to be of sufficiently large amplitudes in order to be clearly detected by both sensors. The strikes have to be selected after some trial and error for each sample.

4) A sufficiently large air flow rate was employed in order maintain a constant source of moisture at the sample surface. However, the flow rate was not permitted to be high enough to generate extraneous vibrations in the sample and hence noisy signals on the oscilloscope. The maximum allowable value of the flow rate depends on the individual sample dimensions and cross-sectional geometry, and is arrived at by trial and error.

5) When reading the time delay off the oscilloscope, care was taken to consistently read between identical phases of the two pulses. The time delay between similar features, such as between pulse initiation points or peak to peak, were measured.

6) Care was taken to trigger pulses immediately after making length corrections, so that accurate readings of sample tension were always assured.

2.4.2 Constant Strain Experiments

The effect of sample strain is an important consideration for low modulus materials which are able to sustain relatively large deformations. The applied strain is particularly relevant in materials where it causes temporary or permanent internal changes in the material. In such cases, it is also useful to study diffusion under constant strain.

As discussed earlier, the Vibrational Time Delay Technique facilitates sorption-desorption experiments under conditions of constant uniaxial (macroscopic) strain. The procedural details are essentially identical to those discussed in the case of constant tension. In a typical constant strain experiment the sample is conditioned by drying under nearly zero stress for about 3 hours. After this preliminary drying period, the sample is extended to the strain required for the experiment, and drying is continued while making periodic linear density determinations. As in constant stress experiments, drying is continued until the lowest constant value is reached. This value is then recorded as the base dry value for the rest of the sequence of experiments conducted on the sample. The sample is then exposed to moisture. The value of the sample tension, T, is recorded as a function of time, for the known value of sample extension (fixed in this case) and provides information

about stress relaxation and recovery (viscoelastic response as well as swelling and shrinkage bchavior).

2.4.2.1 Precautions

1) - 5) Precautions were applied in the same manner as discussed for experiments under constant tension.

6) Care was taken to make force and velocity measurements in simultaneous pairs in order to assure the validity of this technique.

2.4.3 Heat Treatment of Samples

The heat treatment of some samples is used as a pre-conditioning step prior to diffusion experiments. Heat treatment was performed with the sample held at constant length. The linear density was measured as a function of time and temperature along with the sample tension. The temperatures employed in each case are referred to in the discussion of specific samples in Chapter 4. The sample was mounted within the environmental chamber, and then conditioned for 2 to 3 hours in a stream of dry nitrogen. Subsequently, the temperature of the chamber was raised at approximately 1 °C/min. The temperature was then maintained at the required value for one hour in typical experiments. The sample was then cooled in an inert atmosphere at the rate of 1 °C/min. The rate of cooling was controlled by adjusting the flow rate of the nitrogen gas. Temperature regulation was achieved by manually balancing

the cooling effect due to the nitrogen flow (by adjusting flow rate) with the heater output (by adjusting the rheostat).

2.4.4 Materials

Some of the materials used in this study are Kapton® (DuPont, H-type polyimide film), Lexan® polycarbonate (General Electric, calendered film) and monofilaments of Kevlar 49® (DuPont, from 1500 denier yarn). These materials provide a range of samples that have been examined not only for the variations in their transport related properties, but also in order to explore the scope and versatility of this technique. A list of all the materials studied is provided in Table 2.1 at the end of this chapter.

2.5 Calculations

The experiments described above, essentially provided information about the equilibrium solubility (equilibrium moisture gain) and the transient transport characteristic (the apparent diffusion coefficient). In addition, constant stress experiments also provided data on the dimensional change of samples as functions of exposure time and residual moisture content (the swelling coefficient). By the same token, the constant strain experiments yielded information on stress decay or recovery with respect to time, moisture gain, as well as the direction in which the transport progressed.

2.5.1 Equilibrium Solubility

The equilibrium of the various materials were measured under conditions of constant tension and constant strain. The procedure and calculations arc briefly discussed in the following sections.

2.5.1.1 Constant Tcnsion Experiments

In addition to the changes in linear density due to diffusion, therc is also a contribution that results from the compensatory length changes required to maintain thc desired tcnsion. In other words, the applied strain changes thc lincar dcnsity due to the conservation of mass. Hence, thc lincar dcnsity detcrmined experimentally needs to be corrected accordingly. Thc change in length is computed relative to the original unstressed length, L_0 (m). Thc initial dcnsity of thc sample at $t = 0$ and stress $\sigma = \sigma_0$ is ρ_0, in the following discussion. Subscripts are used to denote current values while superscripts refer to the corrected values bascd on the initial state at t=0 and $\sigma = \sigma_0$.

At $t = 0$, let the total initial mass of sample = M_0 and the unstressed length = L_0 and the linear density measured at time t (for a sample of length L_t) = ρ_t. Thus the sample mass at equilibrium, $M_\infty = \rho_\infty L_\infty$ where ρ_∞ and L_∞ correspond to the mass and length of the sample in the equilibrium state at $t = \infty$.

The length of the sample at time t, while diffusion is in progress is:

$$L_t = L_0 + \Delta L = L_0(1+\varepsilon), \tag{2.4}$$

where ε = the axial strain in the sample and ΔL = the incremental change in length.

Let the corrected linear density (based on original length L_0) at time t = 0 be $\overset{0}{\rho}_t$. Hence, the total mass of the sample at time t is

$$M_t = \rho_t L_t = \overset{0}{\rho}_t L_0. \tag{2.5}$$

Thus at time t, the corrected value of the linear density, based on the length L_0, may be obtained by substituting for L_t from Equation 2.4 into Equation 2.5. Thus,

$$\overset{0}{\rho}_t = \rho_t (1 + \varepsilon). \tag{2.6}$$

The percent weight gain of moisture, or residual moisture content is then given by

$$WT\%(t) = \frac{\overset{0}{\rho}_t - \rho_0}{\rho_0} \times 100 \tag{2.7}$$

The data are presented as plots of WT%(t) versus time are plotted for sorption and desorption cycles.

The approach to equilibrium is characterized in terms of the fractional weight gain with respect to the equilibrium sample mass such that:

$$\text{the fractional weight gain} = \frac{M_t}{M_\infty} \tag{2.8}$$

2.5.1.2 Constant Strain Experiments

During constant strain conditions, the only changes in linear density are due to moisture gain or loss. Hence, the linear density determined experimentally, ρ_t, is in this case the linear density of the sample at time t while ρ_0 is defined as the initial density at t = 0 and $\varepsilon = \varepsilon_0$. The weight gain at any time t is given by

$$WT\%(t) = \frac{\rho_t - \rho_0}{\rho_0} \times 100. \qquad (2.9)$$

These values are then presented as before in plots of WT% versus time. The WT% data provide the equilibrium solubility of moisture at different values of sample strain.

2.5.2 Diffusion Coefficients

The fractional weight gain, defined as before is M_t/M_∞ and is typically plotted against $\sqrt{t}$. The fractional weight gain curve has been used to estimate the apparent initial diffusion coefficient D at different values of strain, based on the standard results (Crank 1975) for cylindrical (fiber) and planar (ribbon) geometries. These are defined in Equations 2.10 and 2.11 below. An assumption implicit in this analysis is that the radius or the

thickness of the samples does not change significantly. Further, diffusion coefficients have been estimated for radial diffusion while transport in the longitudinal direction has not been considered. This is reasonable in the context of the very long samples used (having aspect ratios of about 8×10^5). Thus the entire weight gain of the sample has been assumed to be due to diffusion in the radial direction.

The boundary condition has been fixed by assigning the concentration of moisture in the diffusion chamber to be the concentration at the surface of the sample. The initial condition is based on the assumption that samples were completely dry prior to sorption experiments (internal concentration = 0 % moisture) and saturated with moisture, prior to drying experiments (internal concentration = 100 % moisture). In the earlier stages of diffusion, the sample has been considered to act as an essentially semi-infinite medium. Consequently, the fraction sorbed or desorbed via Fickian diffusion, in a typical case, was expected to be proportional to the square-root of the elapsed time. This has been substantiated by the experimental results discussed in subsequent chapters.

For ribbon samples, the diffusion coefficient was determined from the expression:

$$D = \frac{\pi d^2 S^2}{960}, \text{ cm}^2/\text{sec}, \qquad (2.10)$$

where

d = sample thickness, cm,

S = initial slope of the plot of M_t/M_∞ versus $\sqrt{t}$ (units: $1/\sqrt{\text{min}}$)

For fiber samples, the diffusion coefficient is given by:

$$D = \frac{\pi r^2 S^2}{960}, \text{ cm}^2/\text{sec}, \qquad (2.11)$$

where r = fiber radius (cm) and S ($1/\sqrt{\text{min}}$) is defined above.

2.5.3 Swelling Coefficients

The swelling coefficients have been determined as functions of time and applied stress from the dimensional change in the sample during constant tension experiments. The change in length with time was recorded during sorption and desorption experiments and the axial swelling calculated for the transient experiments.

The initial length of the sample = L_0 (cm)

The length of the sample measured at any time t = L_t

Then, L_t follows from Equation 2.4 and the percent change in length at any time t, $\Delta L\%(t)$, is then given by

$$\Delta L\%(t) = \frac{L_t - L_0}{L_0} \times 100\ \% \qquad (2.14)$$

The value of $\Delta L\%$ is calculated as above and then plotted as a function of time. Thus the swelling coefficient β (expressed as the percent strain per percent increase in the moisture content) can be calculated from,

$$\beta = \frac{\Delta L\%(t)}{WT\%(t)} \qquad (2.15)$$

2.6 Conclusions

The technique described above can be applied to the study of stress coupled sorption in polymer fibers or ribbons by making linear density and sample tension or elongation measurements during diffusion. The assumptions associated with the technique, as well as the fundamental principle of this technique have been verified experimentally. Thus it has been shown that for very long samples under at least moderate to high tensions, the propagation velocity of the vibrational pulses is independent of the material's elasticity. Instead it has been shown to depend on the applied tension and the sample's linear density.

The apparatus has been applied to the study of coupling between applied stress and strain and the materials sorption and diffusion characteristics. Swelling under conditions of constant stress has also been investigated. The results of these experiments, conducted on a variety of materials is presented in subsequent chapters.

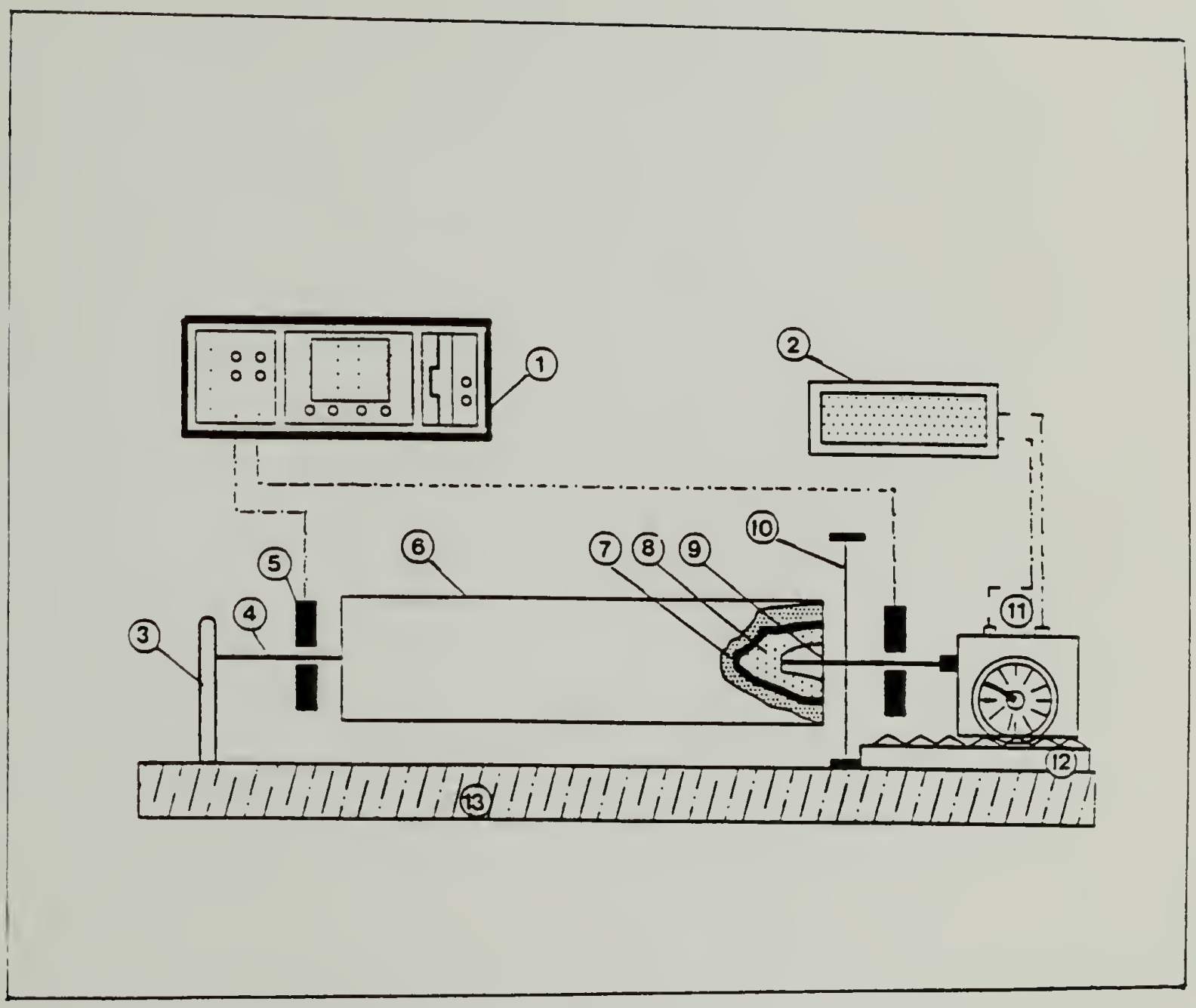

Figure 2.1 Schematic representation of the Vibrational Time Delay apparatus for the measurement of the linear mass of fiber or ribbon samples under tension. 1) digital oscilloscope, 2) force readout, 3) fixed post, 4) sample, 5) vibration sensor, 6) outer tube, 7) insulation layer, 8) heating element, 9) diffusion chamber, 10) striker wire, 11) force transducer, 12) vernier gauge, 13) base.

Figure 2.2 Photograph of the experimental apparatus showing its various components.

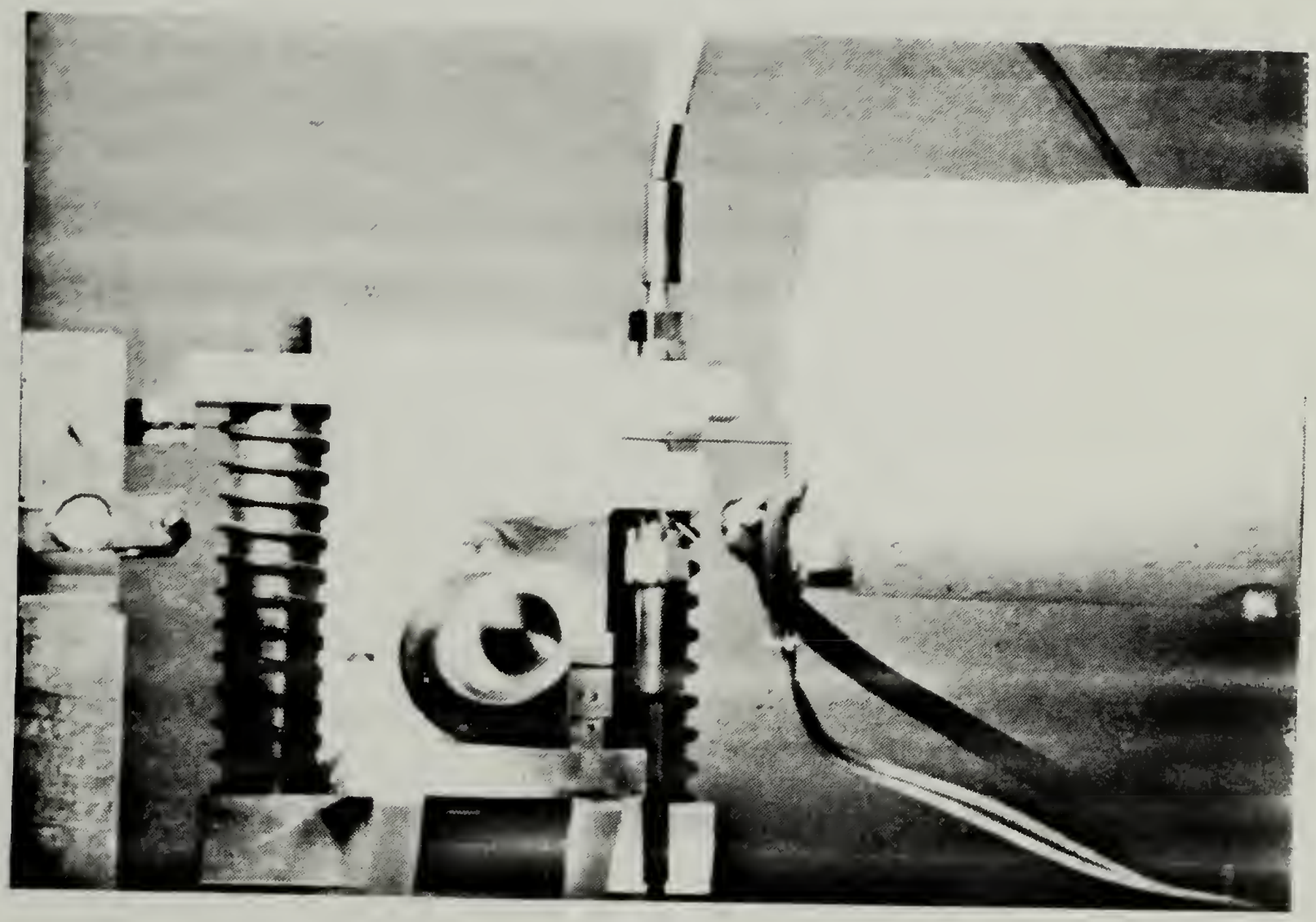

Figure 2.3 Photograph of the vibration sensor assembly showing a fiber sample and the cylindrical diffusion chamber. The sample is threaded through the vibration sensor which is mounted on a vernier assembly.

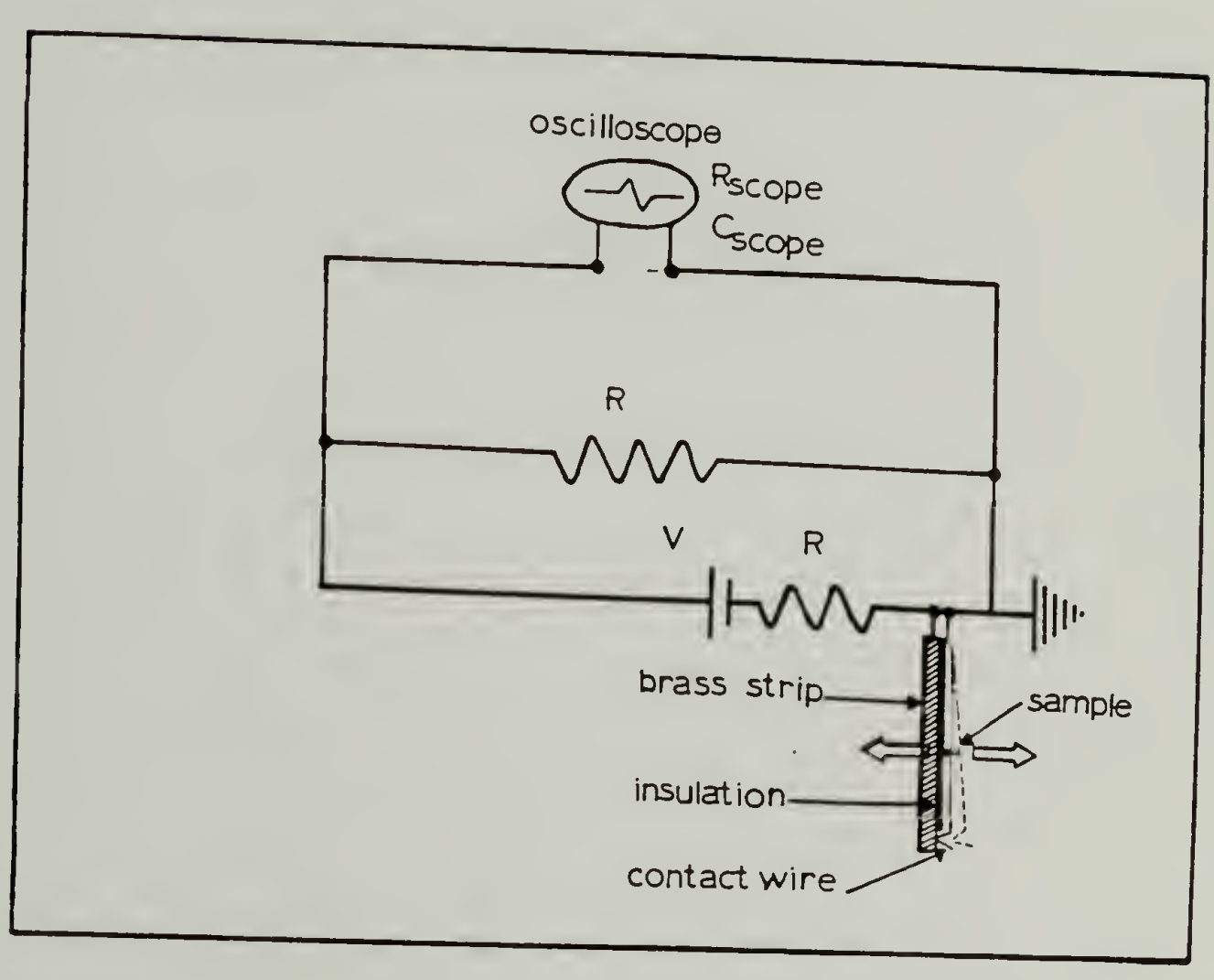

Figure 2.4 Diagram of the "contact wire" vibration sensors for ribbon and thick fiber samples. The sensor acts as a vibration activated on- off switch. The RC circuit ensures sharp cut-offs in the voltage pulse recorded on the oscilloscope.

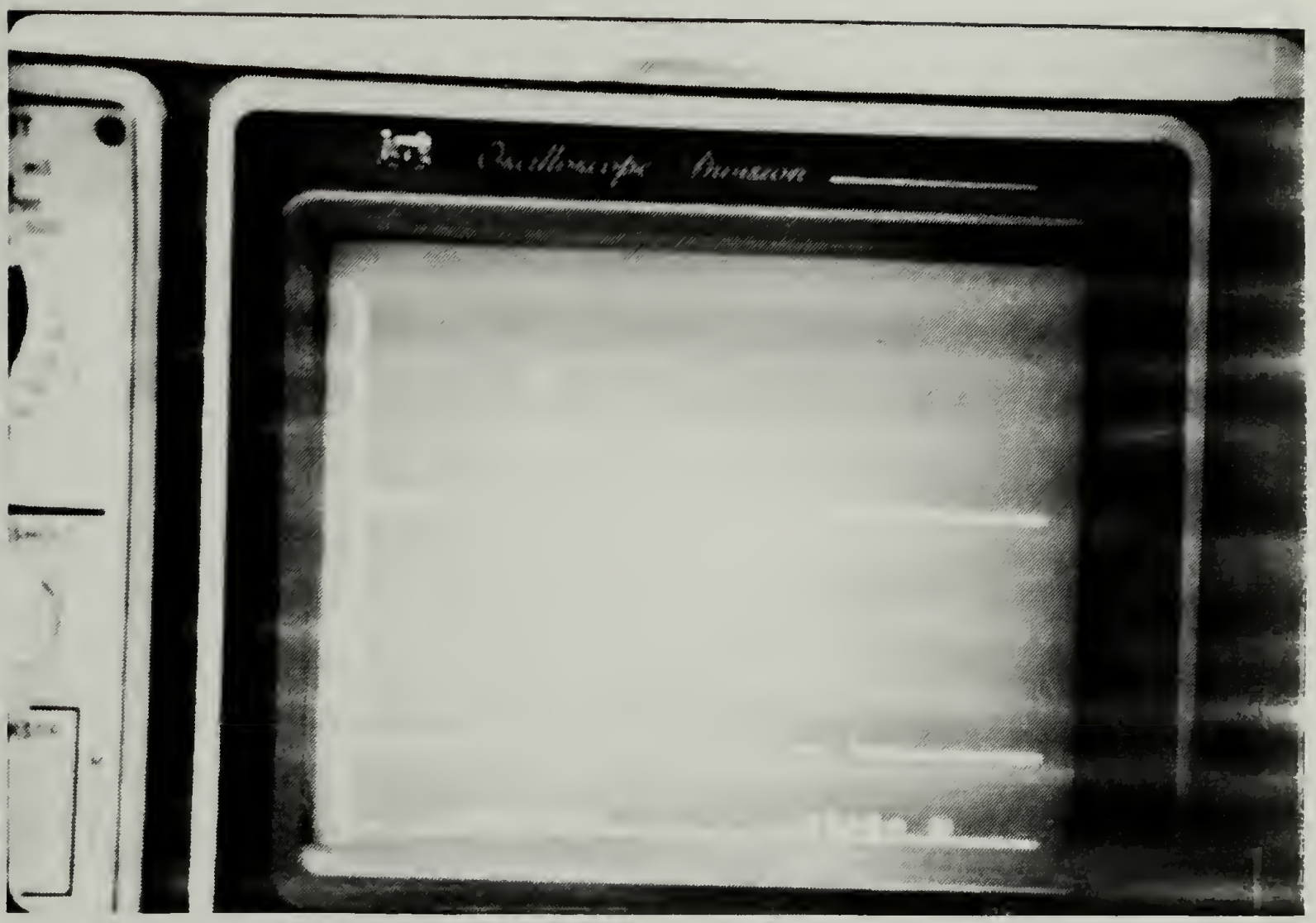

Figure 2.5 Photograph of the digital oscilloscope display showing a typical pair of signals from the vibration sensors resulting from a wave pulse.

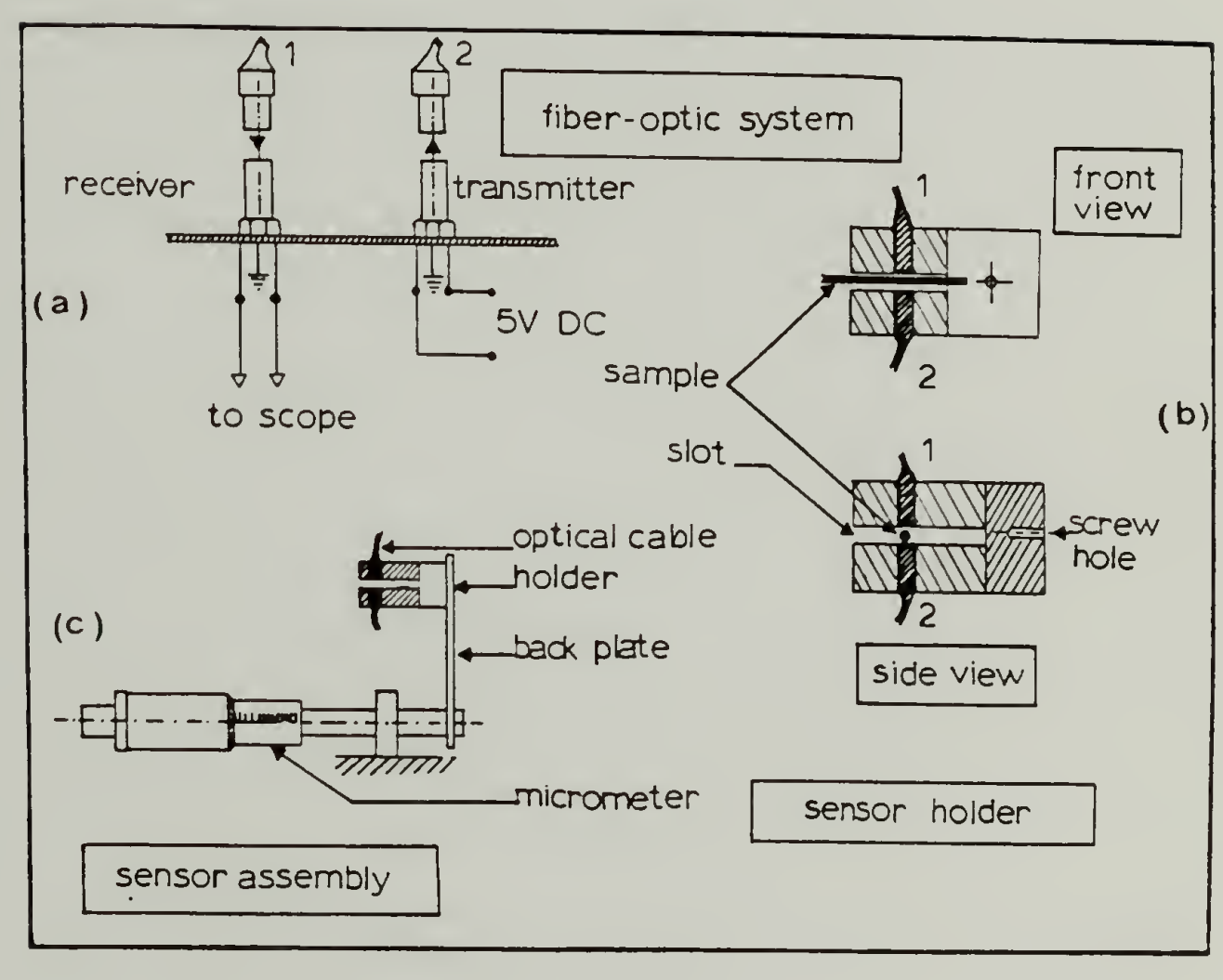

Figure 2.6 Schematic diagram of the fiber-optic laser-activated vibrational sensors (for fiber samples of diameter less than 0.8mm.) (a) emitter-receiver configuration, (b) sensor holders and fiber-optic coupling, (c) sensor assembly. Vibrating samples interrupt beam continuity between emitter and receiver resulting in voltage pulses being transmitted to the oscilloscope. (Not to scale).

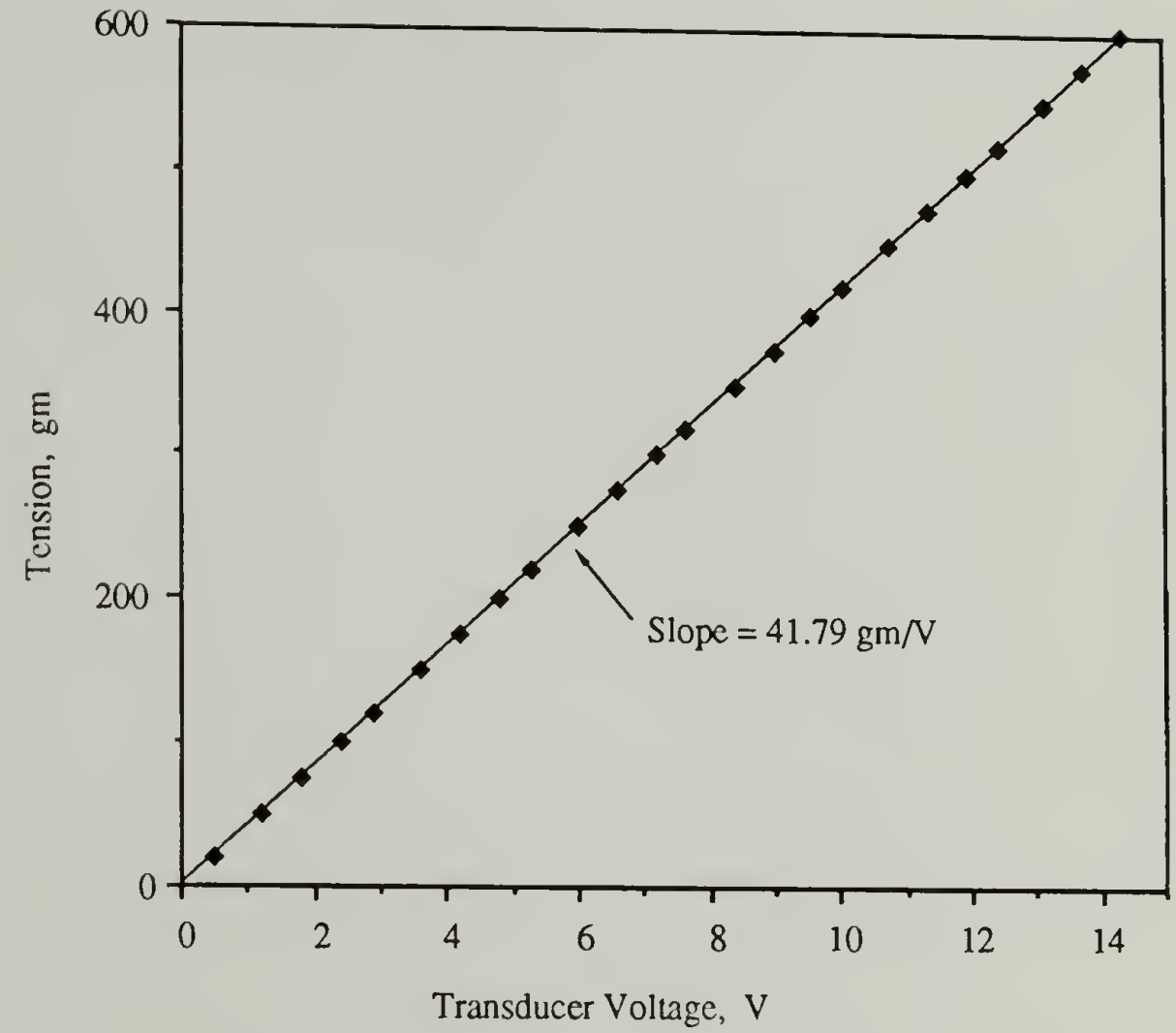

Figure 2.7 Typical calibration curve for the Toyo Measuring Instruments load cell #TI-550-430. Maximum load = 550 gm, Maximum input voltage = 13V, Amplifier gain used = 1000. Calibration conducted at room temperature. The best fit line represents Tension (gm) v/s Transducer Voltage (V). (Loading and unloading cycles were used).

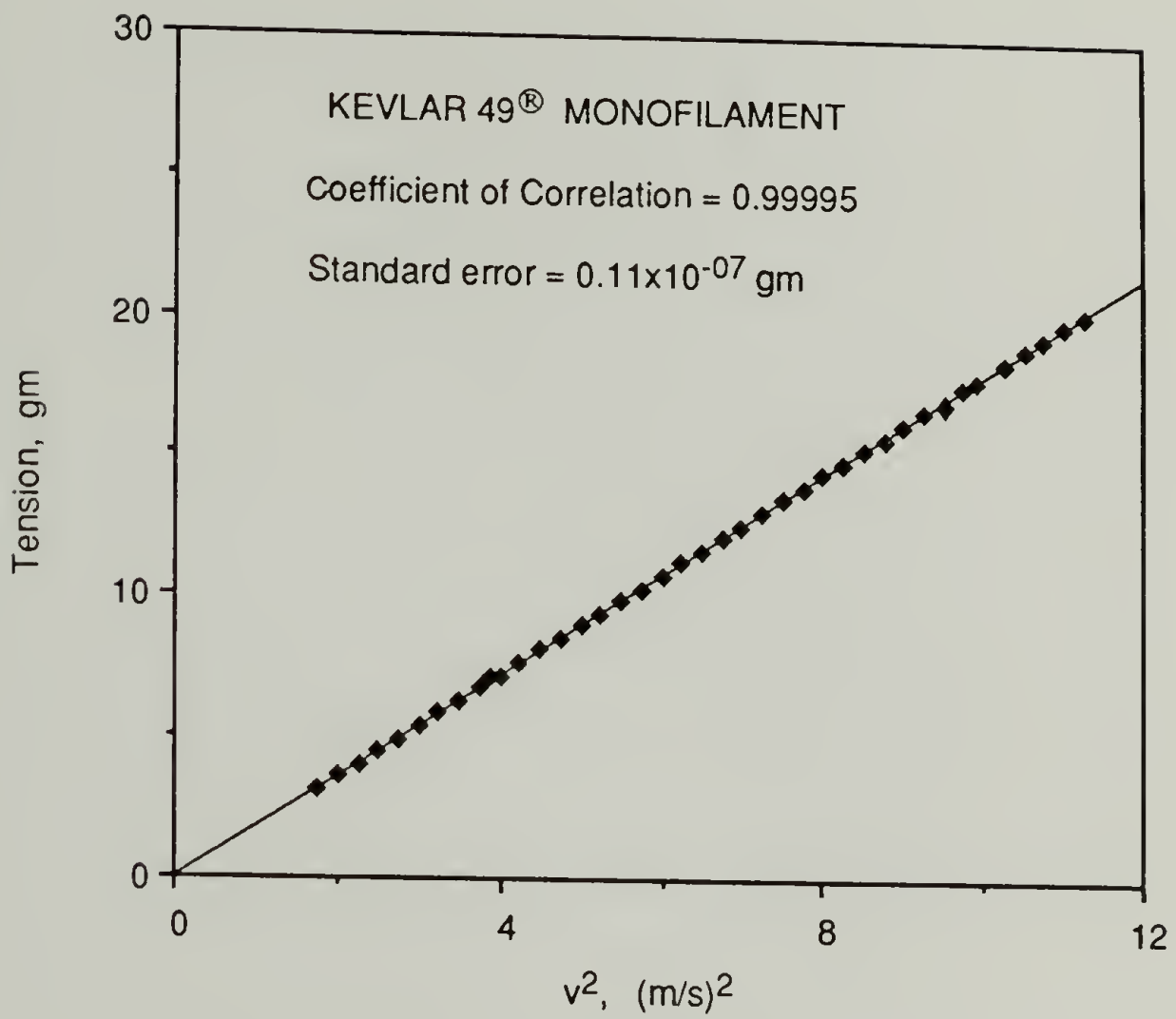

Measured Denier (1.618x10^{-07} kg/m)
Literature Value (1.581x10^{-07} kg/m)*

* From material data

Figure 2.8 Plot of tension versus the square of the wave propagation velocity in a stretched filament of polyaramid (10 μm diameter, tensile modulus = 124 GPa). The straight line fit clearly demonstrates the validity of Equation 2.3 and the principle of the technique.

Table 2.1 List of the materials examined by the "Vibrational Time Delay Technique" in this dissertation.

a) 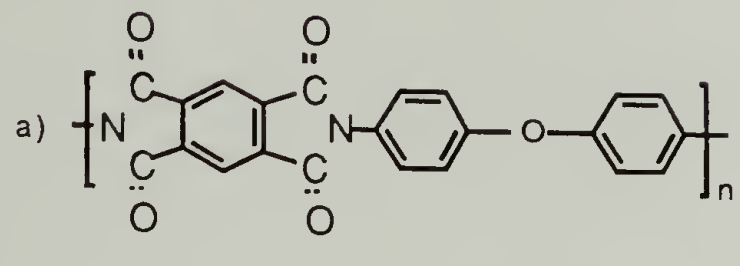

Kapton®, Polyetherimide
(PI)

b) 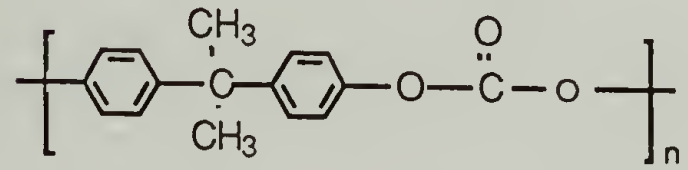

Lexan®, Bisphenol-A Polycarbonate
(PC)

c) 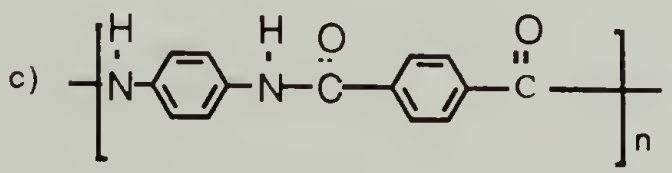

Kevlar® 49, Poly phenylene terephthalamide
(PPTA)

d) 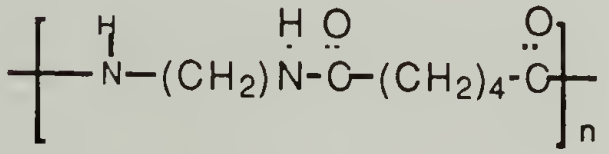

Nylon 6,6®
(N 6,6)

e) 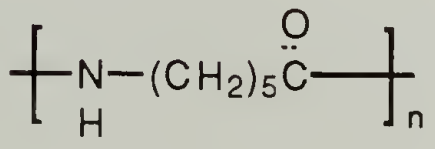

Nylon 6®
(N 6)

f) 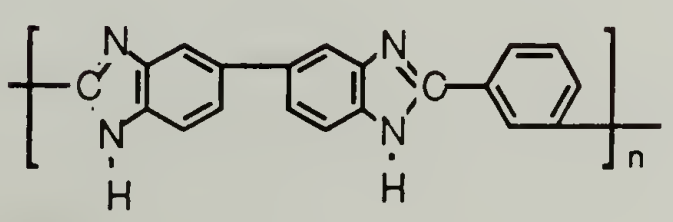

Poly m-phenylene bis-benzomidazole
(PBI)

CHAPTER 3

STRESS-STRAIN COUPLED DIFFUSION

The application of stress on most materials results in deformations at both microscopic and macroscopic scales. The dependence of the solubility of permeants, the diffusion coefficients and swelling on the external applied stress and strain is examined in this chapter. Externally applied stresses result in the macroscopic deformations and exert their influence throughout the material. The effect of internal stresses on the other hand, is contained within much smaller domains. In the linear elastic region of polymers, the applied stress results in proportional strains which vanish on the removal of the stress. Beyond this elastic limit stress and strain no longer remain proportional and ultimately a permanent set results in the material. These regimes of elastic behavior are seen for the case of a PBI filament, in Figure 3.1. In polymers the mode of the mechanical response plays a significant role in determining the qualitative nature of the coupling interactions of stress and transport. This was discussed by Yasuda and Peterlin (1974) for semi-crystalline polyethylene and also observed during this work. The results for PBI are presented later in this chapter, in the form of sorption isotherms for a range of applied strains spanning the linear and non-linear regimes of elastic deformation.

3.1 Experiments

Sorption experiments were performed on samples under constant tension and elongation, by means of the Vibrational Time Delay method. The results are reported and discussed in subsequent sections. The materials examined have been listed in Chapter 2, where a general procedure for sample conditioning was also outlined. Only those aspects of the sample preparation and experimental procedure that specifically deal with the experiments described here are summarized below.

3.1.1 Sample Description and Preparation

Ribbons were prepared in the case of film materials such as polycarbonate and polyimide. Ribbons of widths 2, 3 and 4 mm and lengths ranging from 0.7-1.0 m, were cut by means of a sliding blade paper cutter of photographic studio quality. Individual ribbons were then loosely wound on paper spools and stored inside a dessicator jar. The samples were dried in the dessicator for a minimum period of two weeks prior to use. The ribbons were carefully examined for evenness of cutting and consistency of width by measuring with calipers at random intervals. Damaged or uneven samples were discarded.

Sample preparation was relatively straightforward in the case of fiber samples. Fibers cut into lengths of 0.7-1.0 m as before, were first

examined under an optical microscope for signs of damage. These fibers were then stored in a dessicator jar prior to use. Fiber diameters as well as ribbon widths were measured by means of the graduated eyepiece on an optical microscope. The average value of the measurements made at random intervals along the sample length, determined the fiber diameter.

3.1.2 Experimental Procedure

As discussed in Chapter 2, constant tension experiments were carried out by holding the fiber or ribbon samples under constant tension during diffusion. The tension was maintained by adjustments of the sample length to compensate for any changes due to stress relaxation and swelling. The new linear density resulting from the change in sample length was calculated from Equations 2.6. The measurement of the length change also enabled the determination of apparent swelling coefficients as functions of moisture gain. The description "apparent" refers to the fact that the contribution due to sample creep was not entirely eliminated during the experiment.

Stress-coupled diffusion in glassy (non-equilibrium) materials is interesting from a fundamental and practical viewpoint. It is also meaningful to at least qualitatively determine the manner in which the stress state and transport are related to one another. The extent to which the moisture content in a saturated sample under tension approaches its original dry state on removing the applied stress is indicative of the reversibility of stress effects.

Of course, it is assumed that no permanent physical changes occur in the sample as a result of the applied stress. If equilibrium sorption is only partially reversed on removal of the stress, the contribution due to the stress is identified by the fractional moisture weight recovered.

However, the solubility versus applied stress data is not adequate to make inferences about the transient phenomenon and the diffusion coefficients. For this, the diffusion curves (M_t/M_∞ versus $\sqrt{t}$), for sorption and drying at different stresses as well as their initial slopes need to be examined. Hysteresis in these curves, between sorption and desorption, may be attributed to the coupling interaction and to concentration dependent diffusion coefficients. However, a strong correlation between the changes in the diffusion coefficients and tension is a more definitive indicator of coupling during transient diffusion.

In the section that follows, experiments that examine the reversibility of stresses generated by the sorption of permeants are first discussed. In these preliminary experiments, the samples were held at constant strain and exposed to moisture after some initial delay. The sample tension was then monitored during initial sorption desorption cycles to determine the extent to which the changes in tension corresponded with moisture uptake.

In another series of experiments samples were held under constant tension in the diffusion chamber, while linear density and elongation were determined periodically. A series of sorption and drying cycles were carried out at the same initial stress and repeated for samples subject to a range of axial tension. Thus the dependence of moisture diffusion

transients, solubility and swelling on the applied stress was investigated for a number of independent samples. These samples experienced diffusion under constant tension throughout the entire testing sequence and hence the results are representative of stress coupled transport in materials under a constant applied stress.

An additional series of stress-coupled sorption experiments examined dry samples at some initial stress. These were exposed to moisture until apparent equilibrium was achieved at that stress. When the sample reached saturation and maintained a constant weight, typically for more than an hour, it was considered to be at equilibrium. The material was then made to traverse the stress-solubility equilibrium lines by changing the axial tension. Such a change then resulted in the movement of the equilibrium moisture content to a new value corresponding to the new stress, although the environmental conditions remained constant. This step was repeated many times as the sample traversed from one equilibrium state to another with each change in the applied stress. The experimental procedure is shown schematically in Figure 3.2. In practice, a sequence of such steps was followed by drying and the entire sequence was repeated 2 or 3 times. In this dissertation the stress-solubility equilibrium lines, referred to above, are denoted as the "stress-solubility envelope" of coupled sorption. Furthermore, the diffusion experiments tracing the stress-solubility envelope are referred to as indirect or sequential constant stress/strain experiments.

The implications of the three types of experiments described above are discussed by considering representative results. Constant tension experiments are the main focus of the following sections with the aim of addressing stress-coupled sorption of moisture in polymers. The constant

stress experiments enable the measurement of the equilibrium solubility as a function of stress. They also enable the measurement of apparent initial diffusion coefficients and axial swelling coefficients, both being important descriptors of the stress-transport interaction. The overall scheme of experiments conducted was discussed above and is summarized in Table 3.1

3.2 Results

The first objective of this work was to demonstrate the link between the stress and diffusion by observing stress generated during diffusion. The stresses generated corresponding to the individual phases of diffusion experienced by a sample at constant length, were monitored by measuring the sample tension during sorption and desorption steps. In Figure 3.3 the results of such an experiment on a polyimide ribbon are shown as a plot of sample tension against elapsed time. The change in the tension was monitored during an initial holding phase followed by cycles of sorption and desorption.

During stage A, as seen in Figure 3.3, stress relaxation occurred while the dry sample was held at a fixed initial elongation. In stage B, the stress decay became even steeper as the sample gained moisture. On reversing the direction of moisture transport during drying (phase C), a net increase in tension was observed concurrently with the moisture loss. These trends repeated consistently during additional cycles of sorption and desorption (phases E and F), and are clearly seen to be deviations about the background

stress relaxation which provides a baseline stress. It is thus quite clear that the presence of a permeant in a constrained material generated internal stresses and that these stresses were exclusively associated with the moisture content of the sample. The weight gain of a PI sample exposed to moisture during a similar sequence is presented as a function of time in Figure 3.4.

3.2.1 Constant Tension Experiments: Direct Equilibrium States

It has been seen that it is feasible to measure stresses generated by transport processes within the samples studied. Further transport under applied stress was examined for samples under constant tension, and the data are presented in Figures 3.5 and 3.6. Percentage moisture gain is plotted against the exposure time for sorption and desorption cycles in PC in Figure 3.5. The moisture gain during a sorption cycle is also shown for a dry sample of PPTA in Figure 3.6. The moisture gain versus time data as seen in these figures is quite typical and the stresses shown are approximately median values of the ranges used during experiments.

Transient diffusion characteristics were also examined for sorption and desorption in PI, PPTA and PC. The results are presented in Figures 3.7 - 3.9, as plots of the fractional moisture gain (defined in equation 2.8) against the square root of the exposure time. These results were acquired during experiments conducted on a set of samples, each under a different uniaxial stress. In both these high modulus materials, the application of stress (within linear elastic limits) did not alter the basic mechanism of moisture

transport nor were the water molecules large enough to cause anomalous diffusion. It is seen that the mechanism of diffusion did not behave anomalously (ie. "Case II" diffusion). In this context, it is interesting to see that a similar plot for PC (Figure 3.9) is not a straight line, but instead appears to consist of an initial linear region followed by curved region. This is clearly relatcd to thc multi-stage profile observable in Figure 3.5.

In the context of the swelling versus osmotic pressure intcraction proposed by the equilibrium theories discussed in Chapter 1, a study of swelling versus sorption may provide clues to the coupling mechanism. In Figure 3.10 the percent axial swelling strain, for a ribbon of PI, is plotted against the exposure time. The swelling strain is considered to be zero at the start of the experiment, although the sample had a constant, non-zero initial strain. Swelling occurred during the sorption phase (AB) and shrinkage occurred at a slower rate during drying (BC) and was followed by furthcr elongation during the second sorption (CD). In Figure 3.11, the pcrccnt length change due to swelling is plotted as a function of the moisture content for the phases: first sorption - drying - second sorption. The lines represent linear regression fits for each of the 3 phases and demonstrate that while thc slope is approximately equal for swelling strain during both sorption phases, it is much smaller for shrinkage during drying. During the first sorption the sample started from the dry state and hence the line passes through the origin. However, since both desorption and the second sorption started at the length resulting from the previous phase, non-zero initial strains were observed in these cases.

The swelling of PPTA fibers under constant tension, as seen in Figure 3.12, was small (< 0.01%) just as in the case of PI ribbons. In the case of

PC ribbons, there were some remarkable features in the sorption induced swelling as shown in Figure 3.13. The net dimensional change due to swelling in an as-received sample held at constant tension is shown through two drying and sorption cycles. Sample shrinkage was observed briefly (C'-D) during the second sorption phase (C-D). This may be attributed to the fact that the moisture in the PC became sufficient to induce internal rearrangements and thus induce a recovery of strain energy stored during prior deformation (the material was calendered during manufacture and had been held in its stretched state for about 2 hours during the experiment itself). Similarly, stress recovery was observed in PC samples held at constant elongation during sorption. This recovery phenomenon is discussed at greater length in Chapter 4, specifically with reference to Figure 4.12. Analogous results were demonstrated in the case of cold-drawn PC when heated close to its glass transition presumably due to thermally induced recovery of stored deformation energy (Adams 1987). Finally, the swelling is plotted as a function of the moisture gain for PC and PPTA, as shown in Figures 3.14 and 3.15.

The experiments discussed above examined the dependence of the solubility (equilibrium), the diffusion coefficient (kinetics) and the swelling coefficient (energy of deformation) on the applied stress for a range of stresses. These "direct" experiments, focussed on the influence of a constant applied stress on transport related properties. They provided reference data for comparison with the behavior of samples that were exposed to a sequence of stresses, as they traversed from one equilibrium state to another during these "sequential" experiments. In the high modulus materials discussed above, the diffusion mechanism displayed no significant divergence from the

norm of stress-enhancement under tension, particularly for the PI and the PPTA. Low modulus materials were also examined and are discussed later in this chapter.

The equilibrium solubility, the apparent diffusion coefficient and the axial swelling coefficient were determined as functions of the applied stress by means of the experiments described above. The results are summarized for PI (Figures 3.16-3.18). In these figures, the transport property is plotted along the Y-axis with the axial stress along the X-axis. The equilibrium sorption varied linearly with stress in the "direct" experiments described earlier (Figure 3.16). The value at zero stress was arrived at by vapor phase saturation experiments and agrees very well with the extrapolation of our experimental data. This was compared with the independently determined solubility via "wet" immersion tests (Sackinger 1987). The lower value obtained by the immersion studies is attributed to the egress of small molecules from the PI during the initial stages of sorption. Such a loss in weight of PI followed by a net gain due to water sorption was reported by Yang et al. (1985).

The linear relationship between the fractional weight gain and the square-root of exposure time for the initial stages was discussed by Yang et al. (1986). In this study the diffusion coefficient for PI was also found to be proportional to the applied stress, indicating that rate-controlling aspect of the transport mechanism was proportional to the axial stress (Figure 3.17). An interpretation based on the work of Wolf et al. (1984) on PI insulation, suggested that the applied stress provides some of the activation energy for a mechano-chemical interaction of water with PI. Wolf et al. (1984) also cite the work of Zhurkov and Tomashevskii (1966) who proposed that the energy

supplied or the reduction in activation energy resulting from the application of stress was proportional to the applied stress.

The diffusion coefficients for desorption, as seen in Figure 3.17, were relatively unaffected by the application of the stress and were approximately equal to the zero or low stress values. This is characteristic of the hysteresis typically evident during stress assisted diffusion and the resulting asymmetrical sorption-desorption cycle. As shown by Crank (1975), when the diffusion coefficient increased with concentration, transport during desorption was usually slower. Such a slowing down was reported for PI by Yang et al (1985; 1986). They rationalized this phenomenon by proposing that hydrophilic sites increased during the initial sorption. This was believed to cause plasticization of the polymer and thus enhance additional sorption while it slowed down the subsequent desorption.

In Figure 3.18, the axial swelling coefficients for polyimide determined during sorption and desorption under constant tension is plotted against the applied stress. Significantly, Treloar in his pioneering works (1952, 1953) applied thermodynamic principles to deduce that the swelling coefficient increased on the application of a tensile stress. For desorption however, the swelling coefficient was found to decrease with stress. In this case the sample was initially saturated and swollen and subsequently shrank in length as it lost moisture. When superposed on the elongation due to sample creep, the net strain was relatively small resulting in smaller swelling coefficients.

3.2.2 Constant Tension Experiments: Sequential Equilibrium States

The third series of experiments conducted were related to the generation of stress-solubility envelopes. Stress-coupled sorption was carried out and the tension was changed in incremental steps, from one equilibrium state to another. These experiments have been denoted as "sequential" experiments to distinguish them from the "direct" experiments discussed in the previous section and have been sketched in Figure 3.2. These experiments resulted in determinations of the stress dependent solubilities, the apparent initial diffusion coefficients and the axial swelling coefficients of the samples selected. The significance of these experiments lies in the fact that a typical plot of solubility versus stress represents a sequence of equilibrium states for a sample as it experienced step changes in stress state, while the humidity at the boundary remained constant.

The moisture gain versus time data that resulted from the above experiments are seen for PI, PC, PPTA, Nylon 6,12 and Nylon 6,6 in Figures 3.19 through 3.23. For instance, in Figure 3.19, the exposure time is plotted against the moisture gain as well as the corresponding swelling strain for sorption starting with a dry sample. As before, swelling strains were assumed to be zero at the start of sorption in dry samples at some applied stress or strain. It is seen that sample elongation accompanied the moisture gain during the first stage. The step change in sample length observed between stages corresponds to the adjustments in sample length that were required to change the tension. The sample was observed to reach a distinct equilibrium state corresponding to each stress applied. The subsequent lowering of sample tension resulted in a

"desorption" driven by the reduction in axial stress. Significantly, the value at 12.3 MPa (the lowest stress examined) was approximately equal to that reported in the literature (≈6.0%), based on traditional "stress-free" sorption experiments.

The other materials examined exhibited a similar pattern.as is seen in Figures 3.20 and 3.21 for PC and PPTA samples. In this case samples with a prior exposure to moisture at the initial stress were first dried (AB). This was followed by sorption (BC) at the initial stress and then subsequent stages at progressively lower stresses (CD, DE; EF in case of PPTA). In these cases too, the equilibrium sorption at the lowest applied stress approached the stress-free values reported in the literature (and independently determined during this investigation). Although the samples were at equilibrium at the end of the first sorption (at C), their solubilities shifted to different equilibrium values (at D, E and F respectively). The series of equilibrium states resulted from reductions in the sample tension after each equilibrium state. The environmental humidity remained constant throughout.

Alternatively, when stresses were increased sequentially, the material passed through progressively higher values of equilibrium moisture; though the boundary condition of ≈100% relative humidity remained constant throughout. This was seen for Nylon 6,12 and Nylon 6,6 in Figures 3.22 and 3.23. Figures 3.24 to 3.26 refer to PI, PC and PPTA, and show the stress dependence of equilibrium sorption over repeated cycles including one after heat treatment. They reveal a different stress-coupled sorption behavior for each polymer. The stress-solubility envelopes for PI curved concave upwards while for PC they were concave downward. Remarkably, for the PPTA fibers the equilibrium sorption appeared to be a linear function of the applied stress,

although the data covered a smaller range of stresses (These results will be discussed in greater detail in Chapter 4). Also, for Nylons, the final stage was actually accompanied by a decrease in solubility. It is concluded that the considerable elongation of these relatively low modulus materials, and the associated increase in internal orientation suppressed the stress enhancement of sorption in the final stage. The ability of sufficiently large strains to dominate the coupling highlights the significance of strain dependent sorption in highly deformed flexible materials. This aspect will in fact be addressed in the next section.

The influence of the applied stress on the diffusion mechanism was studied by examining the kinetics of sorption for samples at constant stress. The fractional weight gain in a PI sample was plotted against the square-root of exposure time (Figure 3.27) and the diffusion coefficient as a function of applied stress in Figure 3.28. It is shown by the data of Figure 3.19 and 3.29 that sample length changed concurrently with moisture gain. Only the swelling strain is shown here, with the initial value equal to zero at the applied stress. The swelling coefficient was estimated from the *net* swelling strain for each step, plotted against the corresponding moisture gain at any applied stress, as presented in Figure 3.30 for stress at 50 MPa. The effect of applied stress on the swelling coefficients is demonstrated by the data of Figure 3.31. Similar results were also observed for PC and PPTA. The swelling coefficient was seen to be a linear function of the applied stress (as seen in Figure 3.18 and demonstrated by Treloar 1952, 1953) suggesting that a simple proportionality constant may suffice to describe stress enhancement within the linear elastic limit.

3.2.3 Results: Constant Strain Experiments

In many industrial applications, polymers are used in dimensionally constrained configurations. One example of this is the use of polymers in coatings, paints and laminates such as circuit boards, where the material adheres to a rigid substrate. Alternatively, it may be enclosed in confined spaces such as packing materials, seals and inside composite materials. The literature review of Chapter 1 referred to the study of transport in materials in varying degrees of deformation. It was also pointed out that the direction in which the applied stress influences transport depended on the degree of deformation (Peterlin 1983; Rosen 1960; Smith and Adam 1981). Diffusion coefficients were seen to increase for small deformations, experience a maxima, and ultimately decrease as the strain exceeded the linear elastic limit. Also, for highly deformed low modulus materials it was observed that the moisture gain profiles were atypical in that they demonstrated multi-stage behavior.

Clearly, it is useful to study the effect of applied strain as an independent variable for describing the transport characteristics of low modulus materials. The state of stress is sufficient to determine the change in transport properties only as long as the applied stress remains within the linear elastic limit and the material shows little mechanical hysteresis. The strain may play a relatively significant role when the deformations resulting from the applied stress induce internal changes in structure or orientation. Constant strain experiments, as described earlier, were conducted to generate sorption isotherms (solubility versus relative humidity at constant strain, for a

range of strains) in an attempt to study the changes in the mode of transport as a function of the applied strain.

Typically, a dry sample was conditioned as described in Section 2.4.1, and stretched in the diffusion chamber in a stream of dry nitrogen. The experiments at constant strain were analogous to the sequential constant tension experiments in the determination of the stress-solubility envelope. When the sample reached saturation at the lowest strain (e.g. 1.4%) it was further deformed to the next level of strain (1.7%). At every stage, on reaching apparent equilibrium the axial strain was changed to a new value as the sample traversed from one equilibrium state to another. Thus, as in the case of constant tension experiments, these constant elongation experiments were used to generate the strain-solubility envelope. In Figure 3.32 the weight gain is plotted as a function of the exposure time and it is seen that the solubility increased with applied tension, for strains as high as 2.5%. For higher strains, the solubility subsequently decreased. As a result of the initial increase in stress with each transition to a higher strain, local maxima were seen during individual stages. There was an initial increase in the moisture gain, followed by a decrease with stress relaxation. In this Figure 3.33, the various stages of applied strain are shown with the corresponding stress versus time profiles.

The traditional method for the classification of the diffusion mechanism during sorption experiments (Crank 1968) is based on examining plots of the fractional weight gain versus the square root of exposure time (such as in Figure 3.34). In the case of Fickian diffusion the resulting curve is usually a straight line at short times whereas, proportionality between the fractional weight gain and the exposure time is considered symptomatic of

Case II diffusion. In the case of PBI as well as in the case of the Nylon 6,6 (Figures 3.34 and 3.35) the curves were not simple straight lines in contrast to the constant tension experiments where Fickian diffusion was the norm. In the constant strain experiments, the stress state of the material changed even though the sample strain was kept constant. Thus, it is felt that the anomaly referred to above, is indicative of the relative significance of the stress state as a critical parameter in transport processes under mechanical constraint. The changing state of stress within the material altered the diffusion behavior with time although the sample strain remained constant. This observation highlights the issue of the relative influence of the stress or the strain experienced by a polymer matrix. It demonstrates that in the case of large deformations close to the linear elastic limit of the polymer, the sample strain may play the dominant role in the coupling interaction.

Most studies of the transport mechanism examine plots of the solubility versus the relative humidity to better understand the mode of transport. This was seen in Chapter 1 with regard to the analyses of Barkas (1942a, b) and presented in Figure 1.1. The shape of the isotherm provides clues to the mechanisms involved. Thus Yang et al. (1985) inferred the formation of clusters of penetrating molecules by examining such isotherms. The dominant solubility versus partial pressure relationship can also be inferred from the sorption isotherm, such as the validity of Henry's law or dual sorption mode of transport (Crank 1975; Chern et al. 1983; Hopfenberg and Stannett 1973). The isotherms of Figure 3.37 are therefore presented for qualitative comparison with such "standard" isotherms. They appear to be indicative of the the dual sorption mode which is particularly common for

sorption in polymers and is discussed extensively by Chern et al. (1983) and Hopfenberg and Stannett (1973).

The effect of the applied strain on moisture sorption is clear from the strain-solubility envelopes of Figure 3.36. The solubility increased with the applied elongation in every case but dropped when the strain was close to 2.5%. This was observed for all relative humidities to which the sample was exposed. It is well known that the deformation of a polymer may result in internal rearrangements of chains or chain conformations and subsequently affect its properties (Morton and Hearle 1975). In view of the sorption and diffusion mechanisms referred to above, this clearly alters the solubility in much the same way as described by Peterlin (1983) for diffusion coefficients. The stress-strain behavior observed in PBI fibers demonstrated that the linear elastic region was exceeded at a strain of about 2-3%. This suggests that the final decrease in solubility that we observed was due to the internal changes induced by the large level of deformation.

The sorption isotherms observed for PBI (Figure 3.37) suggest that the mode of sorption indeed closely approximated the dual sorption mechanism. Typically, this is known to result from a superposition of a Henry's law behavior with a Langmuir sorption, yielding the characteristic isotherm observed. It may be noted that the isotherms showed higher levels of sorption at greater strains but continued to retain their overall shape. However, the shape of the isotherm at 2.5% strain, did not follow this pattern, and instead intersected the the low strain isotherms. Clearly, the "excessive" strain applied altered the relative contributions of the two transport modes and resulted in the skewed profile that was observed.

3.3 Conclusions

The following section discusses the main conclusions of sorption and drying experiments conducted with samples held under constant tension. The main results of both sequential and direct experiments are summarized.

3.3.1 Constant Tension Experiments

The significance of the stress coupled sorption of moisture has been established in the materials studied in this work. It has also been also demonstrated that there was coupling between equilibrium sorption and the applied tension in the materials selected. The diffusion and swelling coefficients also increased with the sample tension. Furthermore, the equilibrium sorption was shown to depend on the applied stress. There is no doubt that local stresses may arise during diffusion, because of the concentration gradients in the sample, and may in turn affect transport in those cases where the diffusion and stress are coupled. However, these transient local perturbations gradually vanish as equilibrium is approached, while only the external stress continues to act. Since the local stresses and gradients vanish at equilibrium, the thermodynamic analyses proposed by Barkas (1940), Treloar (1952) and Sternstein (1972) are in fact among the best models of the equilibrium condition. The results of their work qualitatively corroborate some of the experimental observations made during this study.

Treloar (1952) showed that for a material with a positive moisture swelling coefficient, the solubility increased with sample tension. Thus, if the moisture sorption at equilibrium were considered to be proportional to the relative humidity at the boundary (Henry's Law type of dependence), then the swelling strain would increase in proportion to the moisture gain. This was experimentally observed for all the materials considered. Also, the equilibrium moisture content typically increased with tension, consistent with Treloar's deductions. However, Treloar's approach was applicable as long as stresses did not result in large deformations. Also inherent in Treloar's analysis was the limit to the validity of Henry's Law at higher concentrations.

The analysis developed by Sternstein (1972) based on considering the work of deformation and energy of mixing, provides insight into the stress-coupling mechanism. Sternstein's analysis was less restrictive than Treloar's analysis and also enables a qualitative interpretation of the case of stress on a material in swelling equilibrium. It can be modified to suit a wider range of materials depending on the assumptions for heat of mixing and the work of deformation that are employed. It was shown by Sternstein that for a rubber-like material exposed to a solvent, the application of tensile stress results in an increase in the concentration of the solvent within the material. A rationale was also provided for the enhancement of equilibrium sorption with applied stress. The theory can be suitably modified for more complex materials by employing the appropriate work function and free energy of mixing relationship. The analysis may also be extended to glassy polymers by

relaxing the condition of incompressibility. The high strain region of coupled sorption may be addressed by also including the contribution of deformation energy.

In conclusion, the analyses referred to above provide the basis for future comparison with experimentally observed results. The analyses discussed are versatile enough to address a variety of polymers as well as experimental conditions. Also, recalling the anomalies observed in oriented materials like PC (overshoots in the sorption-time profile), it becomes clear that the independent effect of strain on diffusion in polymers cannot be ignored. Strain effects are particularly important for low modulus materials at applied stresses where the strains are large enough to cause internal changes in the material. The next section deals with the conclusions resulting from constant-strain experiments conducted with a view to evaluating the significance of strain-coupling in moisture transport.

3.3.2 Constant Strain Experiments

It was seen that the coupling between the stress and sorption resulted in transport characteristics that were distinct from the stress-free case. The applied stress was the primary independent variable in this relationship. In the constant tension experiments, the solubility and diffusion coefficients were seen to vary directly with the external stress, at lower tensions. Incontrast, during constant strain experiments where stress varied

continuously, the diffusion characteristics as well as sorption profiles were multi-staged. These experiments also demonstrated the critical role of the applied strain in determining the limits within which the mode of interaction or coupling remains unchanged. Thus, the sorption isotherm underwent a qualitative change when the magnitude of the applied strain was of the same order or exceeded the linear elastic limit.

The effect of the instantaneous stress or strain applied to polymer samples was examined in this chapter. In particular, the nature of the influence of the applied stress on the equilibrium solubility, diffusion coefficient and the swelling coefficient was studied. A further dimension to the interaction is contributed by the time dependent processes that prevail in polymers. Since most engineering applications of polymers extend over protracted periods of time, their long term behavior is of great interest. Hence, the issue of history dependence of stress-coupled transport, and in particular the influence of mechanical conditions, is addressed in the following chapter.

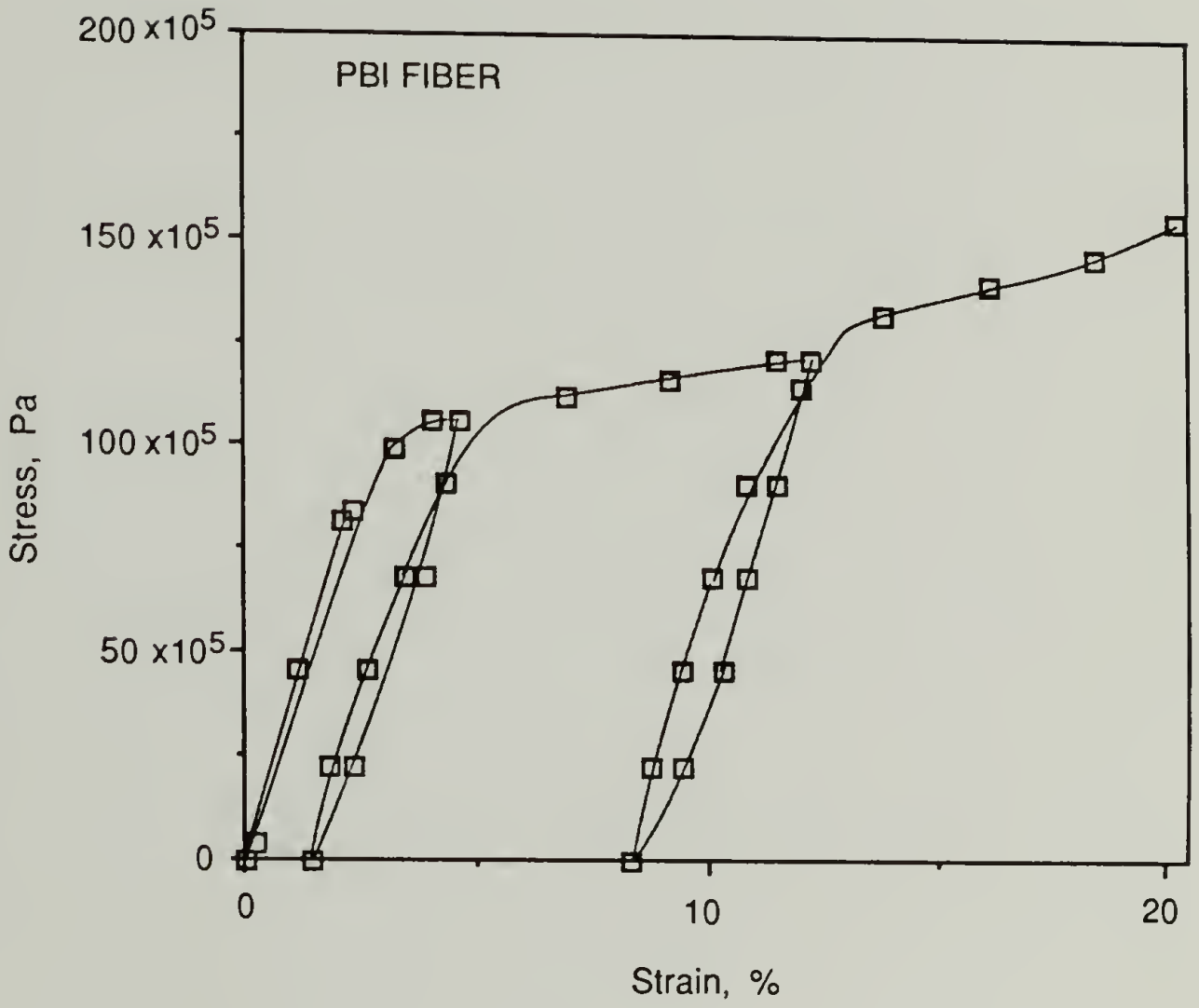

Figure 3.1 The stress versus strain curve for a PBI fiber under repeated loading and unloading demonstrating the regions over which reversible and irreversible changes occurred. In the initial elastic region, on the removal of stress the strain followed the same initial curve. At higher levels of stress, a permanent shift occurred and the stress-strain curve was no longer linear.

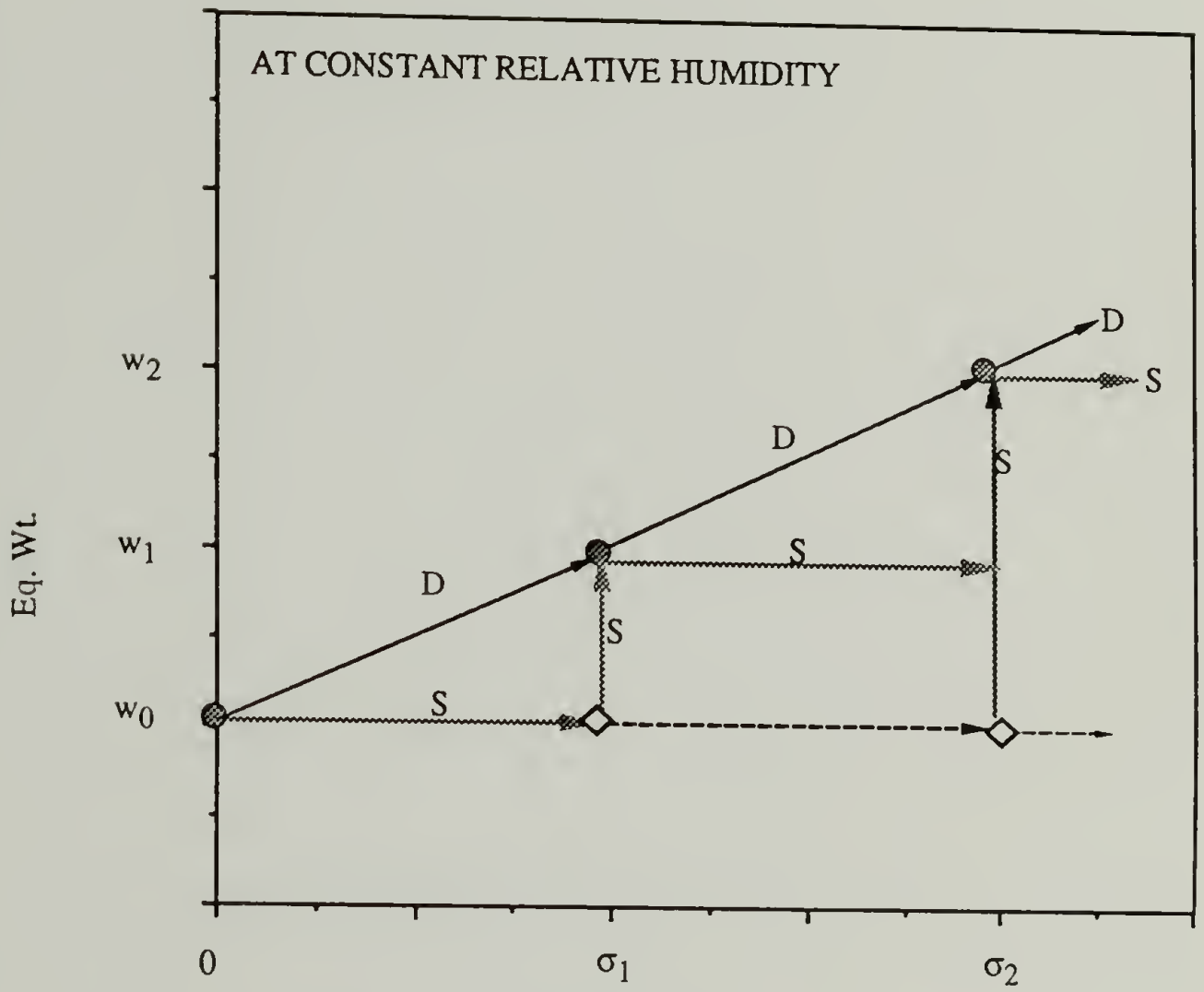

Figure 3.2 Schematic representation of the direct and sequential constant tension(strain) experiments. The applied stress and equilibrium weight gain values are denoted as σ_i's and w_i's respectively. For constant strain experiments the σ_i's are replaced by ε_i's. The diagonal line passing through σ_1, w_1 and σ_2, w_2 etc. is referred to as the stress-solubility envelope.

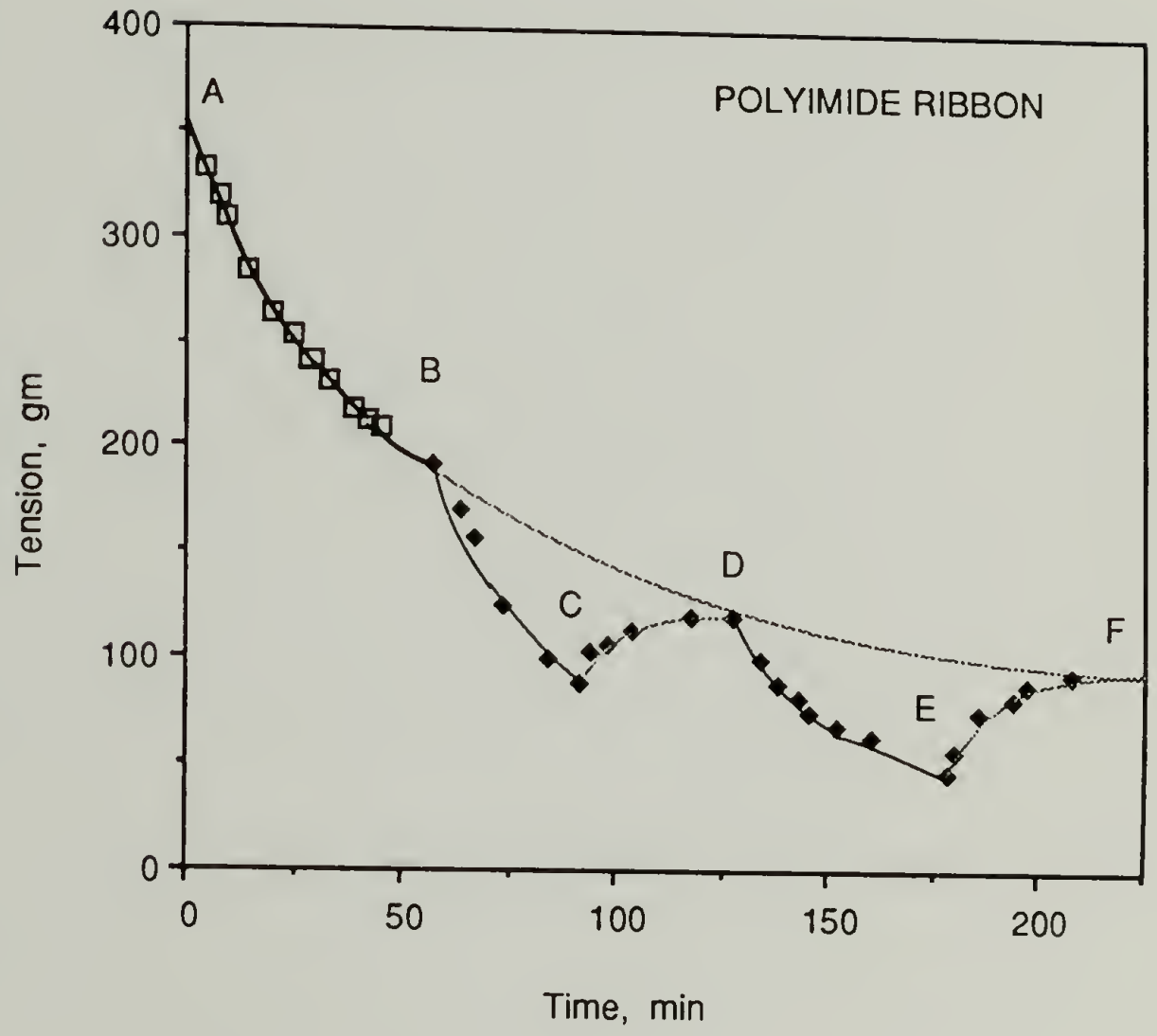

AB - Initial relaxation
BC - Sorption
CD - Desorption
EF - Second sorption

Figure 3.3 Plot of the sample tension versus time during moisture diffusion in a polyimide ribbon with its length held constant. The trend in sample tension is shown during initial stress relaxation followed by two cycles of sorption and drying. The fluctuations are seen to be superimposed over the usual stress relaxation curve.

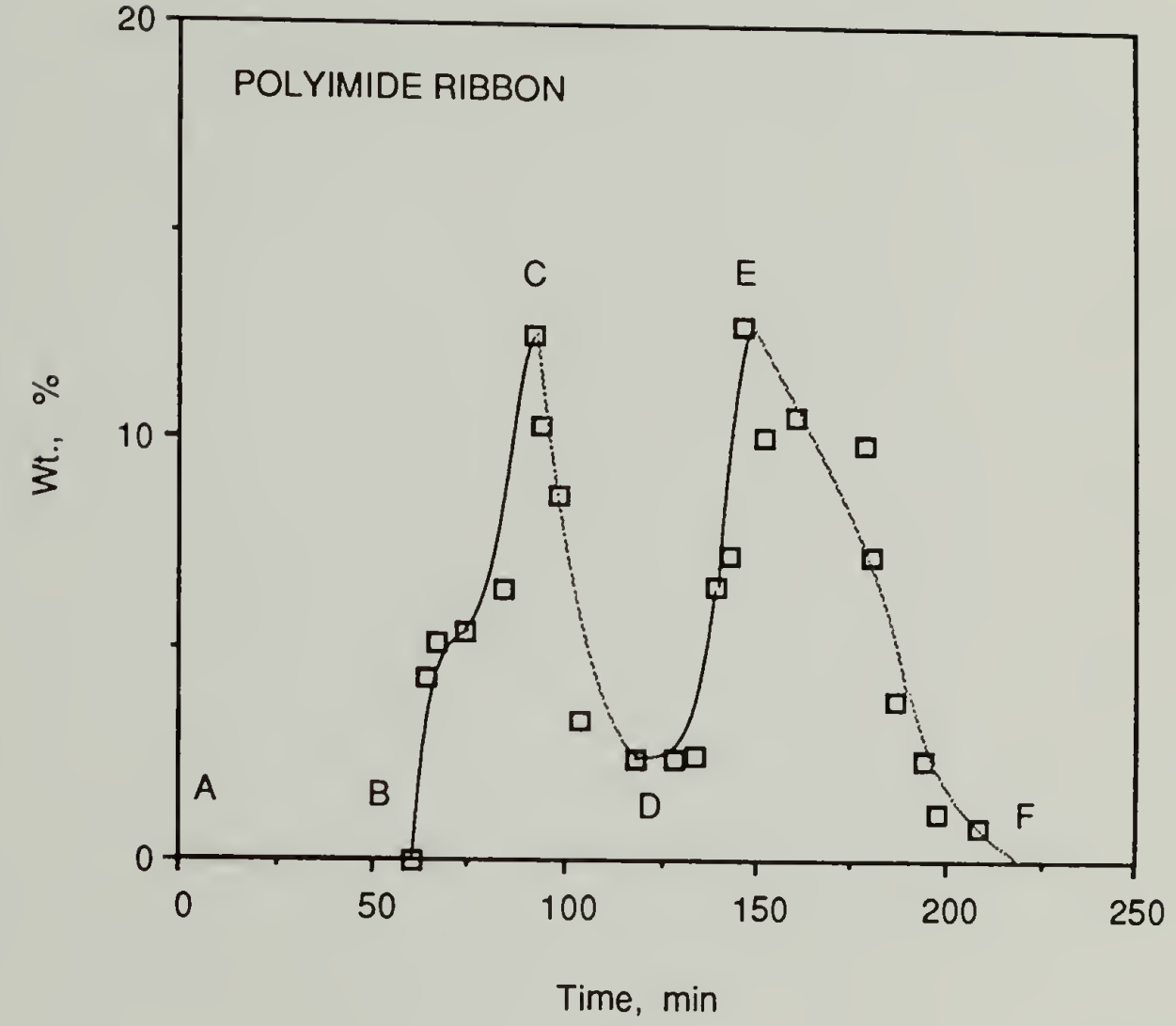

Figure 3.4 Plot of the moisture content versus exposure time in a polyimide ribbon under constant elongation. The sample was exposed to repeated sorption and drying after an initial holding period.

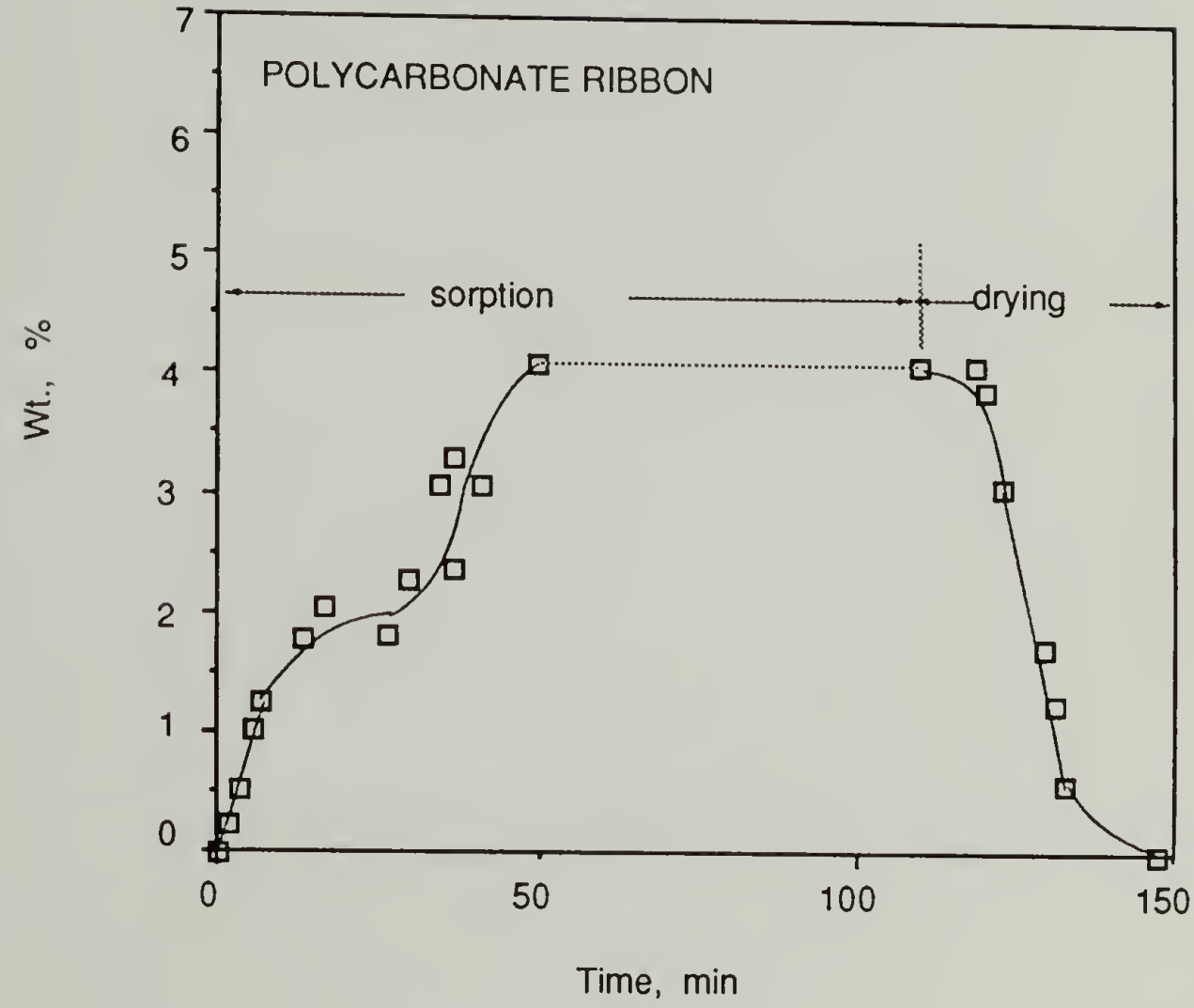

Figure 3.5 The moisture content versus exposure time in a PC ribbon under constant tension while it was exposed to a cycle of sorption and drying.

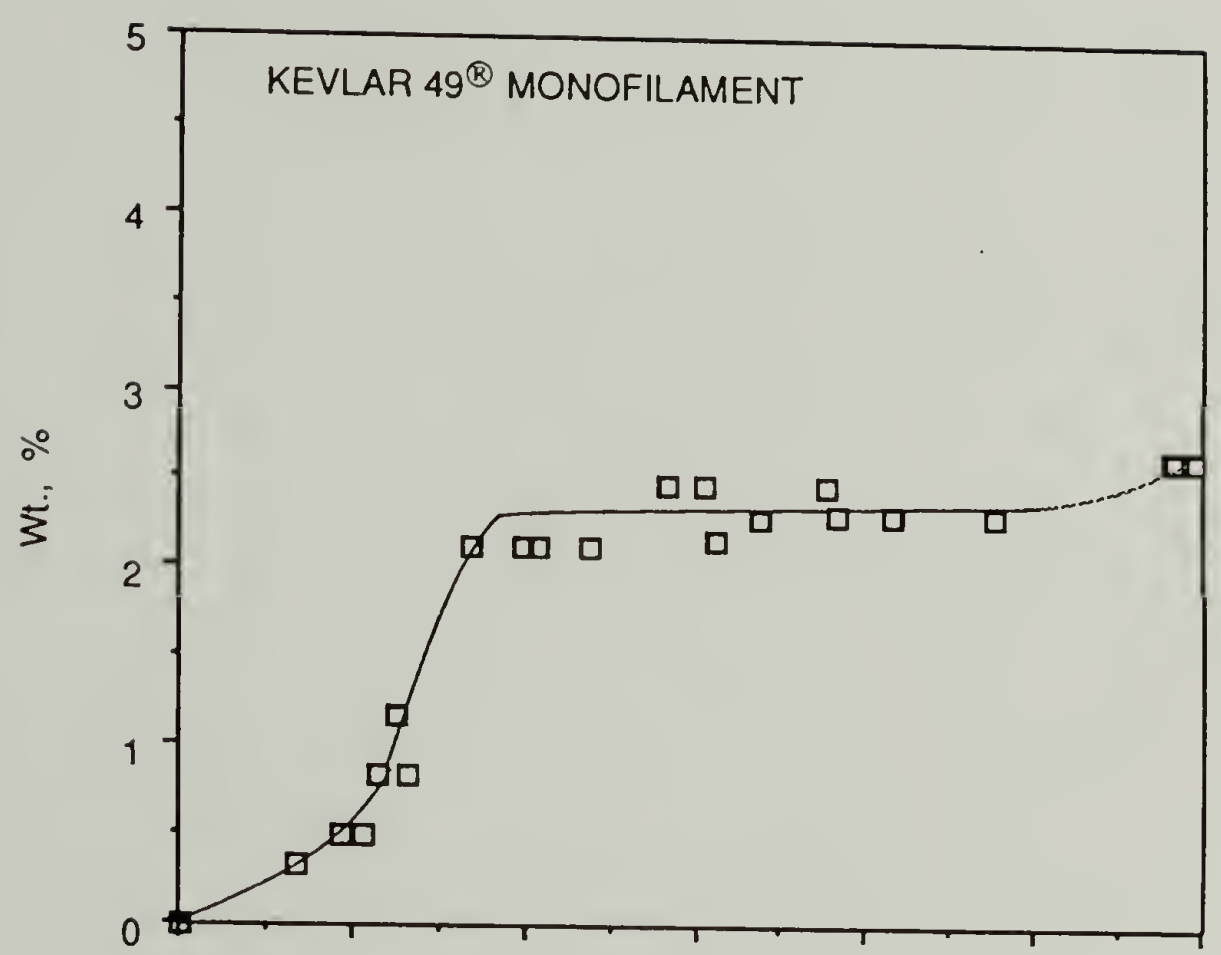

Figure 3.6 Percent moisture gain versus exposure time in a dried PPTA fiber at constant elongation.

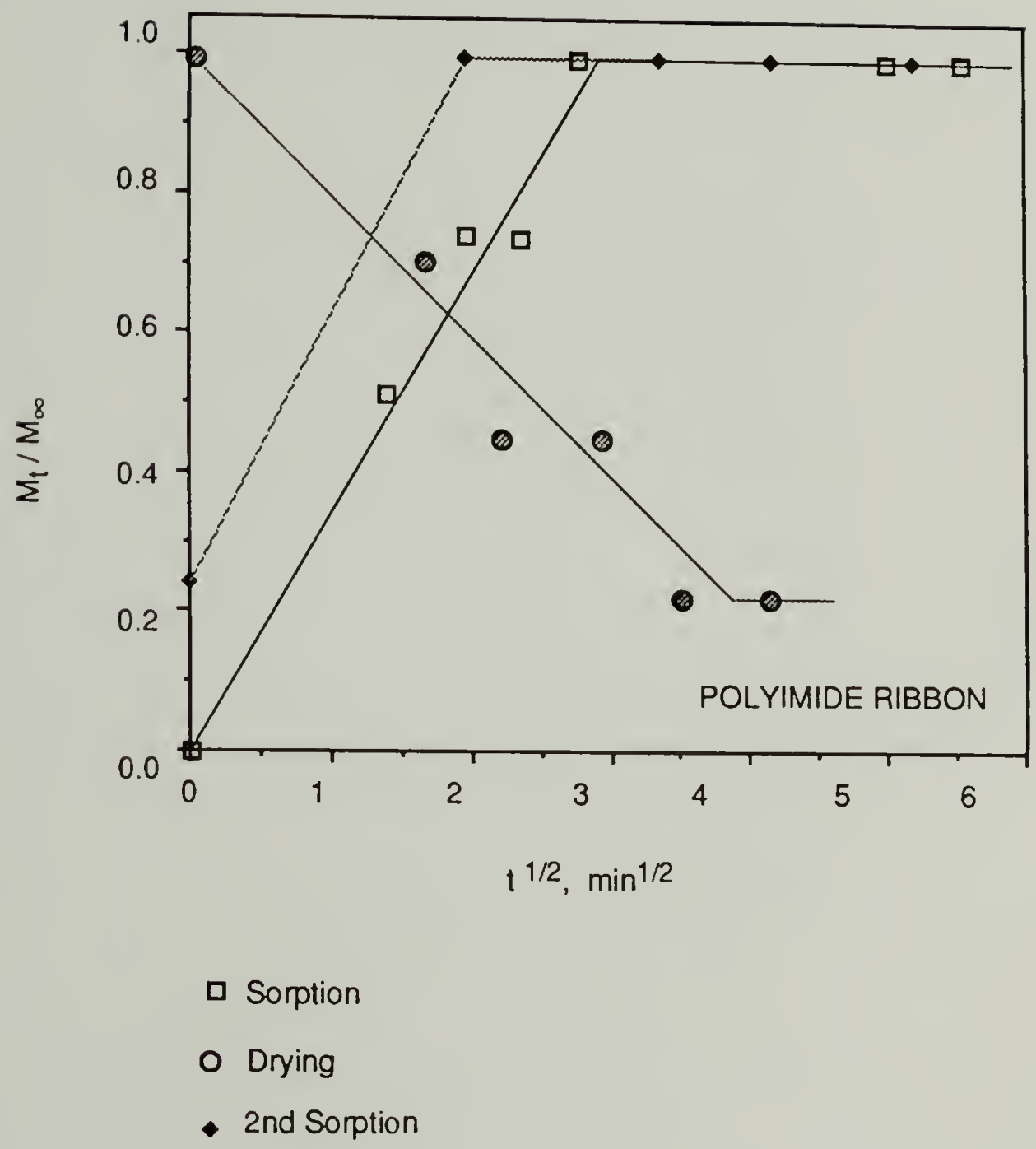

Figure 3.7 Fractional weight gain versus the square root of exposure time in a PI ribbon under constant axial applied stress (30 MPa). A dried sample was subject to a cycle of: sorption - desorption - second sorption. The transport mechanism was Fickian.

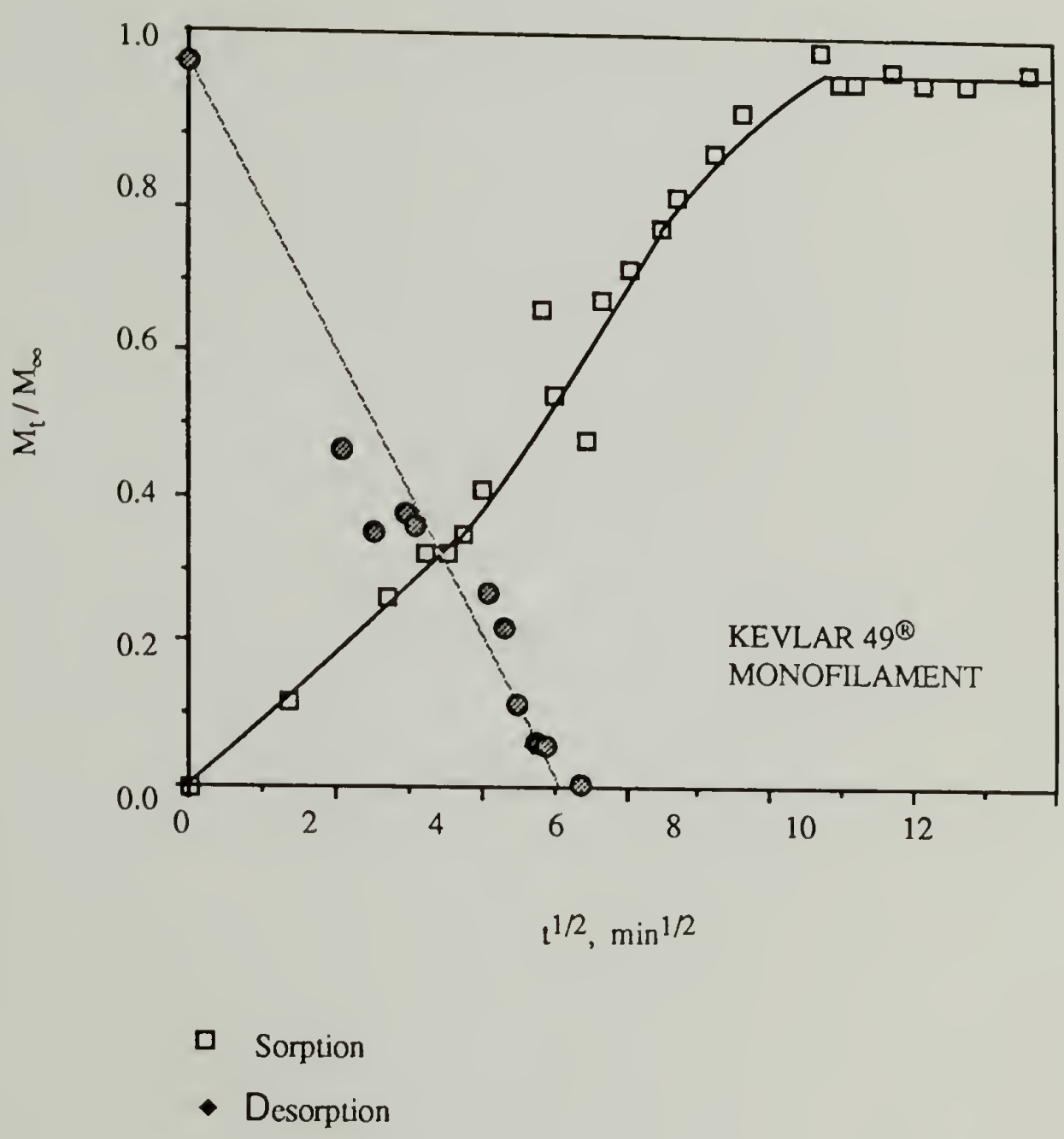

Figure 3.8 Fractional weight gain versus the square root of the exposure time in a PPTA filament under constant axial applied stress (1.4 GPA). A dried sample underwent: sorption - desorption.

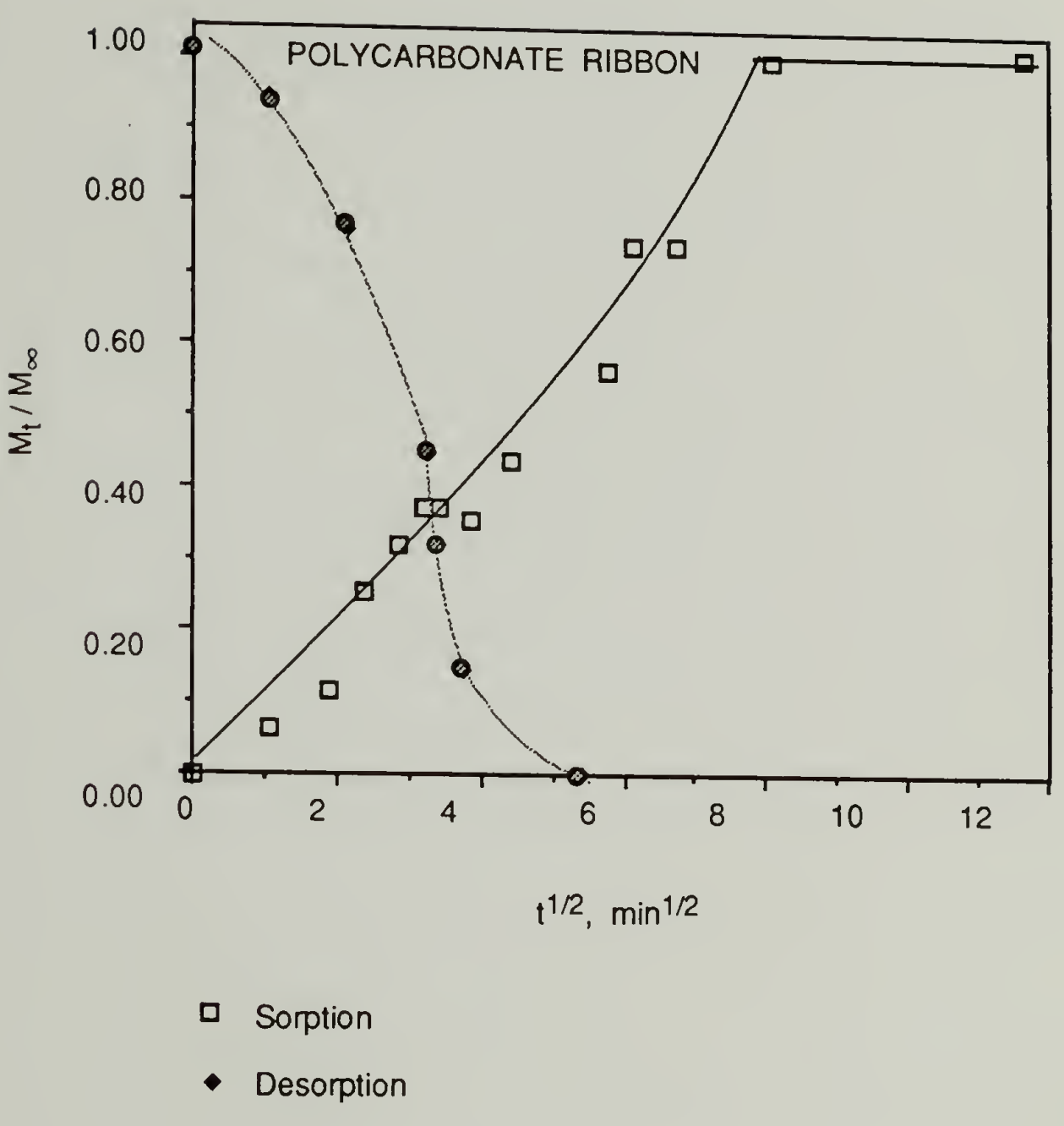

Figure 3.9 Fractional weight gain versus the square root of exposure time in a PC ribbon under constant axial applied stress (17.5 MPa). A dried sample was subject to: sorption - desorption. The sorption appeared to be multi-staged with a linear initial region while the desorption was non-linear throughout.

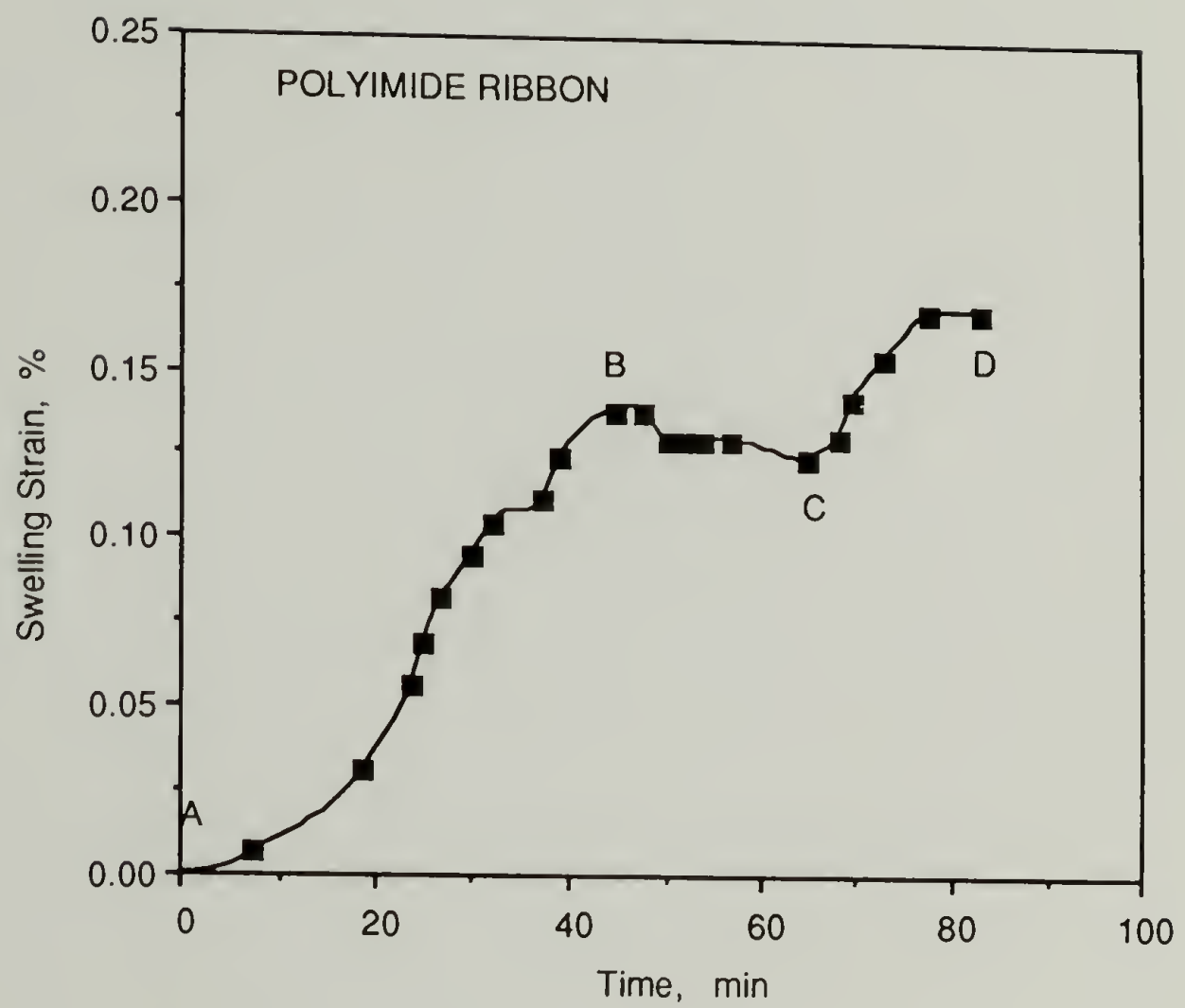

Figure 3.10 Axial swelling strain (%) versus the exposure time in a PI ribbon under constant axial applied stress (20 MPa). A dry sample was exposed to a cycle of sorption (AB); drying (BC); and a second sorption (CD).

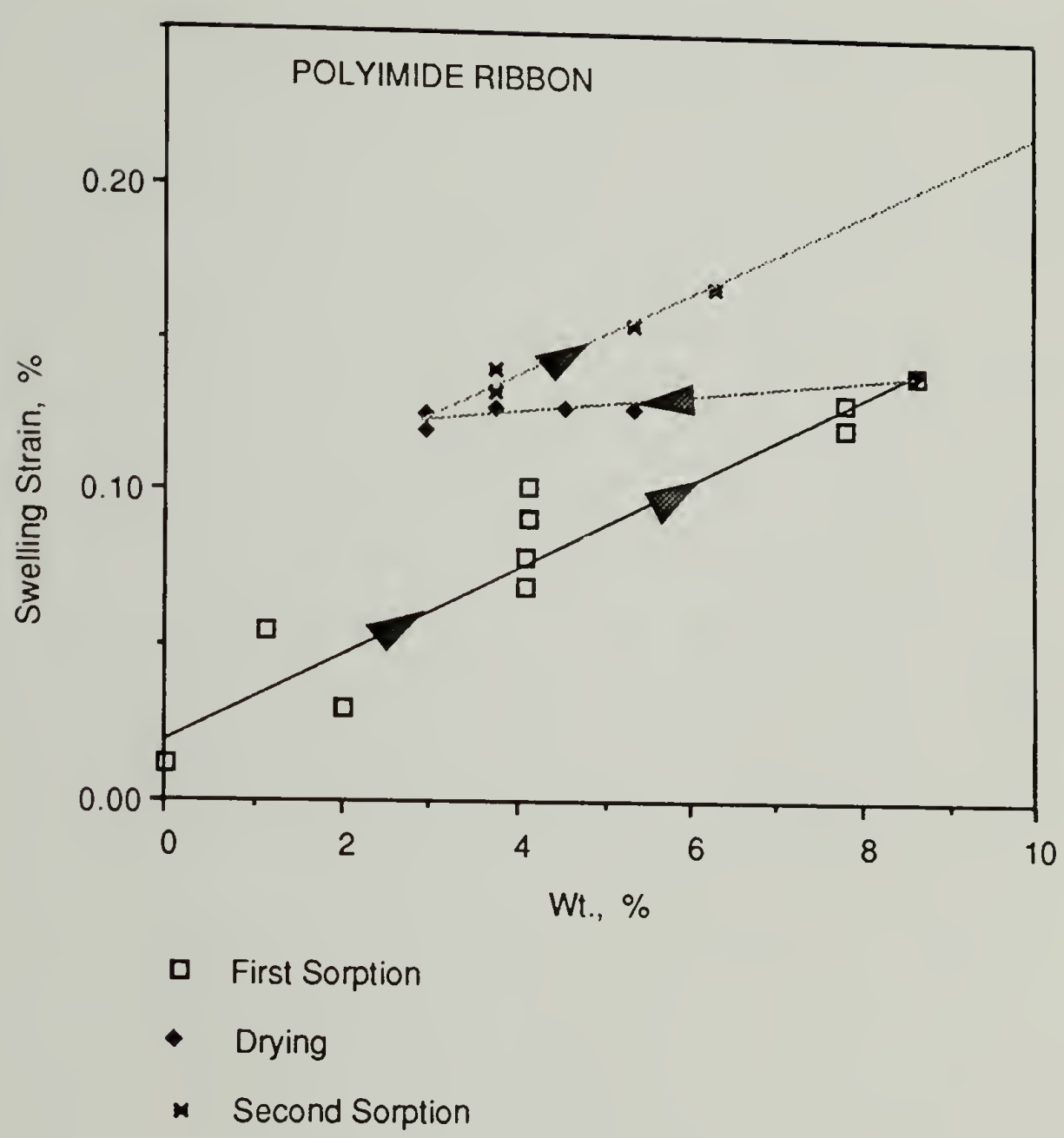

Figure 3.11 Axial swelling strain (%) versus the percent moisture gain in a PI ribbon under constant axial applied stress (20 MPa). A dry sample is subject to: first sorption - drying - second sorption.

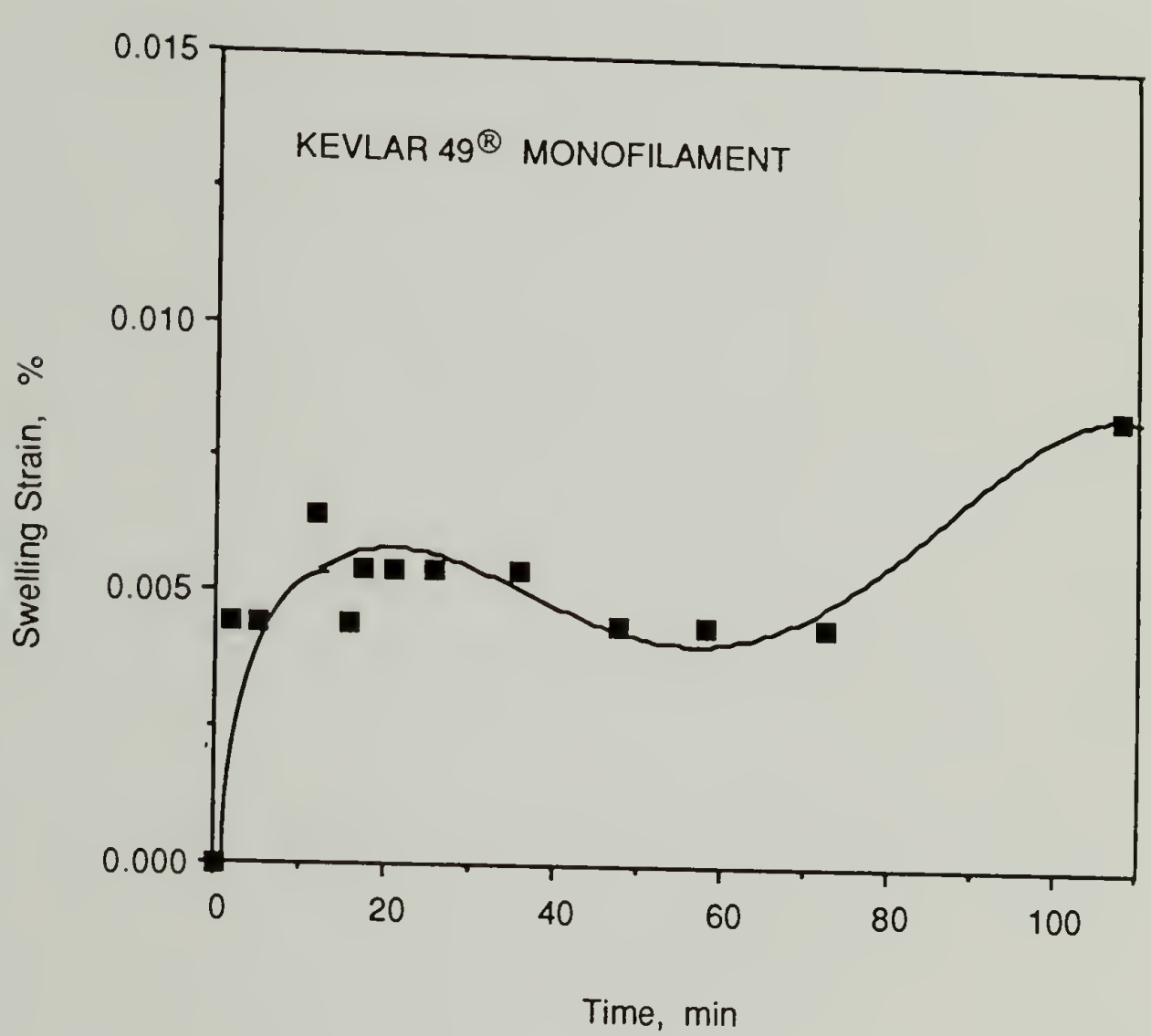

Figure 3.12 Axial swelling strain (%) plotted against the exposure time for a PPTA filament under constant axial applied stress (1.4 GPa). A dry sample was exposed to moisture until the equilibrium weight gain was attained. Sample length continued to increase beyond this due to the applied tension.

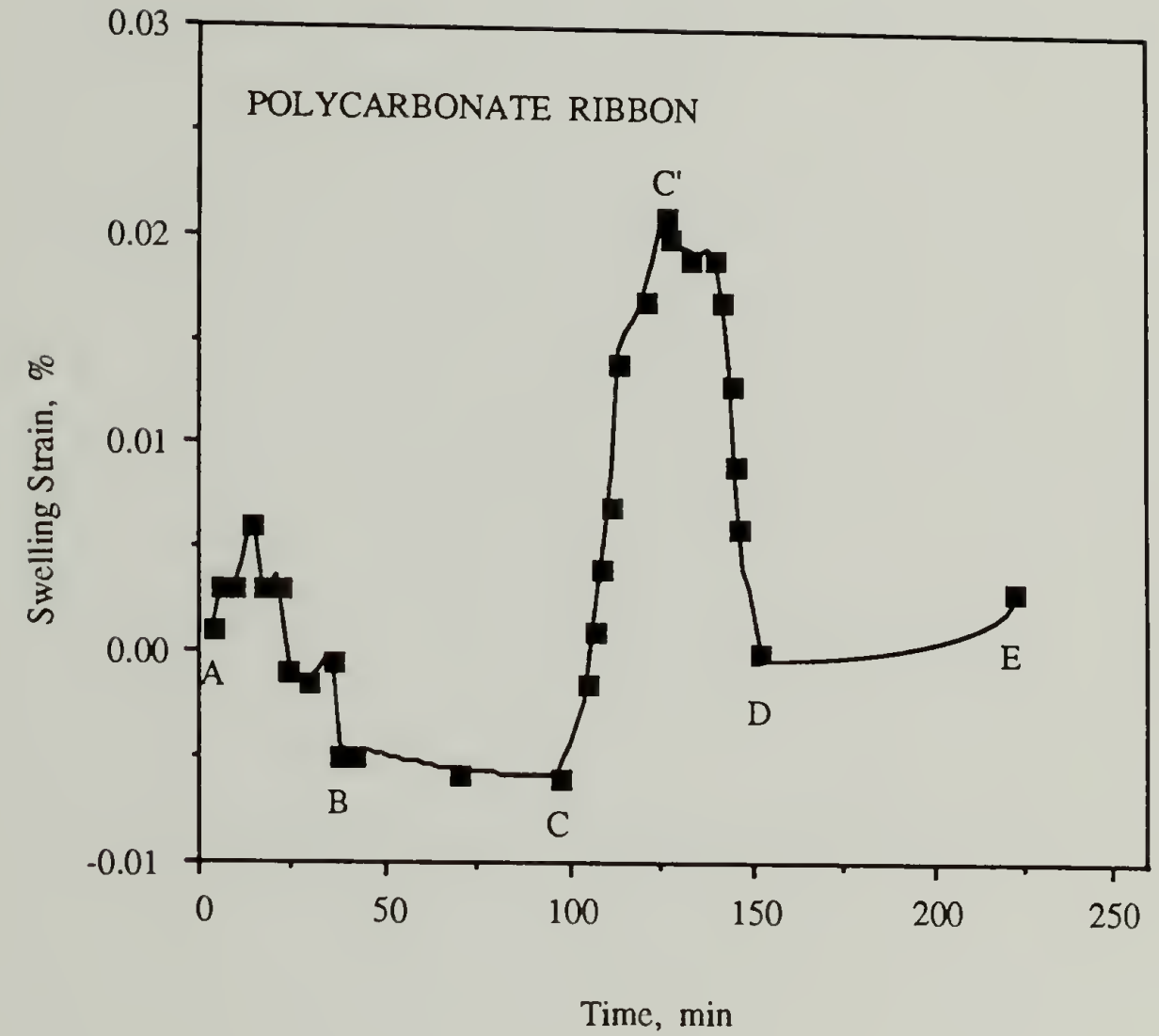

Figure 3.13 The axial swelling strain plotted against the exposure time in a PC ribbon under constant axial applied stress (33 MPa). An as-received sample of PC was exposed to desorption (AB), sorption (BC), a second sorption (CD) and a second drying (DE). "Anomalous" shrinkage was observed during the phase C'D even as sorption by the sample continued through CD.

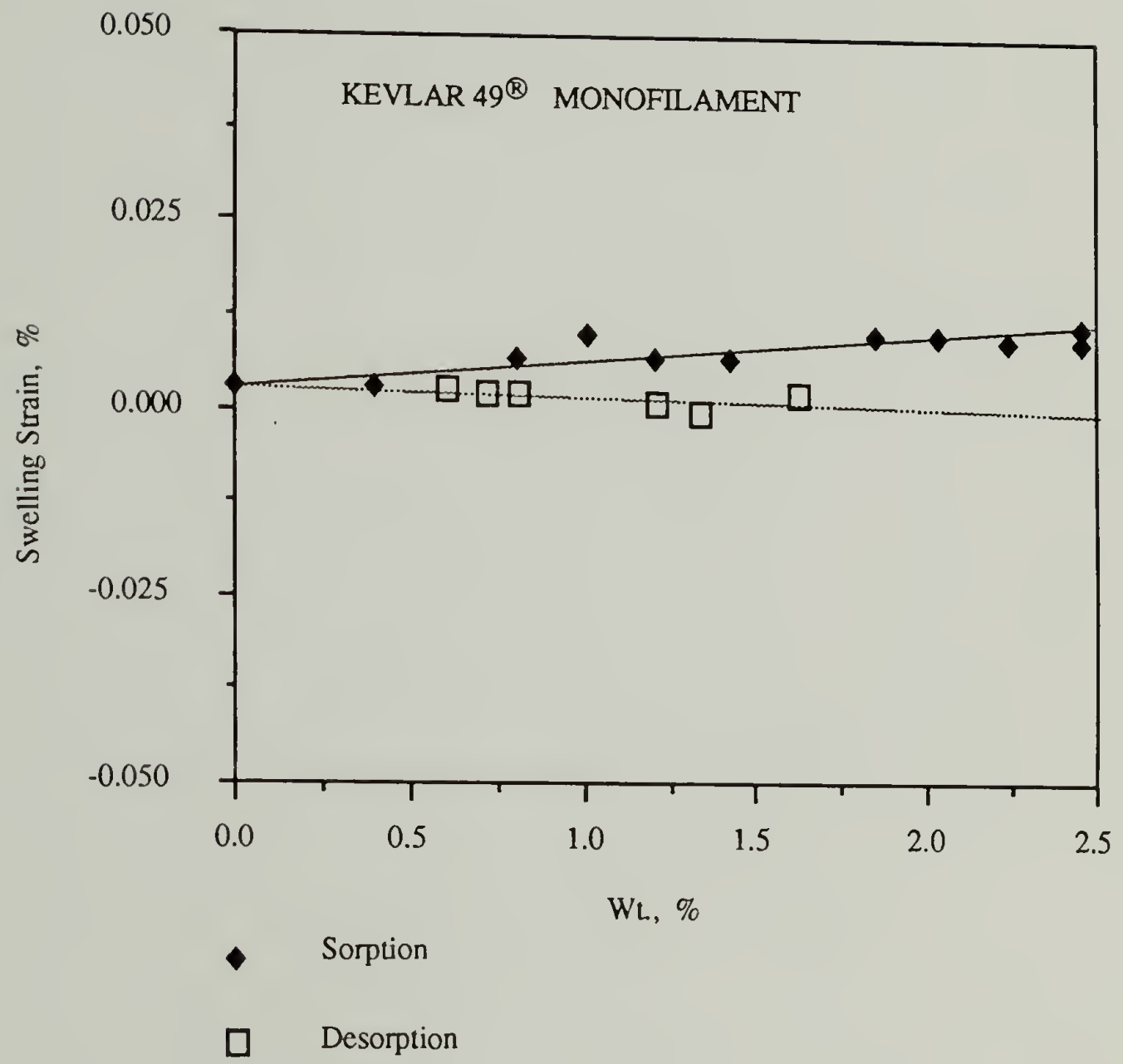

Figure 3.14 Axial swelling strain (%) versus the moisture gain (%) in a PPTA fiber under constant axial applied stress (1.2 GPa). A dry sample was subject to a sequence of sorption followed by desorption.

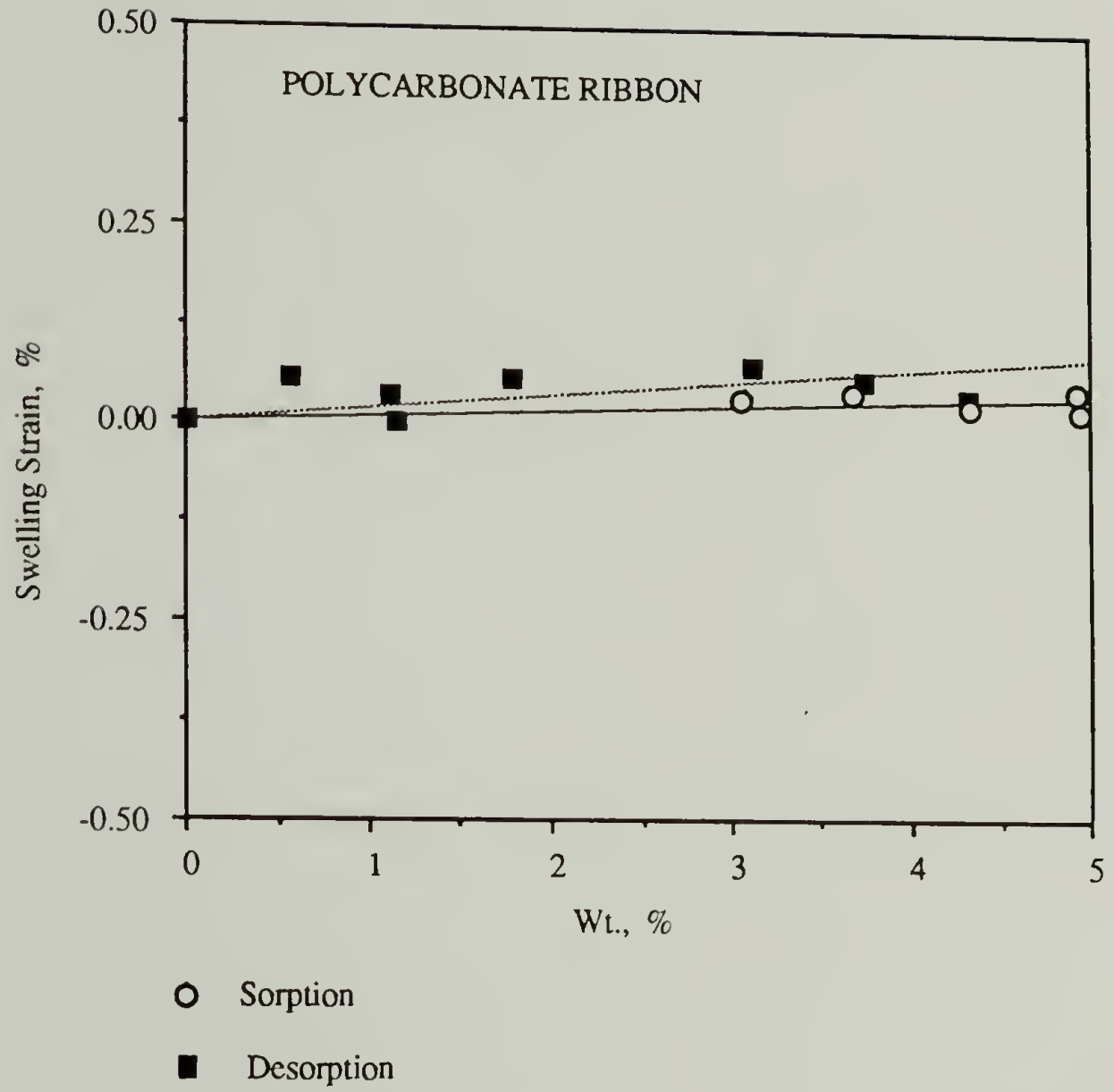

Figure 3.15 Axial swelling strain (%) versus the moisture gain (%) in a PC ribbon under constant axial applied stress (33 MPa). Data for one cycle of desorption and sorption experienced by an as-received sample are shown.

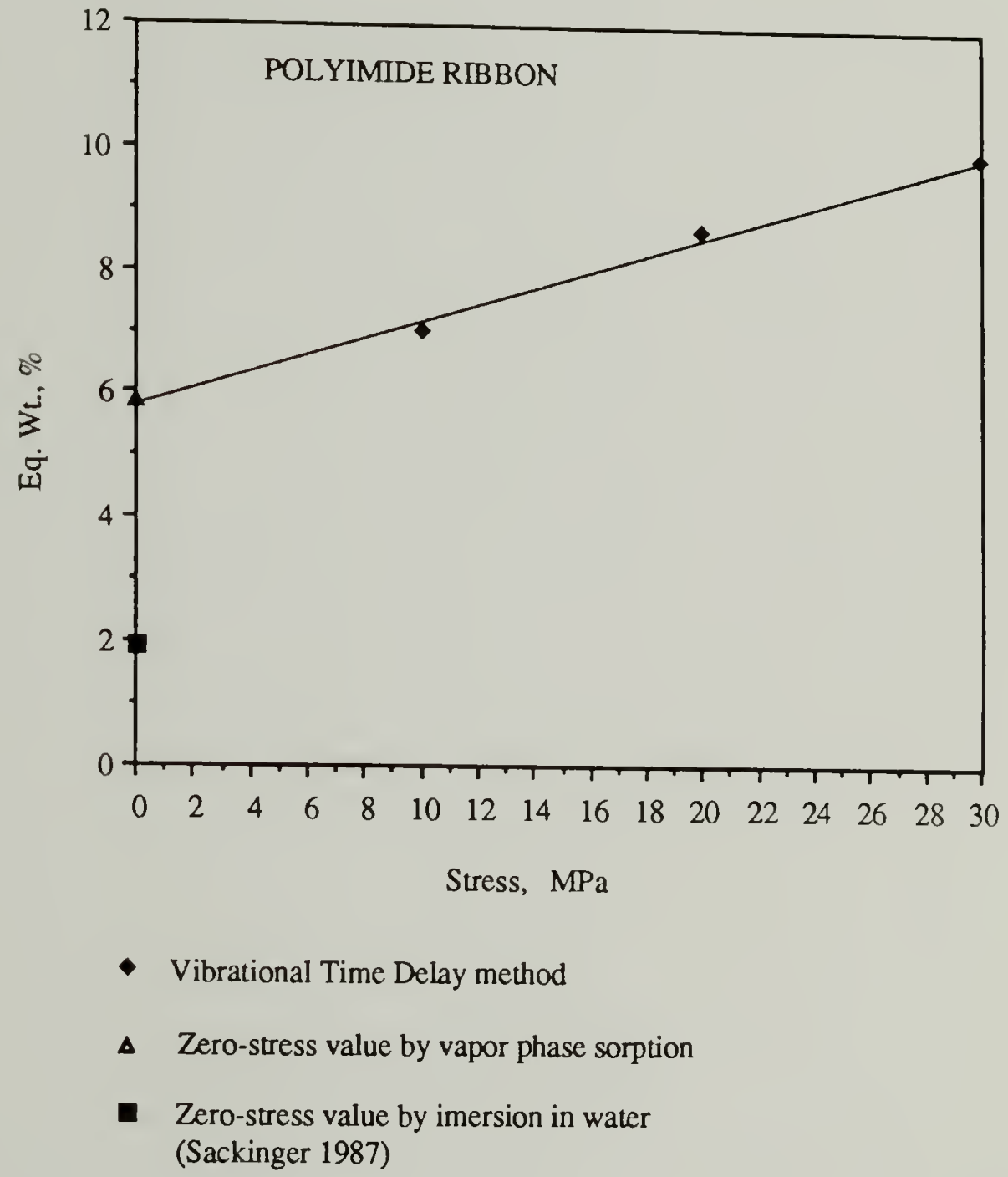

Figure 3.16 The equilibrium moisture solubility plotted as a function of the applied stress during direct moisture sorption in PI. Dry samples under constant applied stress were exposed to 100% relative humidity until equilibrium was attained. Independent zero stress values based on vapor and liquid phase sorption are also compared.

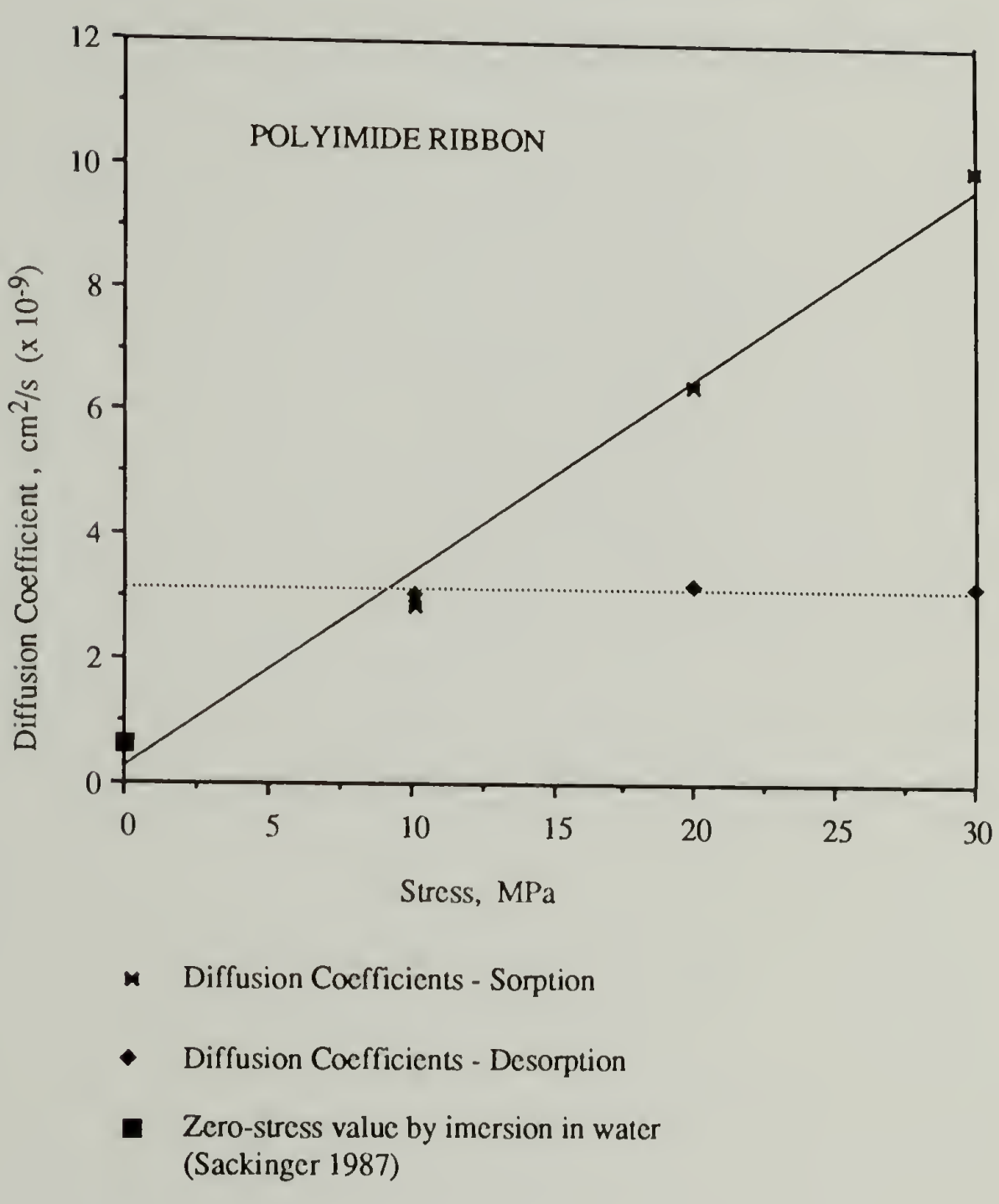

Figure 3.17 The diffusion coefficient versus the applied stress during direct sorption in individual samples of PI is shown. Dry samples under constant applied stress were exposed to 100% relative humidity until equilibrium was attained. Data for sorption and desorption are presented along with an independent liquid phase sorption result.

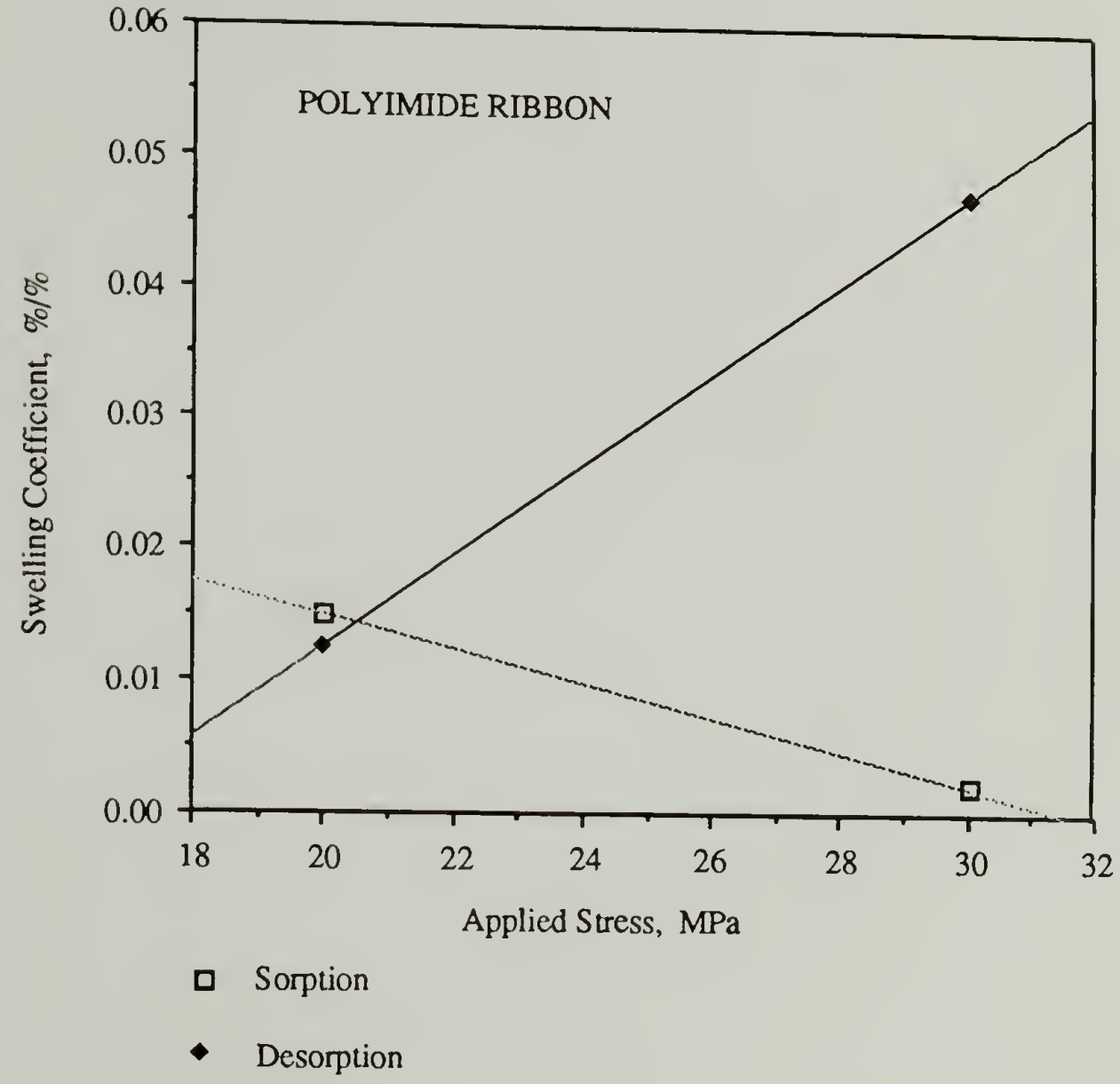

Figure 3.18 The axial swelling coefficient plotted as a function of the applied stress during direct sorption in individual samples of PI. Samples under constant applied stress were exposed to a sorption and a desorption respectively.

(a)

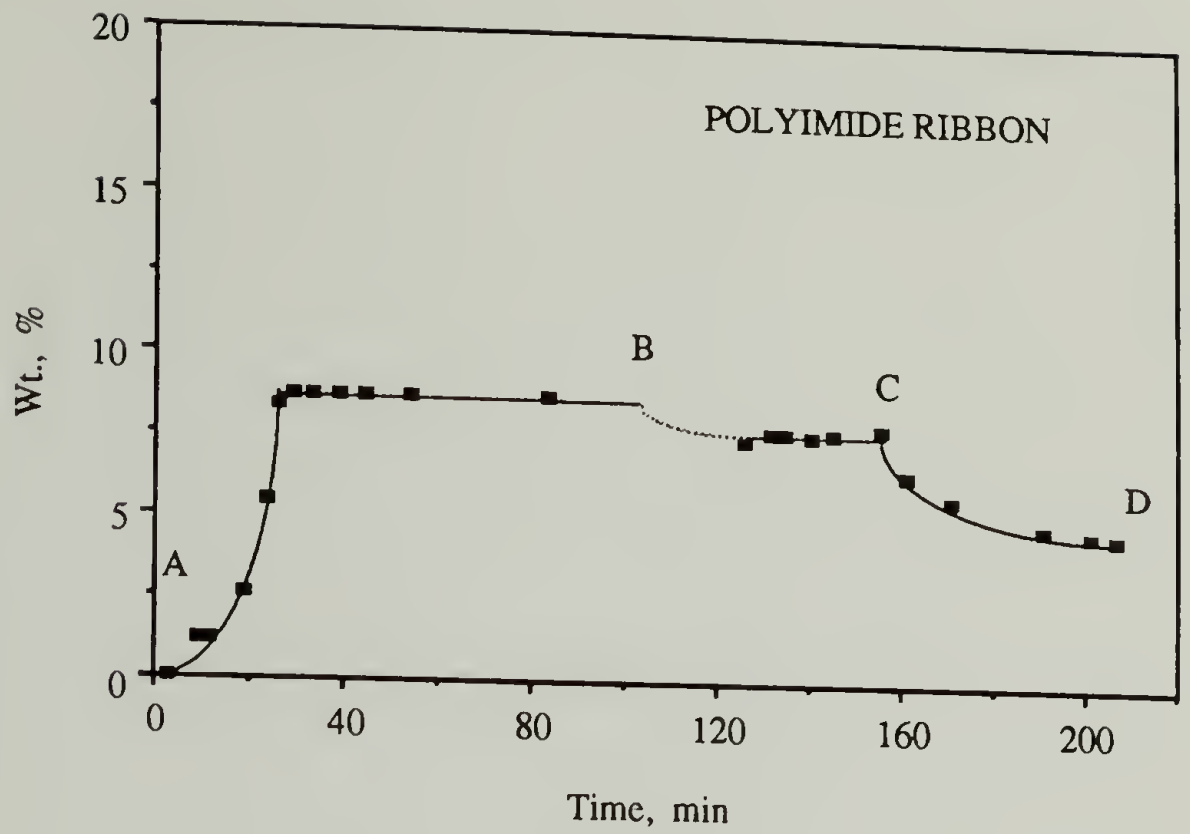

(b)

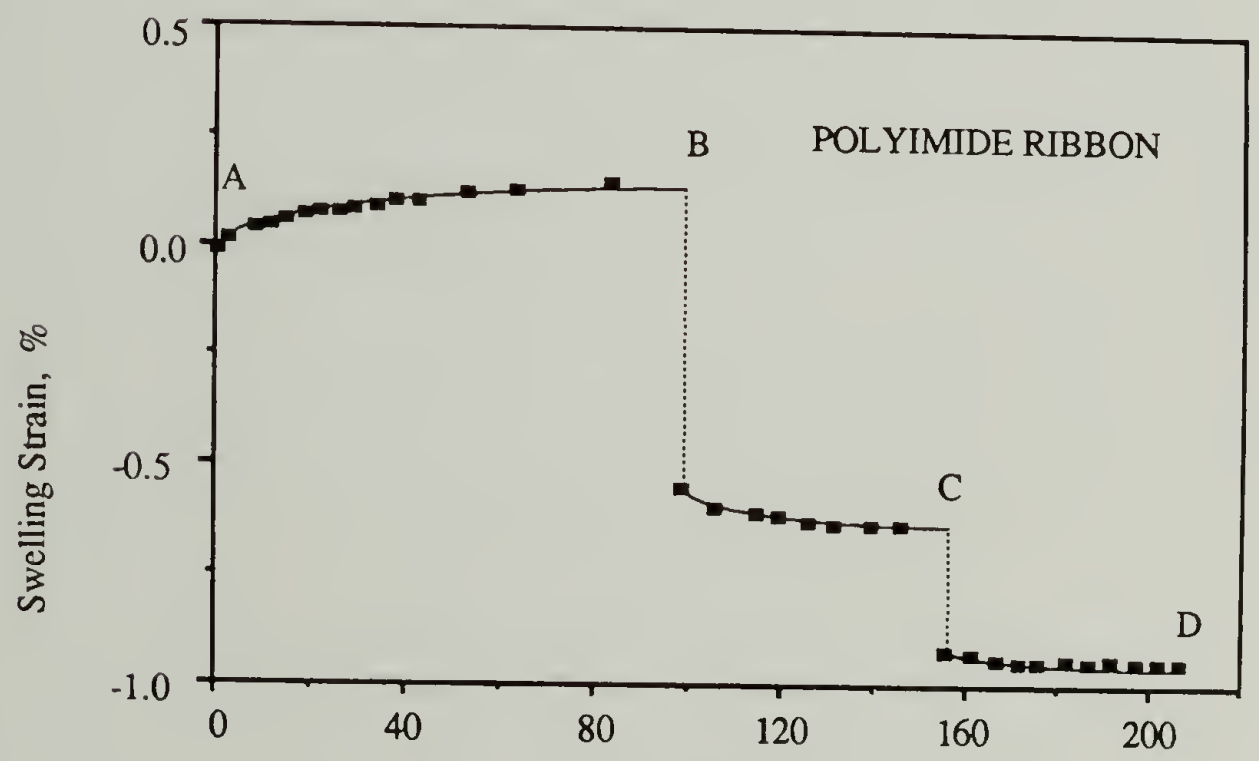

Figure 3.19 Percent weight gain versus exposure time during a typical sequential applied stress experiment on a PI ribbon (a). A dry sample at initial stress = 50 MPa, was saturated with moisture (AB). On achieving equilibrium, the axial stress was changed to a new value = 25 MPa (BC) and then 12.3 MPa (CD), resulting in new equilibrium states. The sample traversed from one stress-solubility equilibrium state to another with each change in the applied stress. The corresponding changes in sample length due to swelling are shown by the bold lines of Figure 3.19 (b).

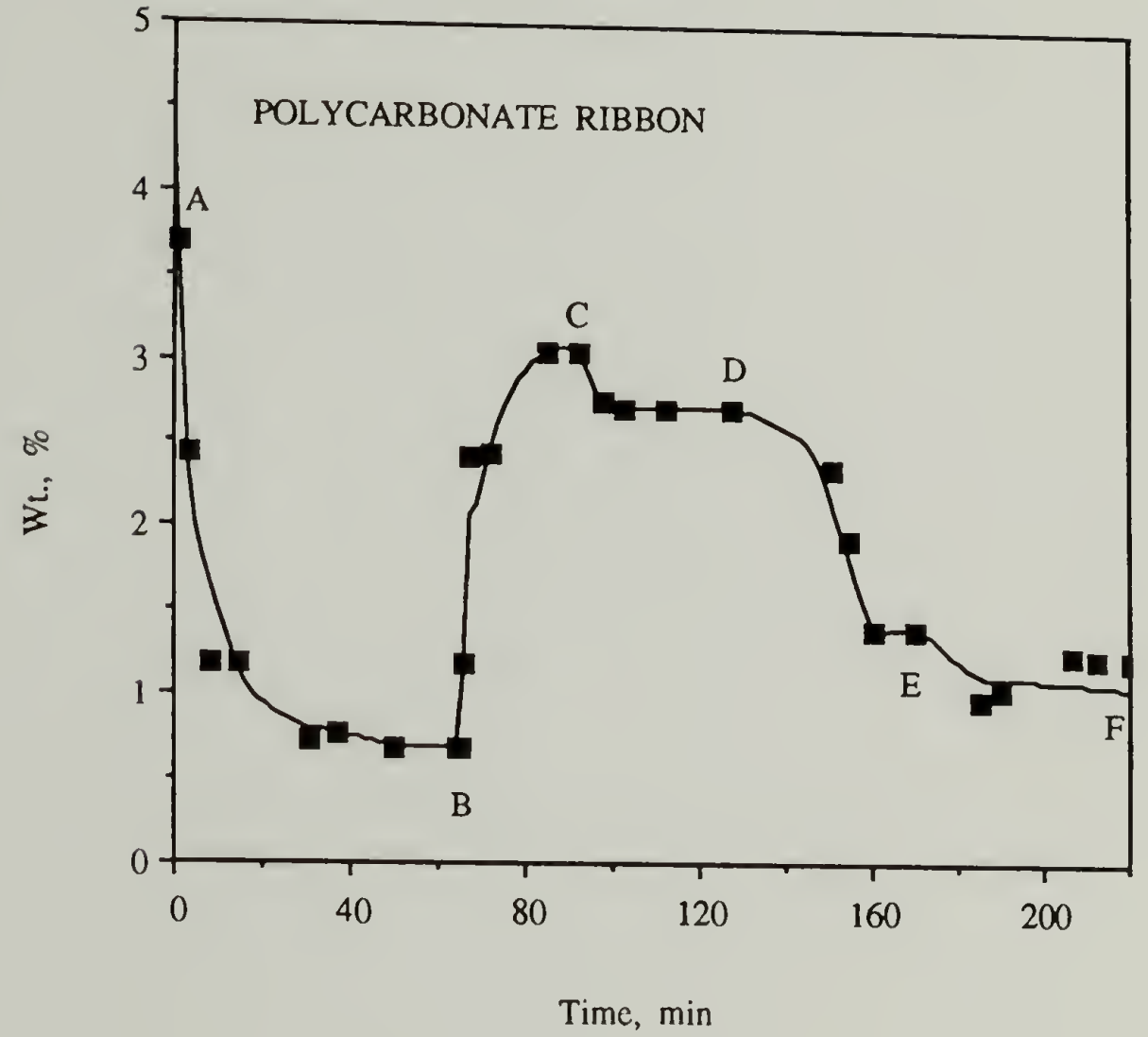

Figure 3.20 Percent weight gain versus exposure time under sequential applied stress for a PC ribbon. A previously saturated sample at initial stress = 33 MPa, was first dried (AB). This was followed by sorption (BC). At equilibrium, the axial stress was changed to new values = 26 MPa (CD); 20 MPa (DE)and 10 MPa (EF) respectively resulting in a sequence of equilibrium states. The sample traversed from one stress-solubility equilibrium state to another with each change in stress.

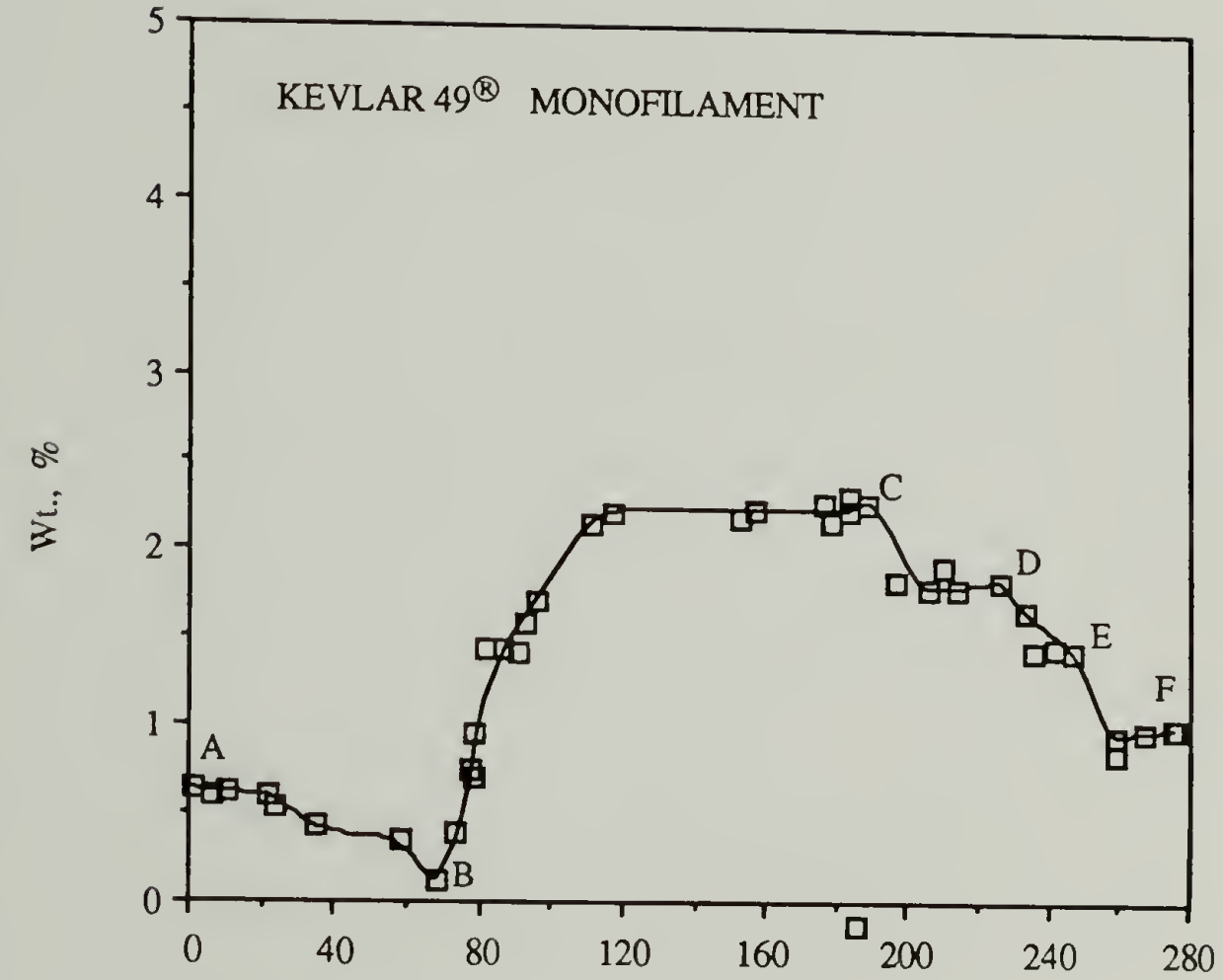

Figure 3.21 Percent weight gain versus exposure time under sequential applied stress for a PPTA ribbon. A previously saturated sample was dried at an initial stress = 1.4 GPa (AB) and then saturated with moisture (BC). At equilibrium, the axial stress was changed to a new value = 1.2 GPa (CD); 0.8 GPa (DE) and 0.6 GP (EF), resulting in a sequence of equilibrium states.

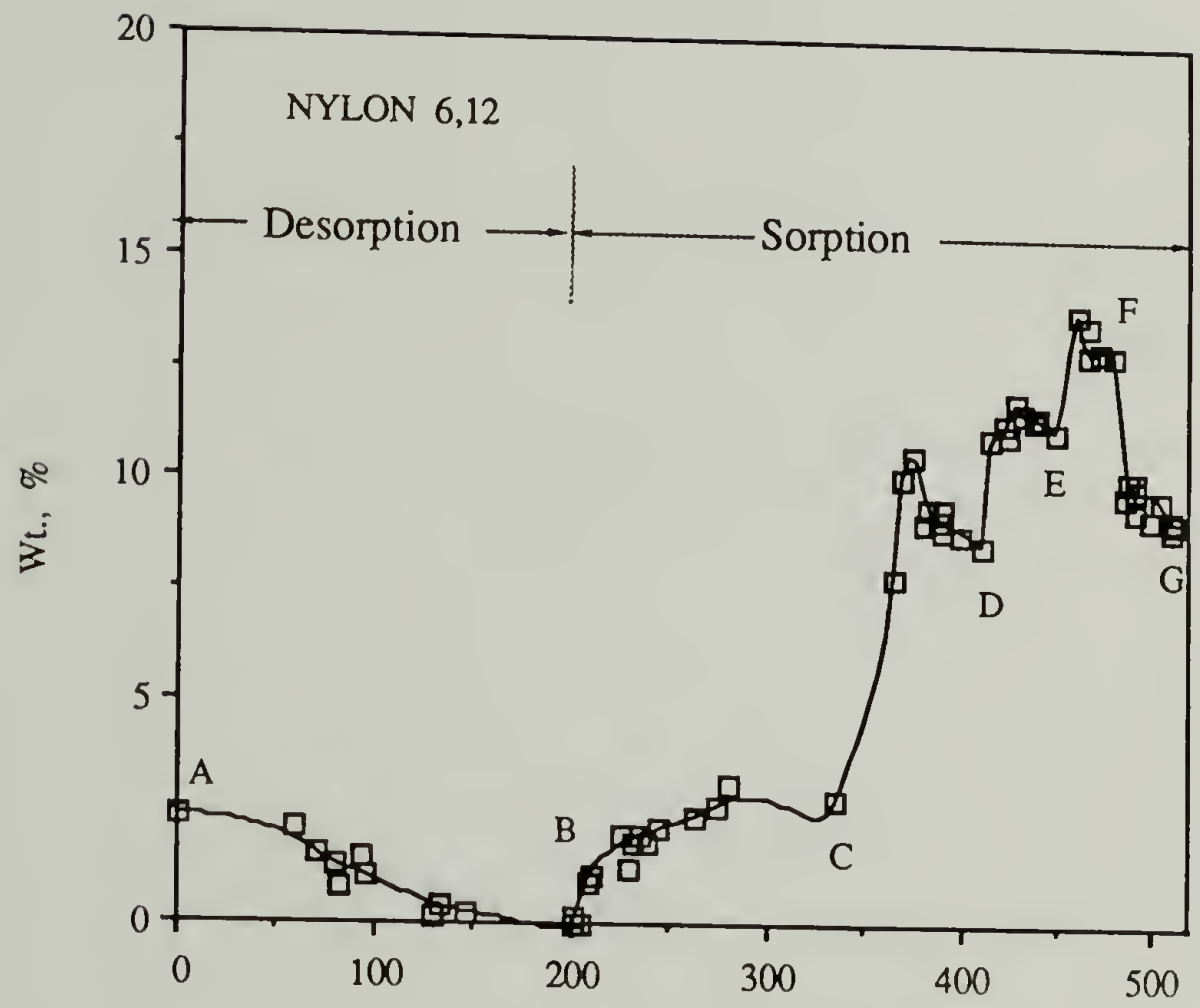

Figure 3.22 Percent weight gain versus exposure time during sequential applied stress for a N 6,12 ribbon. An as-received sample was dried at an initial stress = 8 MPa (AB) and then saturated with moisture (BC). At equilibrium, the axial stress was changed to new value = 16 MPa (CD); 24 MPa (DE); 32 MPa (EF) and 16 MPa (FG) resulting in a sequence of equilibrium states.

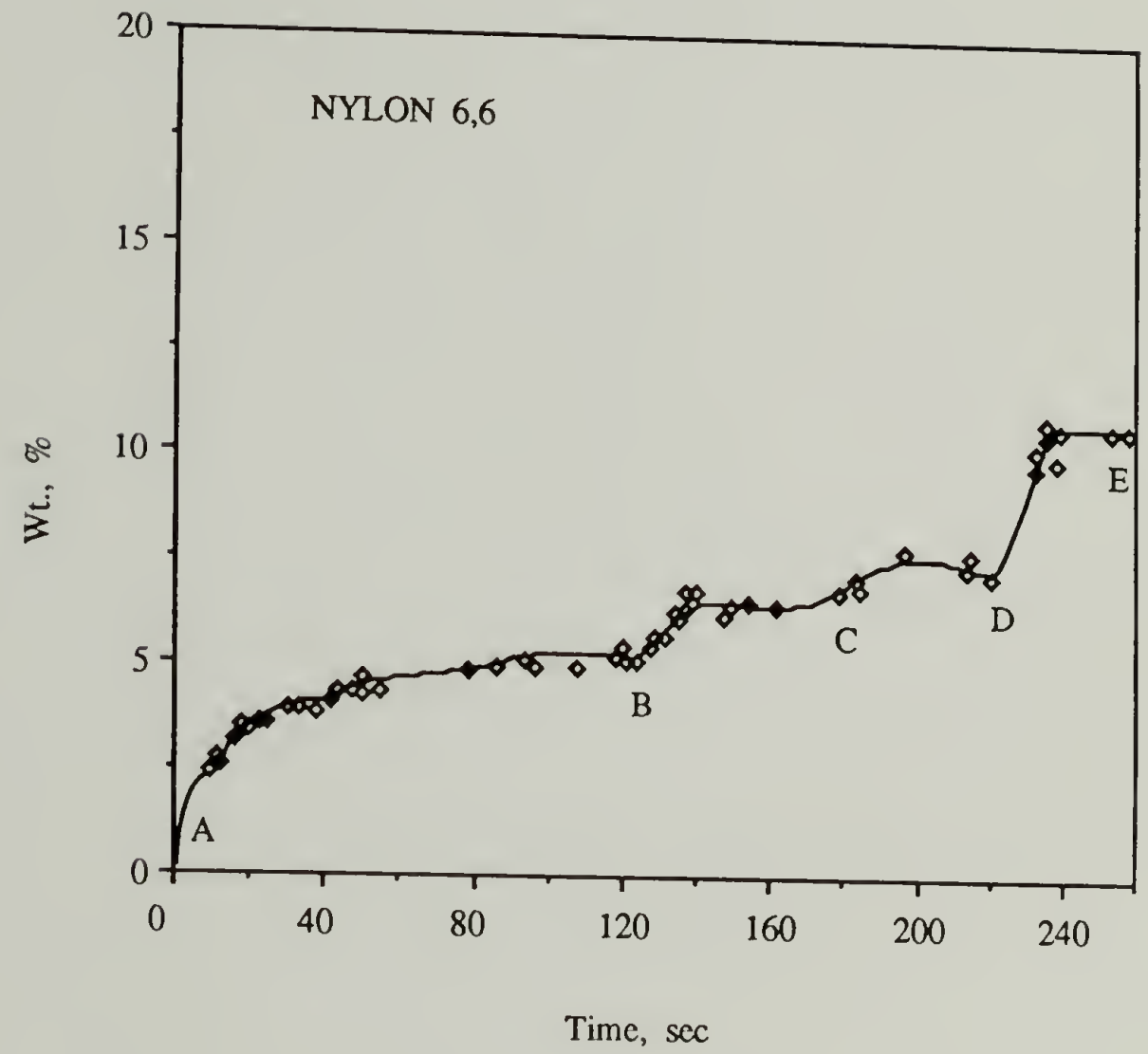

Figure 3.23 Percent weight gain versus exposure time under sequential applied stress for a N 6,6 ribbon. A dried sample at an initial stress = 6 MPa was first saturated with moisture (AB). At equilibrium, the axial stress was changed to a new value = 9 MPa (BC); 11 MPa (CD) and 16 MPa (DE) resulting in a sequence of equilibrium states.

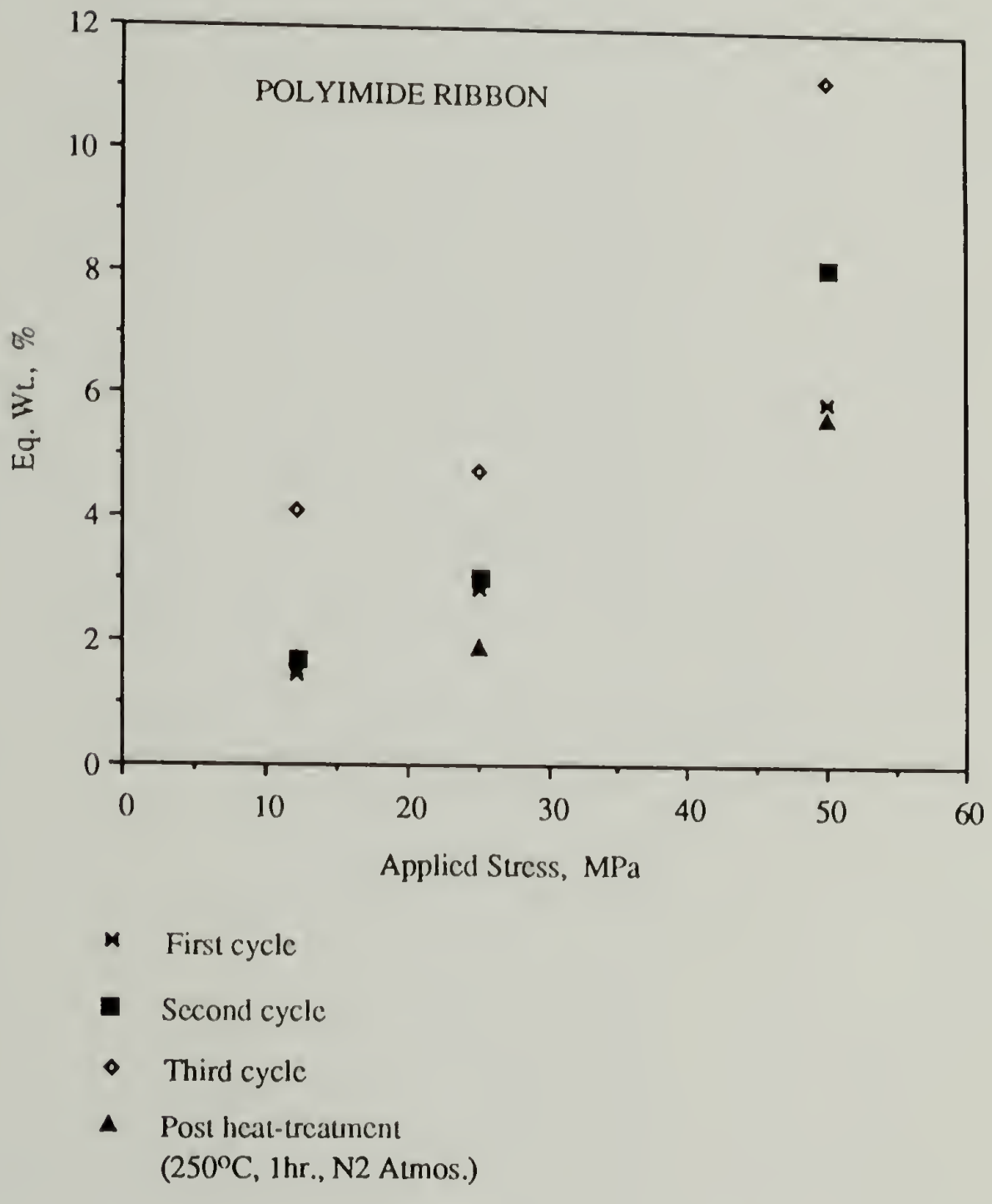

Figure 3.24 Equilibrium moisture solubility plotted as a function of the applied stress in a sample of PI: A dry sample under constant applied stress was exposed to 100% relative humidity until equilibrium. On achieving equilibrium, the axial stress was changed with the humidity constant. The points represent equilibrium states corresponding to the sequential stress-solubility experiments for a repeated cycles.

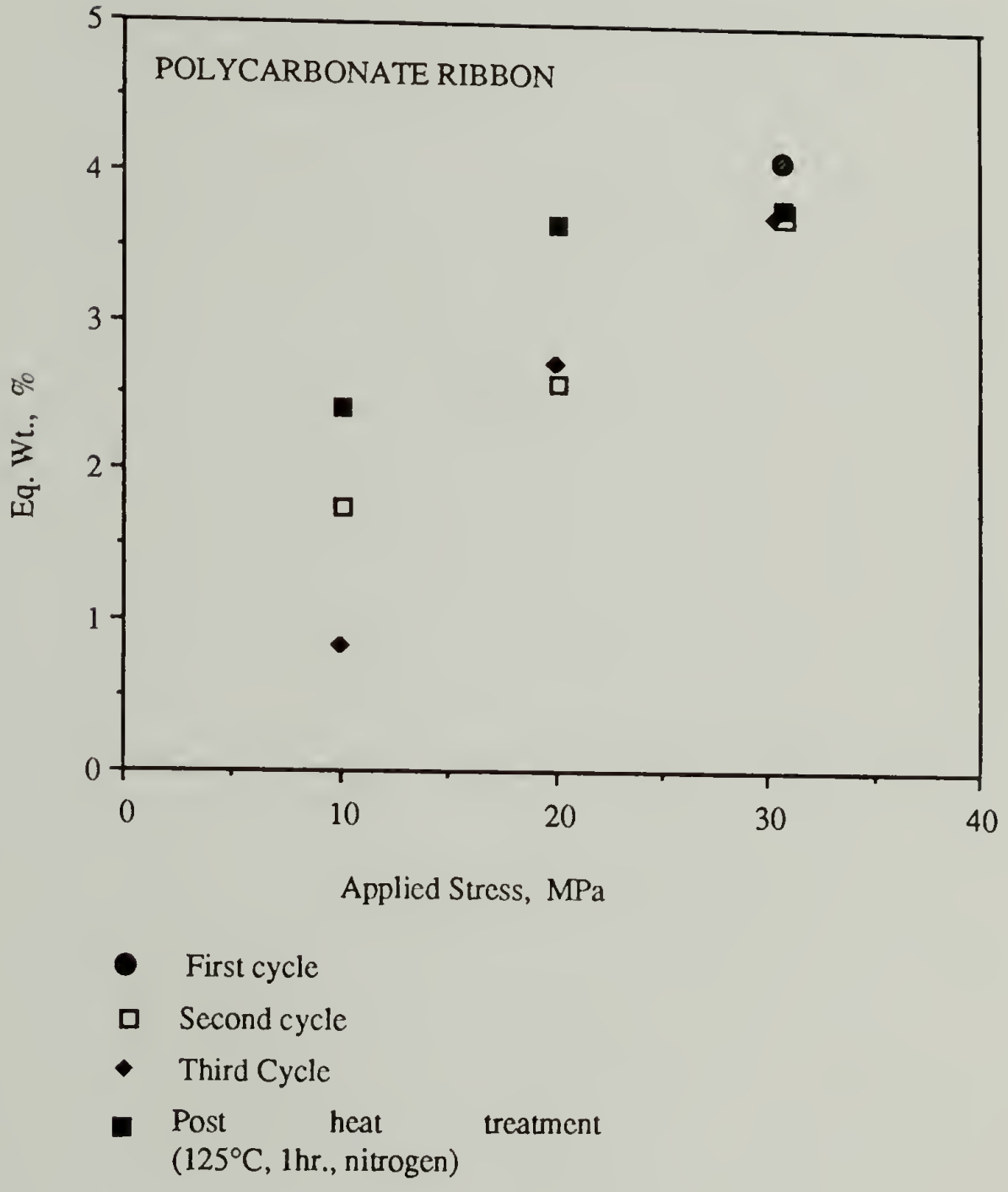

Figure 3.25 Equilibrium moisture solubility as a function of the applied stress in a sample of PC: A dry sample under constant applied stress was exposed to 100% relative humidity until equilibrium. On achieving equilibrium, the axial stress was changed with the humidity kept constant. The points represent equilibrium states corresponding to the sequential stress-solubility experiments for repeated cycles (Only one value of stress was examined during the first cycle).

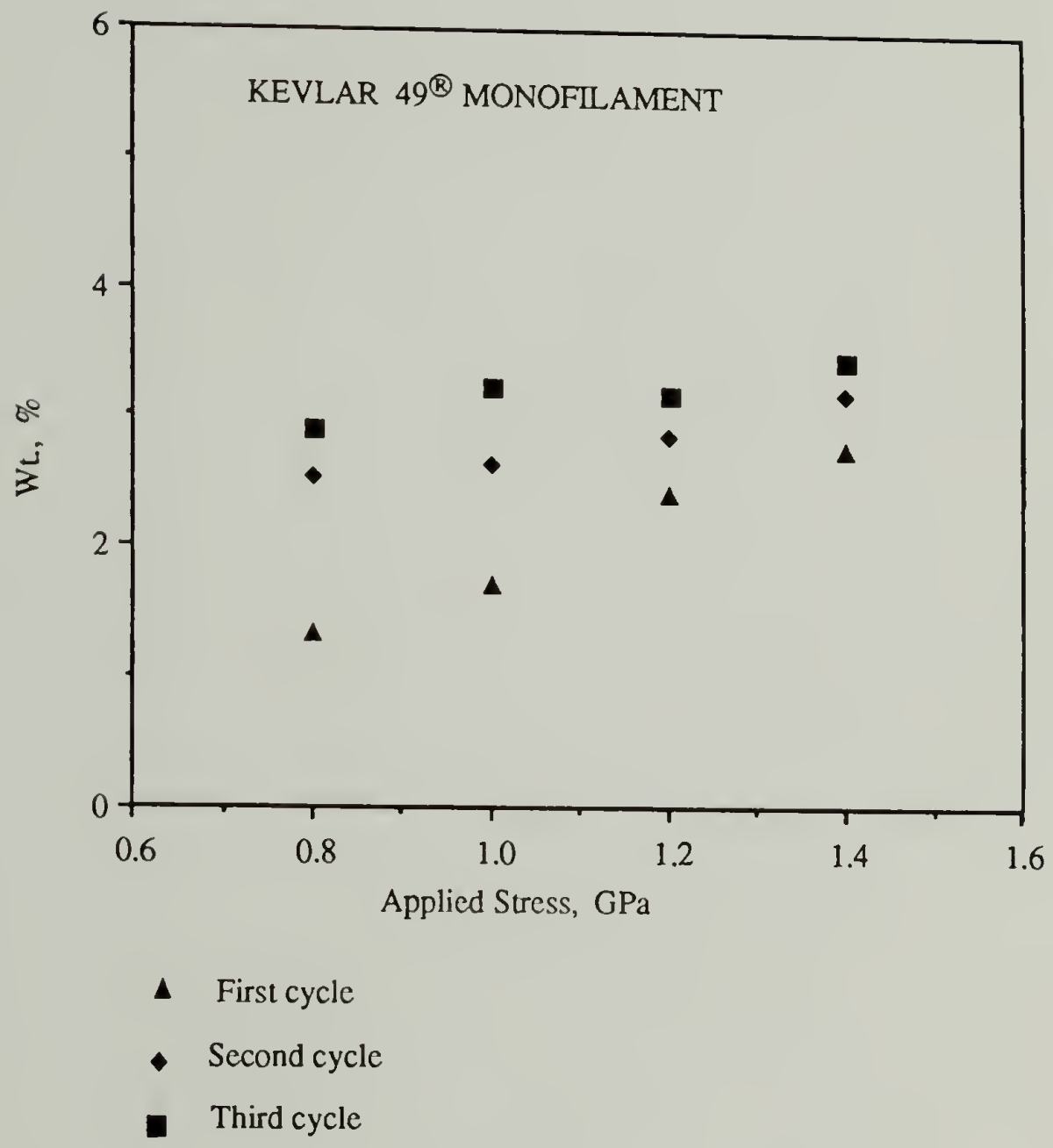

Figure 3.26 Equilibrium moisture solubility as a function of the applied stress in a sample of PPTA: A dry sample under constant applied stress was exposed to 100% relative humidity until equilibrium. On achieving equilibrium, the axial stress was changed with the humidity kept constant. The points represent equilibrium states corresponding to the sequential stress-solubility experiments for repeated cycles.

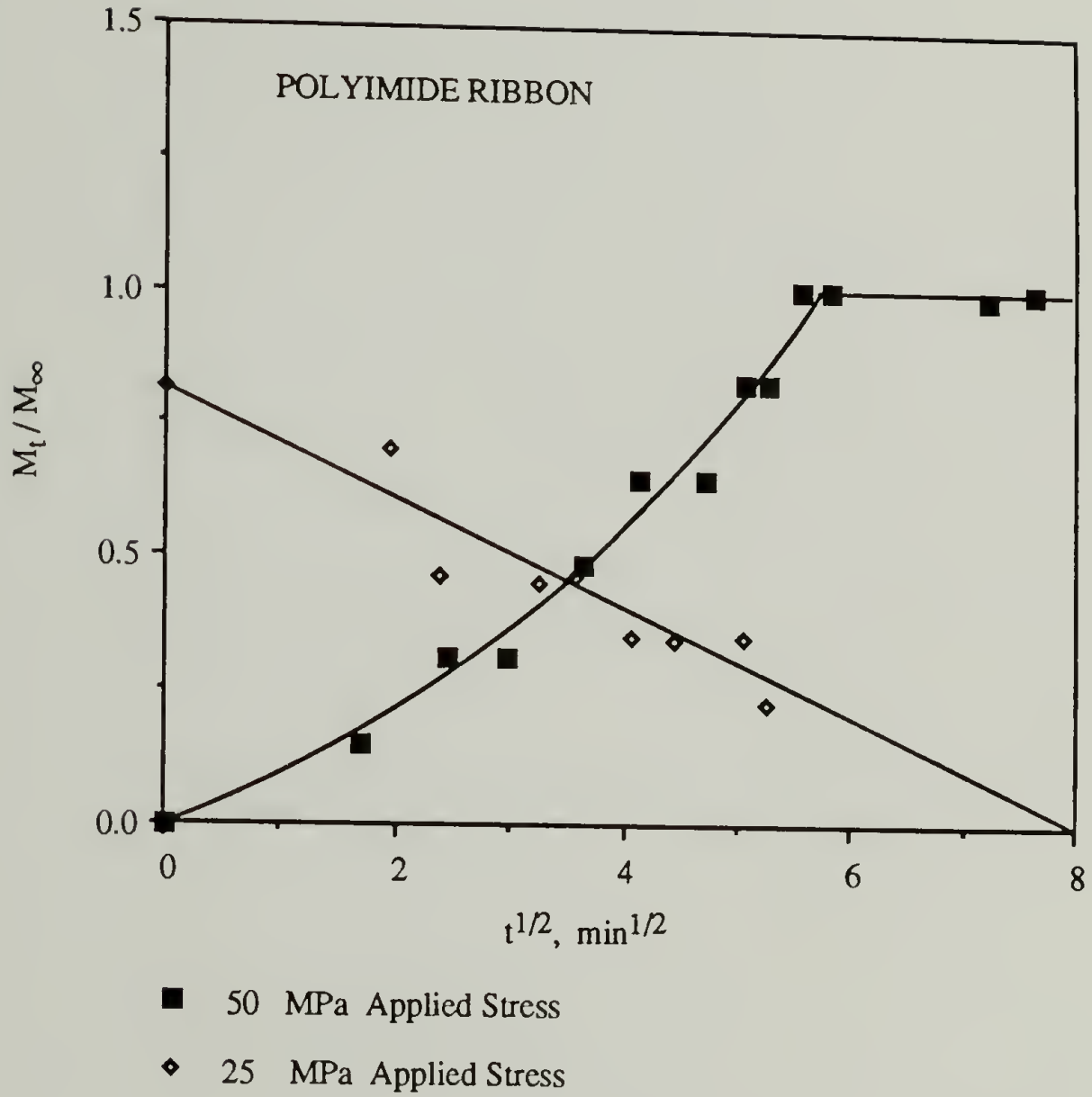

Figure 3.27 The fractional weight gain versus the square root of exposure time for a PI ribbon under constant axial applied stress during sequential experiments. Dry samples were exposed to 100% relative humidity until equilibrium at 50 MPa. when the axial stress was changed to 25 MPa, while the humidity remained constant. Desorption occurred during the second stage.

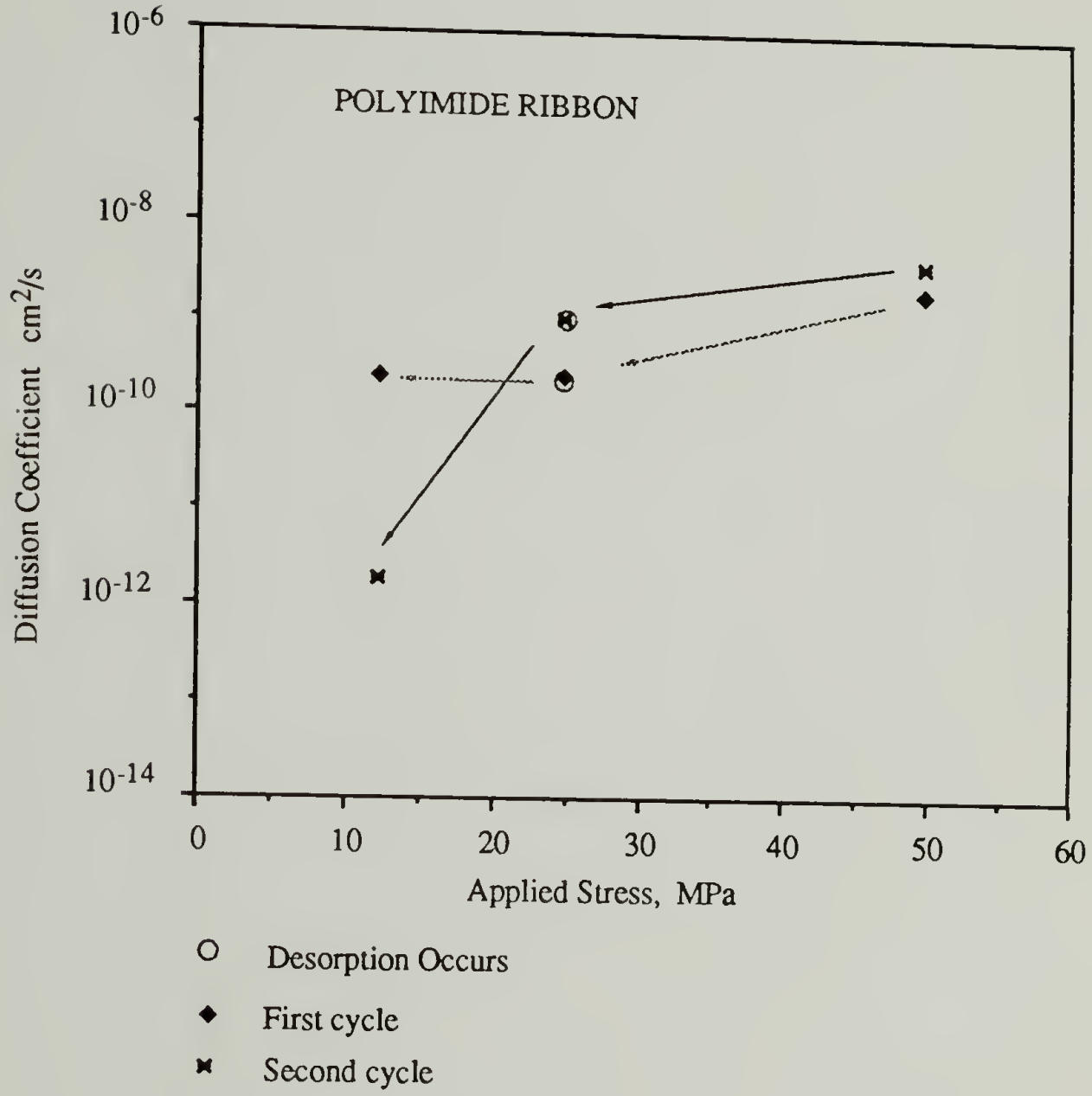

Figure 3.28 The diffusion coefficient plotted as a function of the applied stress for a sample of PI. Dry samples were exposed to 100% relative humidity until equilibrium under constant applied stress (50 MPa). This was followed by transitions to new stress-solubility equilibrium states as the applied stress was varied (to 25 MPa and 15 MPa). Desorption was observed after the first stage. The change in diffusion coefficient with stress is shown for two such cycles.

(a)

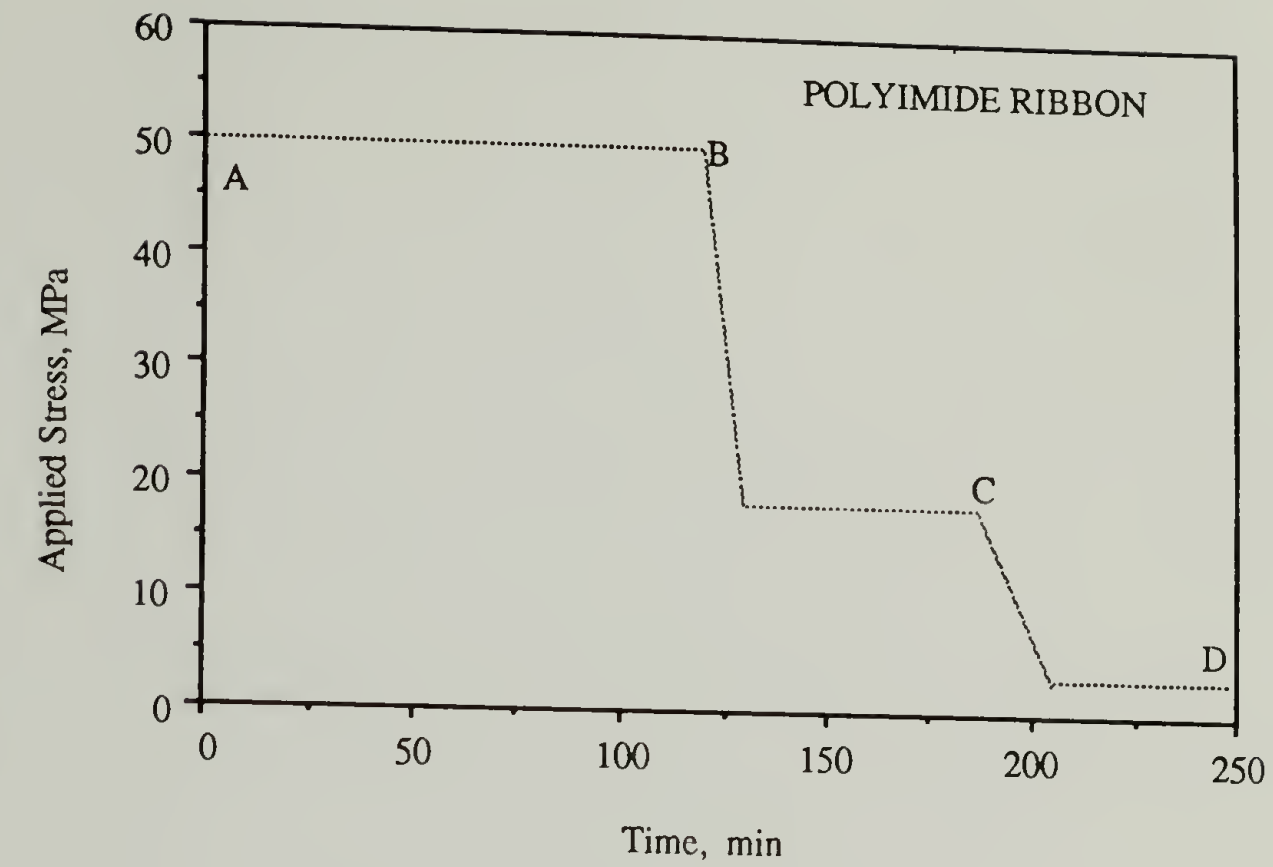

(b)

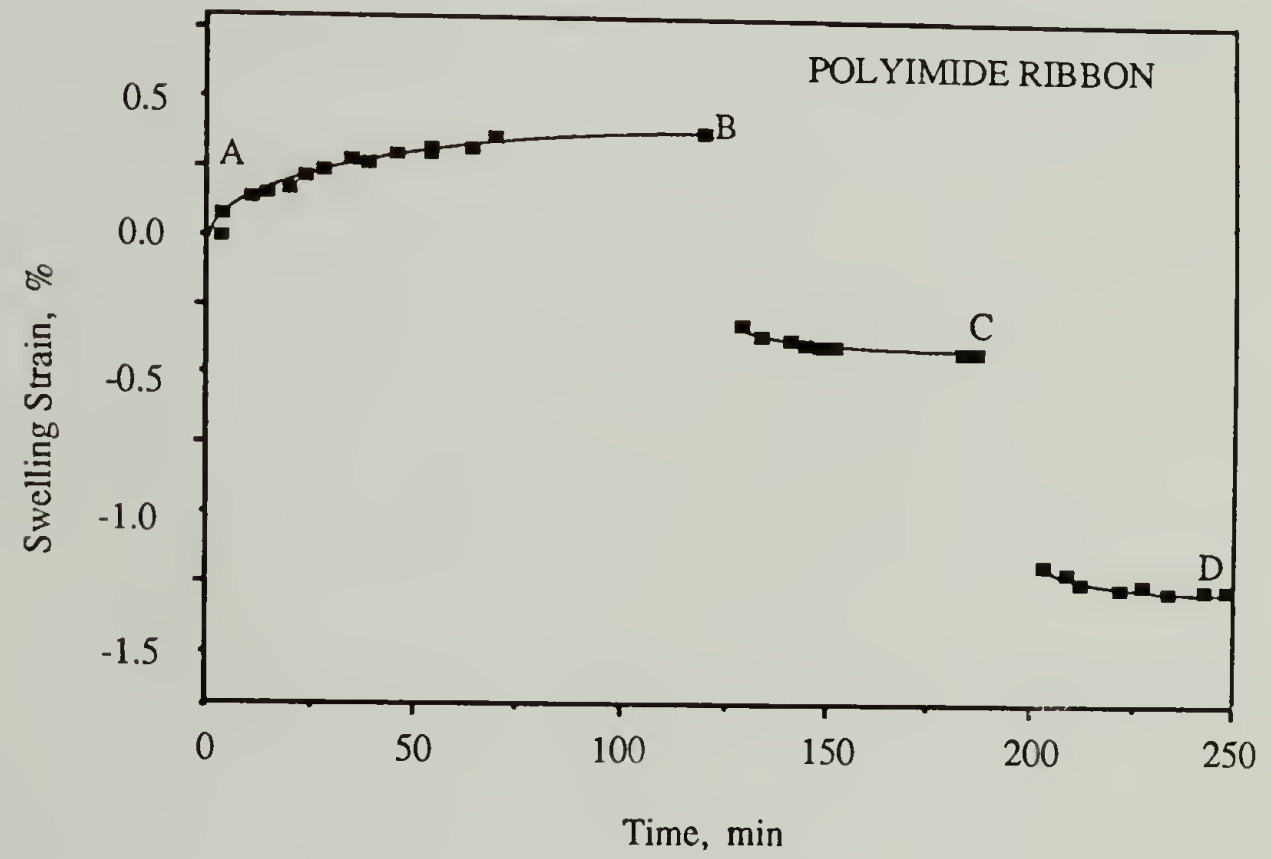

Figure 3.29 A dry PI sample was exposed to 100% relative humidity until equilibration at the initial stress, followed by transitions to new stress-solubility equilibrium states on reducing the applied stress (a). The axial strain resulting from moisture gain is plotted as a function of time during a sequence of constant stress experiments (b). The net strain during each step corresponds to the swelling strain.

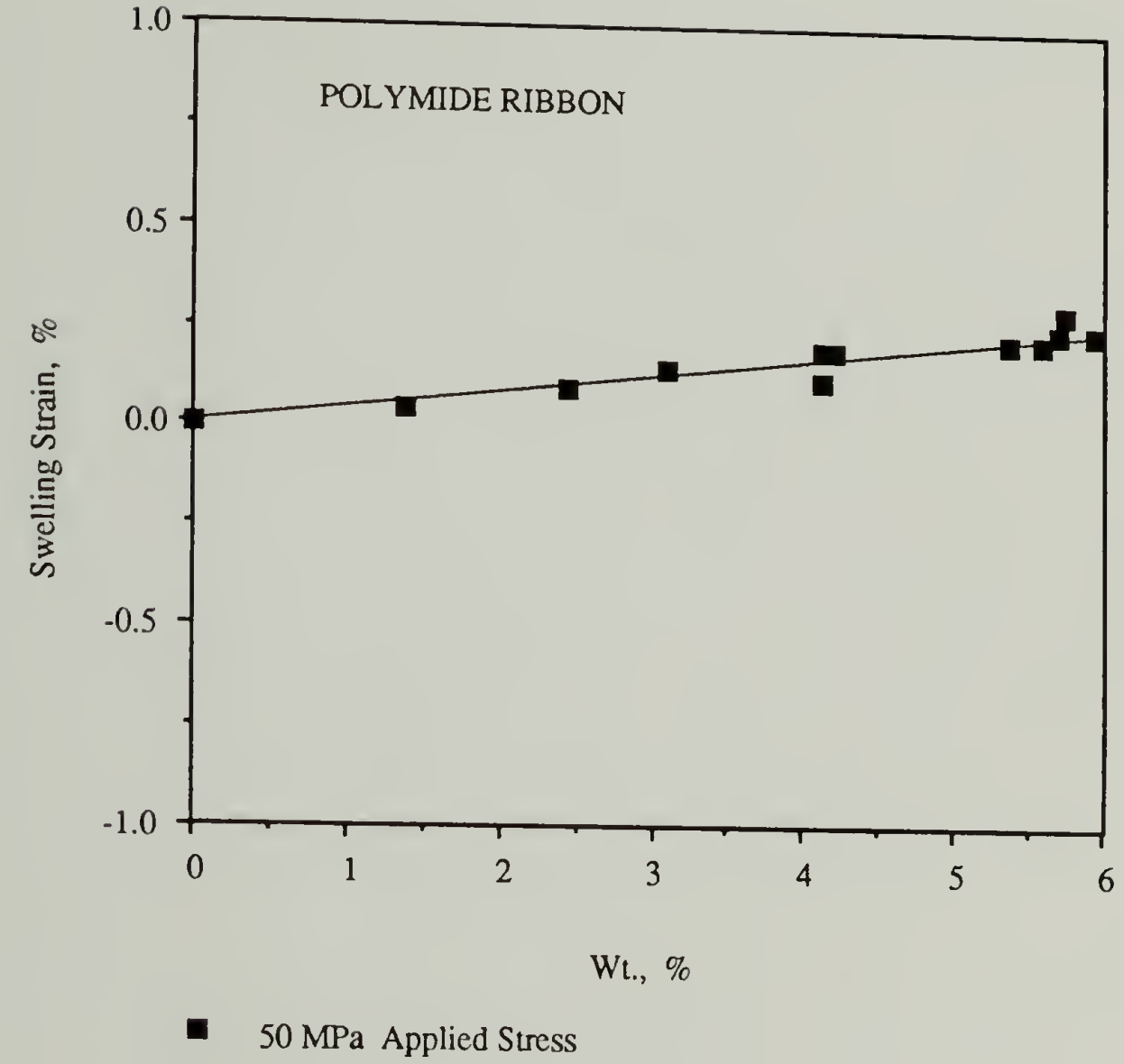

Figure 3.30 The axial swelling strain for a PI ribbon during sorption under constant stress (50 MPa), plotted as a function of the moisture content.

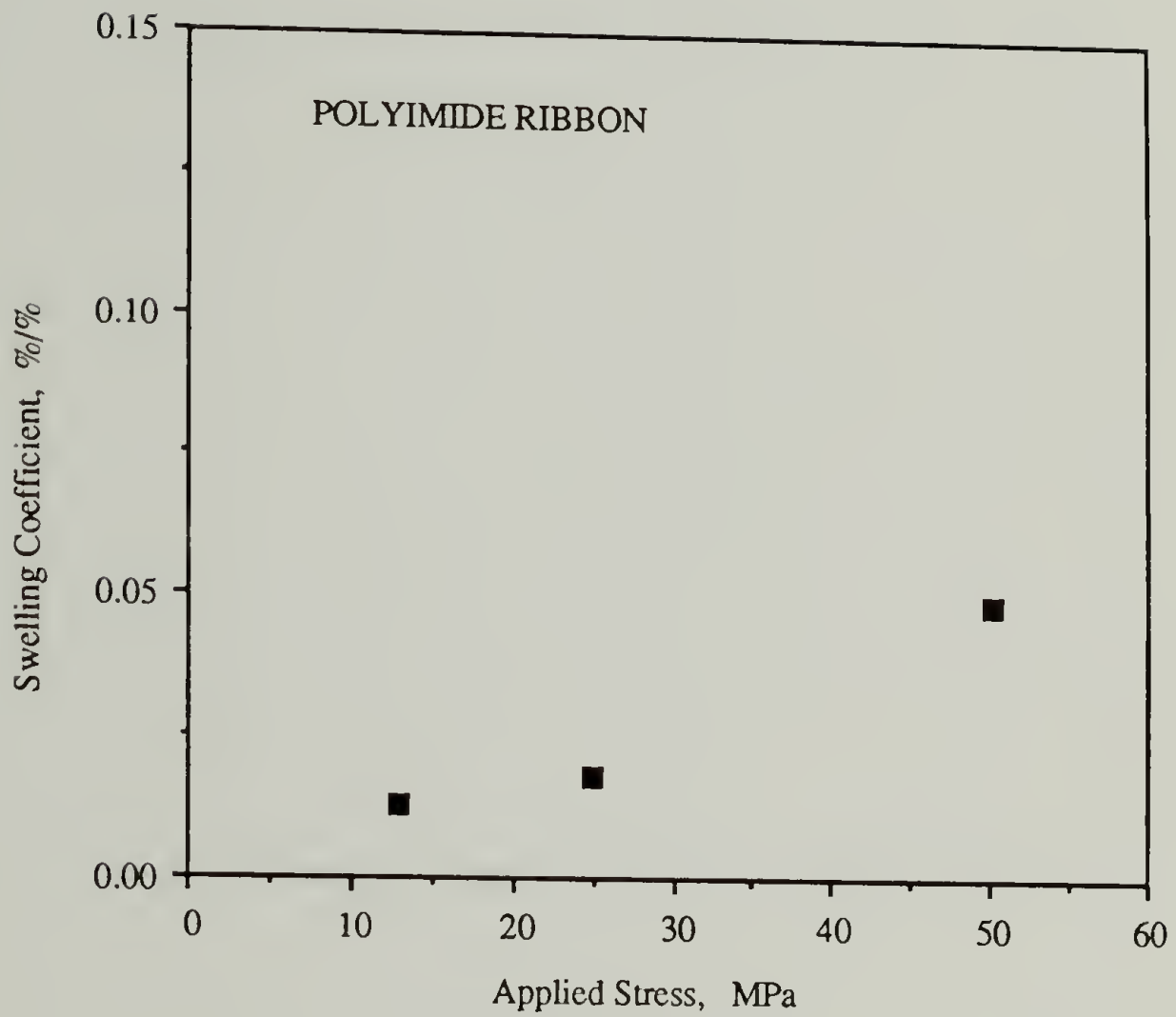

Figure 3.31 The axial swelling coefficient plotted as a function of the applied stress during a sequential constant stress experiment on a PI ribbon. The points represent solubility coefficients determined at the different stresses for the given sample.

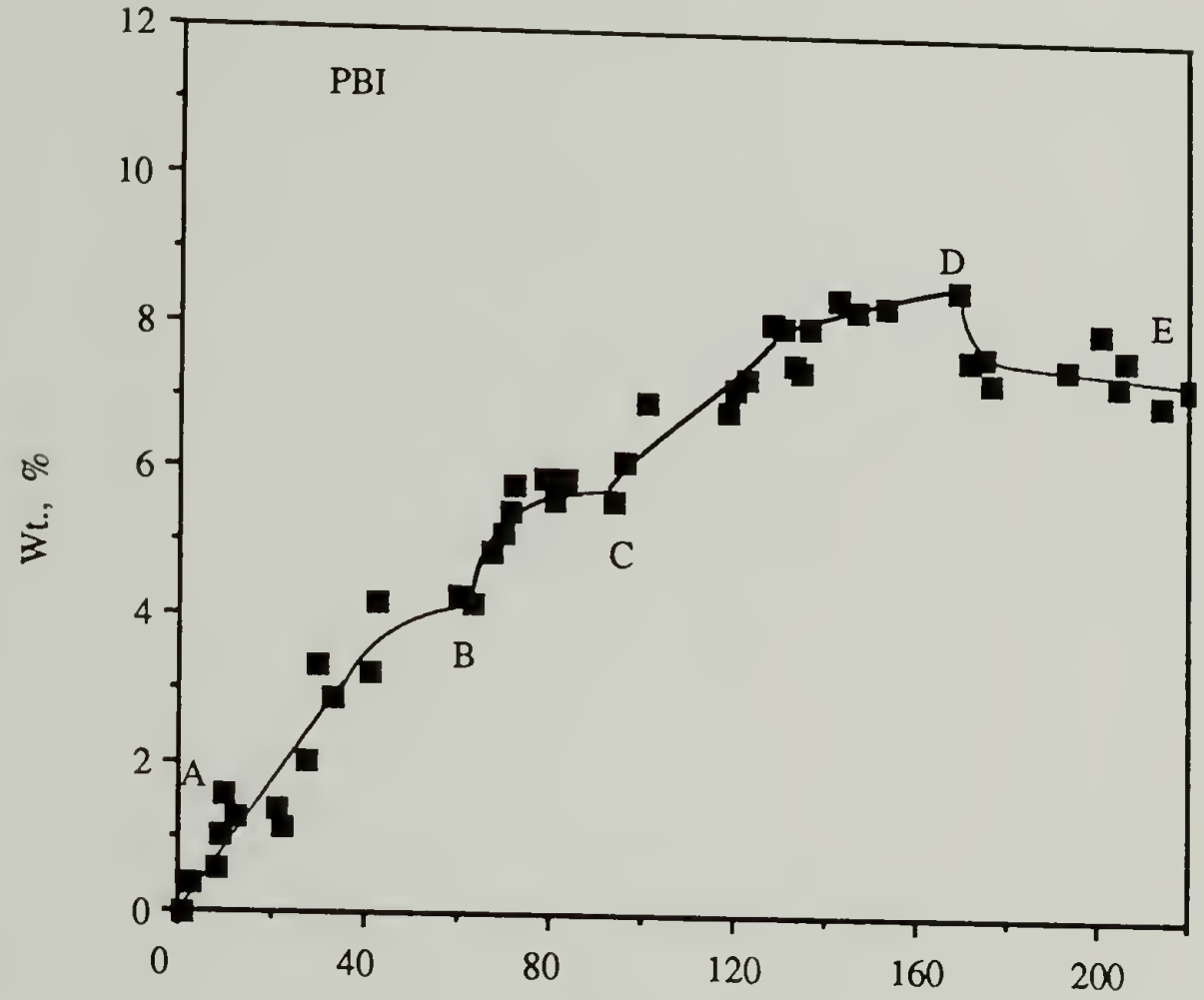

Figure 3.32 The moisture gain for a sample of PBI under constant strain, plotted as a function of exposure time in 85% relative humidity. A dry sample was held under constant initial elongation at 1.4% and exposed to moisture until equilibration. The strain was increased sequentially from 1.4 % (AB); 1.7 % (BC); 2.0 % (CD); 2.5 % (DE) until equilibrium was achieved at each elongation.

(a)

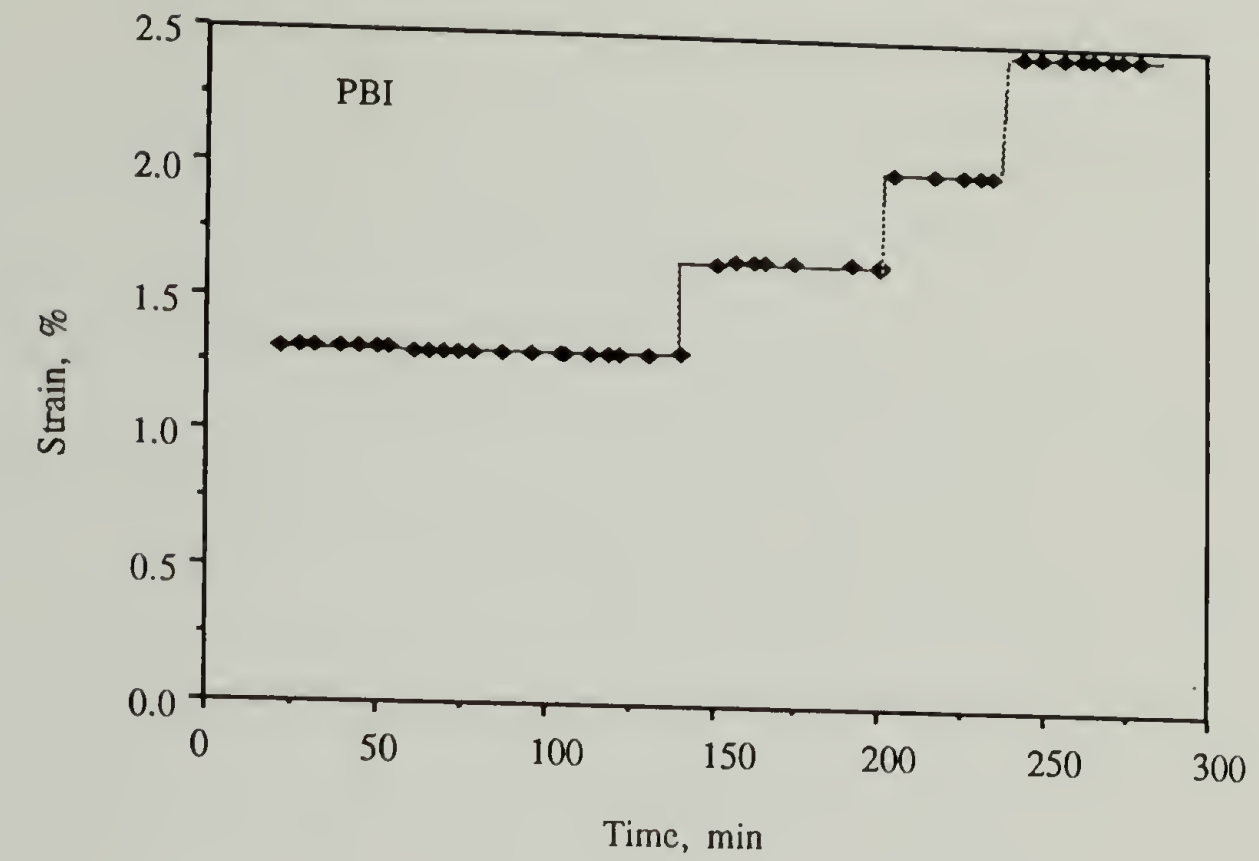

(b)

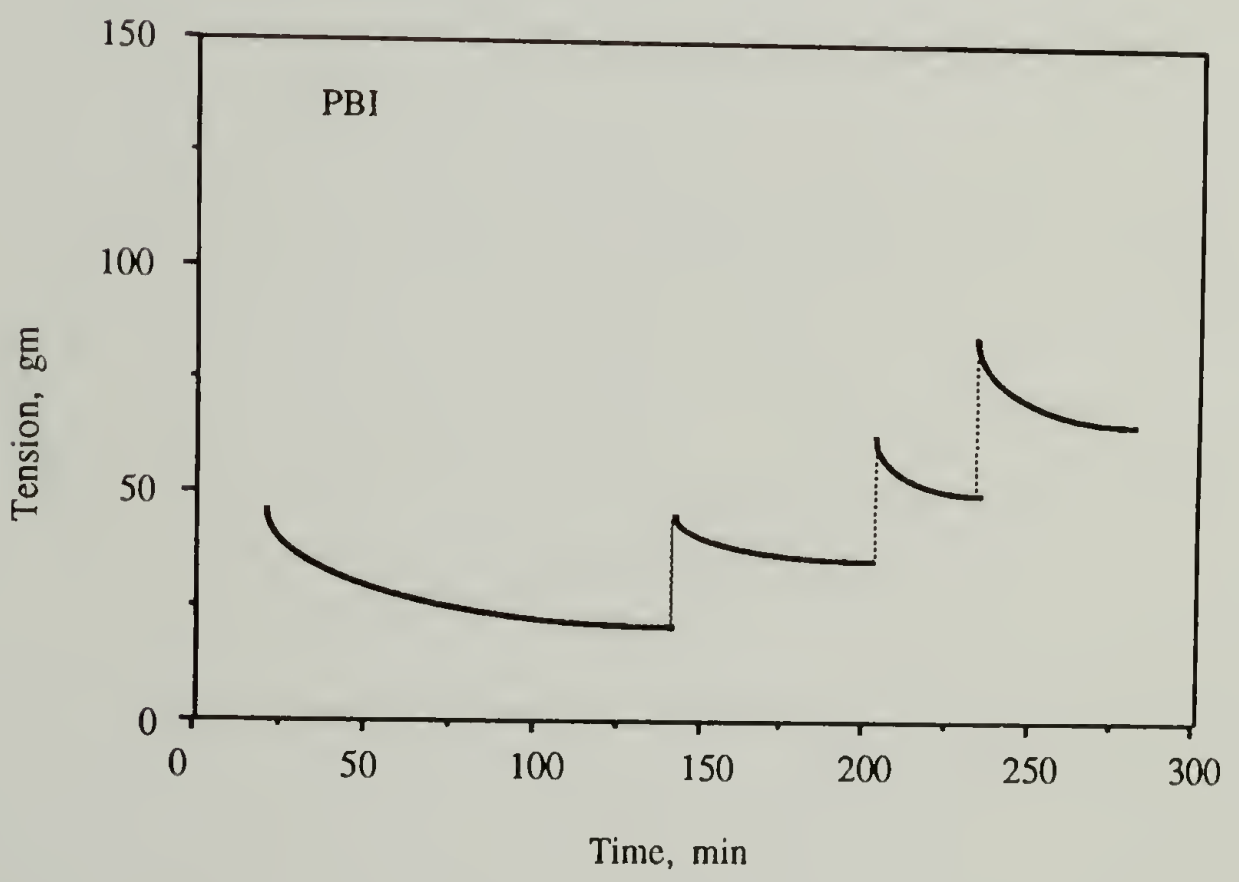

Figure 3.33 The *total* sample strain (a) and the corresponding sample tension (b) are plotted against the time of exposure in 65% relative humidity, for a PBI sample. A dry sample was held under constant elongation at 1.4% and exposed to moisture till equilibrium sorption is achieved. The strain was increased sequentially as equilibrium was attained at each elongation.

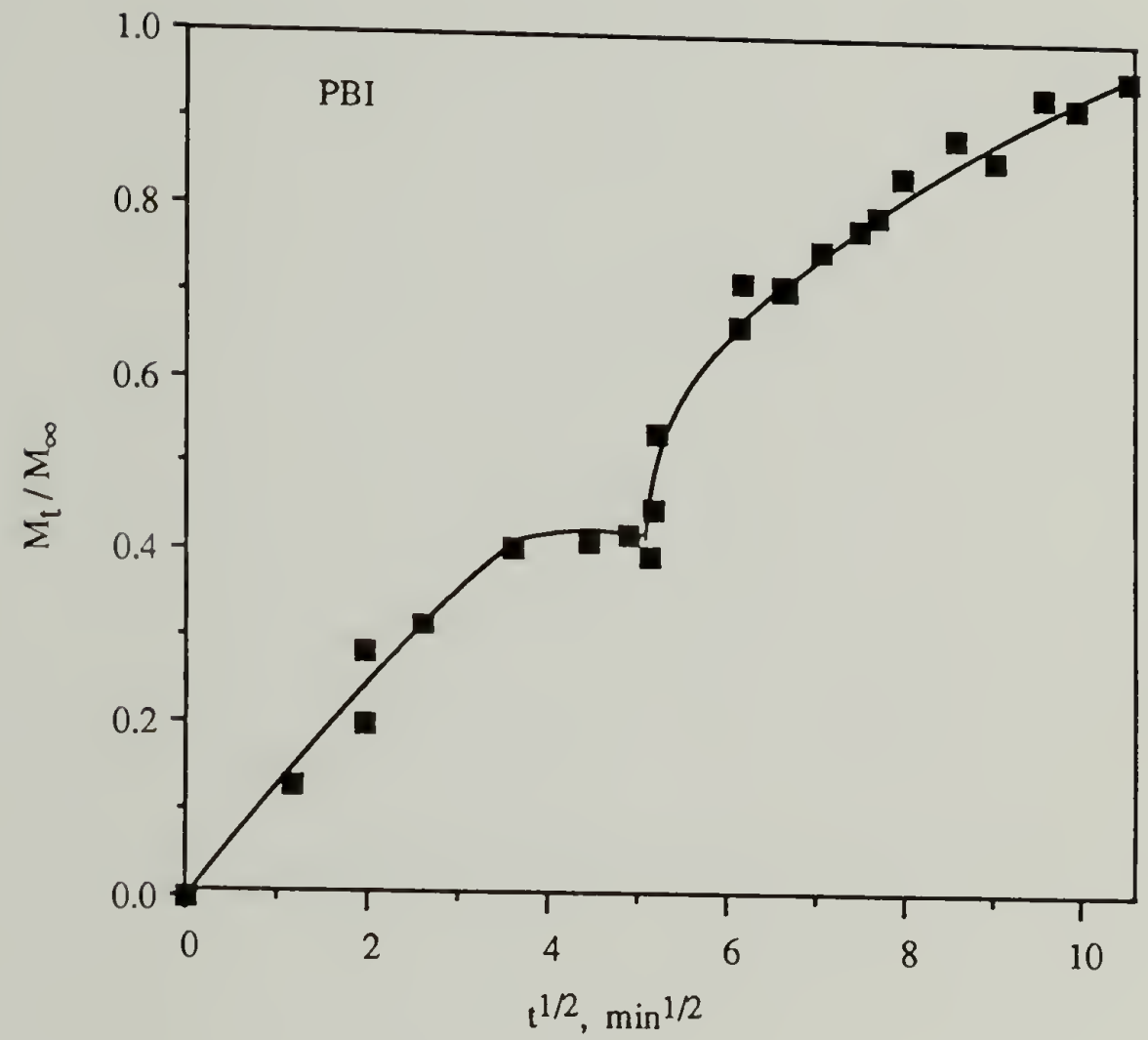

Figure 3.34 The fractional weight gain versus the square root of the exposure time for a sample of PBI held under constant strain (1.4 %) and exposed to 100% relative humidity. A dry sample held at an elongation of 1.4% was exposed to moisture until equilibration.

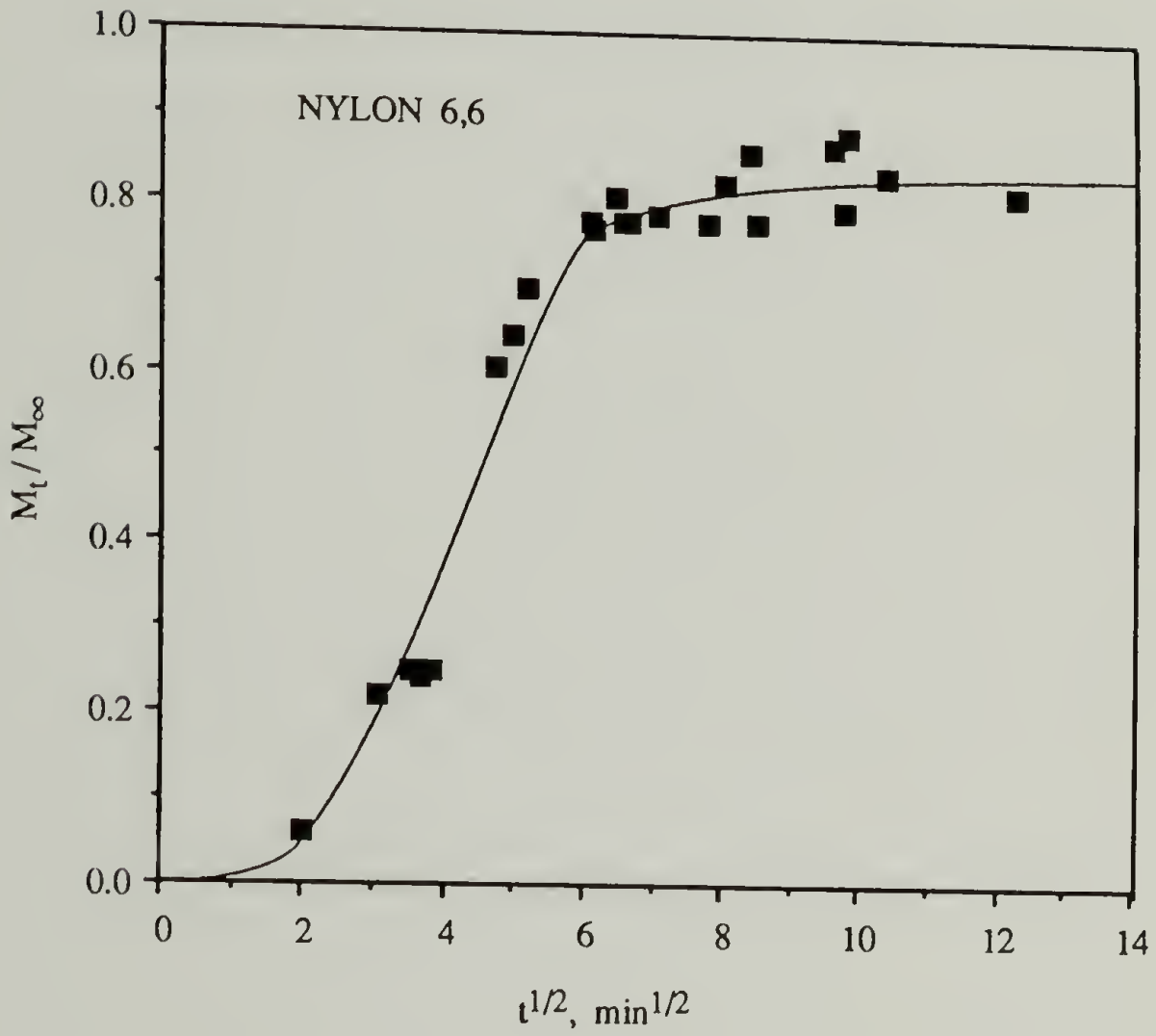

Figure 3.35 The fractional weight gain plotted against the square root of the exposure time for a sample of Nylon 6,6 held under constant strain and 100% relative humidity. A dry sample was held under constant initial elongation and exposed to moisture till equilibrium sorption was achieved.

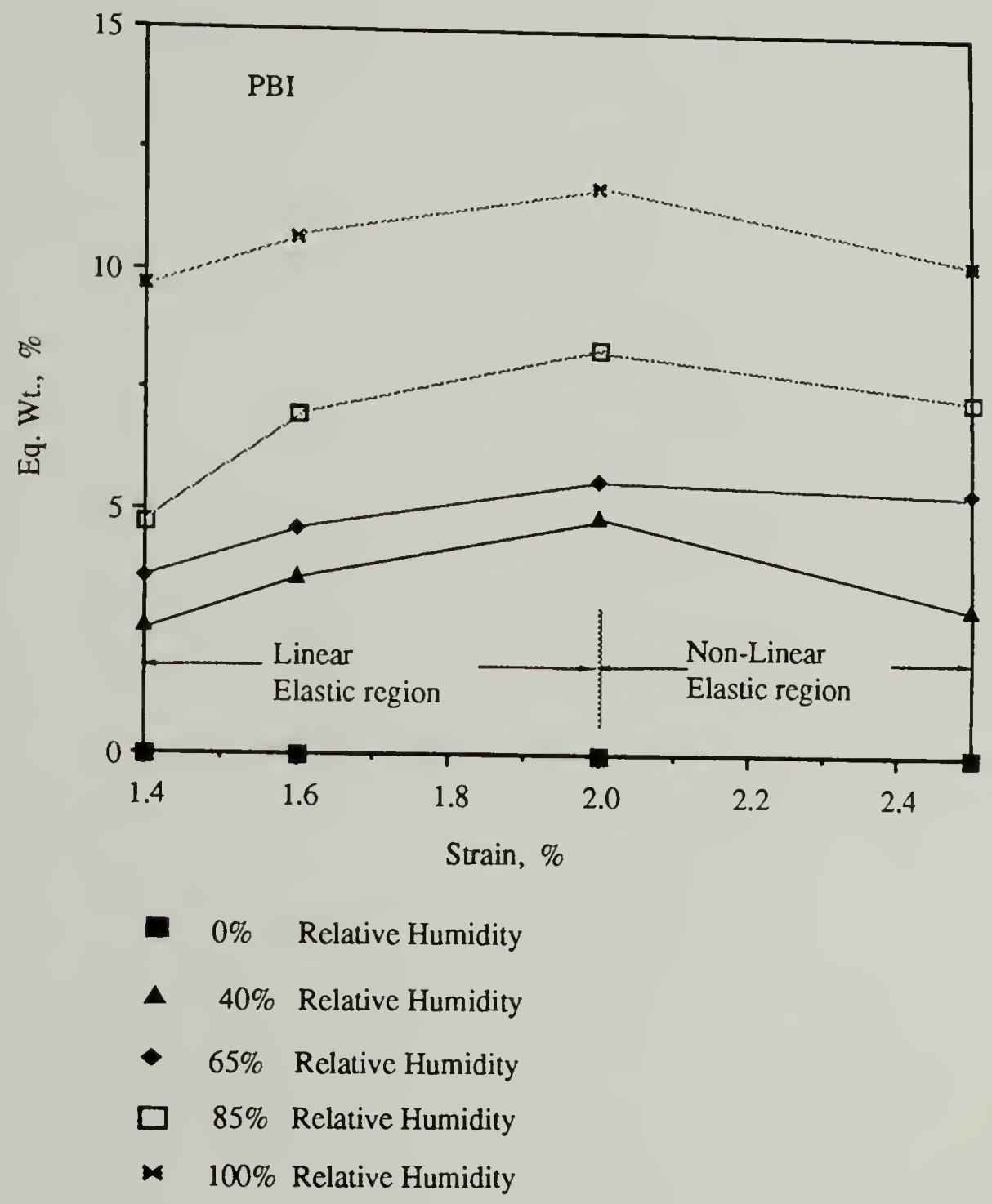

Figure 3.36 The equilibrium solubility plotted as a function of the applied strain for PBI samples under constant strain during a set of sequential strain conditions. Samples were dried and exposed to moisture while being held under a constant initial strain. On equilibration of the moisture content, the axial strain was changed to a new value for a sequence of strains, as the sample traced the strain-solubility envelope. Similar experiments were then repeated for a range of humidities.

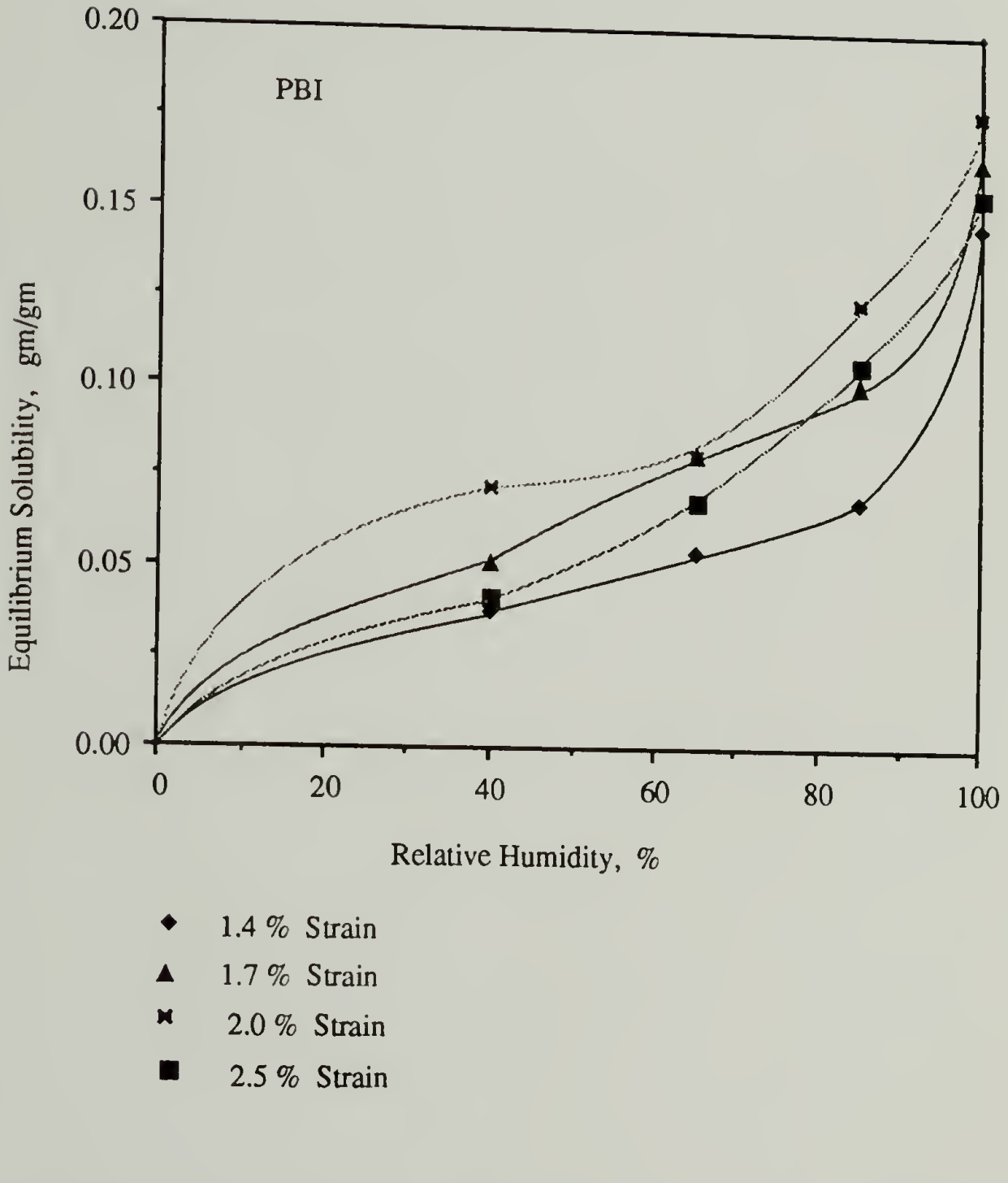

Figure 3.37 The equilibrium solubility versus the relative humidity for samples of PBI held under constant axial strain. Samples initially dried, were exposed to moisture at a constant initial strain until equilibration. These *sorption isotherms* were then generated by conducting such experiments over a range of relative humidities. These experiments were repeated for different values of axial strain.

Table 3.1 Tabular overview of the experiments that are discussed in the Chapters 3 and 4, listing the materials and experimental conditions employed. The heading "driving force" refers to whether diffusion in a given sample at equilibrium (stress, strain, and solubility) was initiated by a change in the state of stress, strain or concentration of moisture at the sample boundary.

Materials	Experimental Conditions	Driving Force	Properties Determined
Polyimide Kapton®	Constant stress (100% R.H.)	Concentration stress/strain	Equ. solubility Diff. coefficient. Swell. coefficient.
	Constant strain (100% R.H.)	Concentration stress/strain	Equ. solubility Diff. coefficient. Swell. coefficient.
Polycarbonate Lexan®	Constant stress (100% R.H.)	Concentration stress/strain	Equ. solubility Diff. coefficient. Swell. coefficient.
	Constant strain (100% R.H.)	Concentration stress/strain	Equ. solubility Diff. coefficient. Swell. coefficient.
Polyaramid Kevlar 49®	Constant stress (100% R.H.)	Concentration stress/strain	Equ. solubility Diff. coefficient. Swell. coefficient.
	Constant strain (100% R.H.)	Concentration stress/strain	Equ. solubility Diff. coefficient. Swell. coefficient.
Nylon 6	Constant strain. (100% R.H.)	Concentration stress/strain	Equ. solubility Diff. coefficient. Swell. coefficient.
Nylon 6,6	Constant strain (100% R.H.)	Concentration stress/strain	Equ. solubility Diff. coefficient. Swell. coefficient.
Poly m-phenylene-bis-benzimidazole	Constant strain (100, 85, 65, 40% R.H.)	Concentration stress/strain	Equ. solubility Diff. coefficient. Swell. coefficient.

CHAPTER 4

HISTORY DEPENDENCE IN STRESS COUPLED TRANSPORT

4.1 Introduction

The non-equilibrium nature of polymers results in property variations not only as result of their "hygro-thermo-mechanical" history but also because of their inherent time dependence. The stress and strain coupled transport discussed in previous chapters examined mostly instantaneous effects on materials. In the cases discussed so far, interactions were mostly elastic and only the instantaneous response to applied stress or strain was examined. However, what remains to be studied is the behavior of the stress coupled transport phenomena over extended periods of time and as functions of sample history. History effects are important in nearly all applications of polymeric materials, particularly when mechanical or hygro-thermal conditions occur cyclically and when consistent performance over extended periods of time is required.

The nature of hysteresis in polymer properties is usually determined by prevalent time-dependent relaxation phenomena in conjunction with prior mechanical and hygrothermal exposure. The interaction of stress-coupling with history dependent behavior provides insight into internal mechanisms and also the modes of coupling between mechanical and transport variables. The results of experiments examining

the effects of prolonged exposure to moisture, through sorption-desorption cycles under applied stress or strain, are discussed in this chapter. Time-dependent effects were extensively described in the literature and a survey of the relevant publications has also been provided in section 4.2.0. This chapter is aimed at extending the study of stress-coupled sorption by employing the technique developed during this work to the investigation of history-dependence in stress coupled transport.

4.2 Background

It has been widely held that the transport of permeant molecules through a polymer matrix can result in the formation of microvoids or crazes. These "micro-defects" are in fact considered to provide additional sites for solvent penetration and thus promote sorption in subsequent cycles (Crank 1953, Browning 1978, Apicella et al. 1981). This "damage" was found to be permanent to the extent that the material did not "heal" during desorption, suggesting that solvent induced deformation was not an elastic process, particularly for thermoplastic materials. In another study related to epoxy materials, it was shown that the "damage" was in fact reversed by heat treatment (Wong et al. 1985). It was concluded that changes in network conformation altered the material's sorption characteristics and that these changes were thermo-reversible. Thus, samples were exposed to repeated cycles of sorption and desorption over extended periods of time. In all instances the moisture diffusion increased with each cycle of sorption.

In contrast to the above cases, Yasuda and Peterlin (1974) demonstrated a decrease in the diffusion coefficient with increasing strain, in cases where the internal chain orientation increased with applied deformation and reduced the tortuosity of diffusion pathways. It was concluded that a reduction of available sorption sites due to internal reorganization similarly resulted in a lower equilibrium solubility. A wide range of strains were examined in their study of the effects of strain on the permeability of gases in semi-crystalline polyethylene. Two distinct regimes of influence were identified: 1) a small strain region of recoverably elastic deformation (where all applied deformations were completely reversible); 2) a large strain region of non-recoverable plastic deformation (where a permanent deformation occurred due to the applied stress).

Yasuda and Peterlin (1974) noted that polymer diffusivity and permeability increased for small strains, while they decreased for large strains. The authors attributed this effect to an initial increase in free volume (in the elastic regime) via dilatation due to the applied stress. A permanent change in morphology (in the plastic regime) was believed to ensue at higher strains, as chains of polyethylene were drawn out of crystallites. The authors postulated that the spherulitic structure became increasingly fibrillar as a result. Observed diffusivities lower than in the original undeformed polymer were attributed to the reduced tortuosity of diffusion paths and closer transverse packing of the increasingly oriented polymer chains. A strain-induced maxima in diffusion coefficients was observed as they increased in the low strain regimes (elastic regime) and subsequently decreased in the high strain (plastic) regime. A similar effect was also reported for PI and PC films (Smith and Adam 1980).

It is well known that the superposition of time-dependent effects onto "elastic" or equilibrium effect results in history-dependent behavior in non-equilibrium materials such as polymers. Time dependent effects in polymcr segments; manifested by stress relaxation, volume retardation and physical aging, havc been to considered to influence the distribution of the "frce volume" and segmental mobility. This relationship underscores the significancc of comparing the time scales of diffusion relative to the relaxation timcs, particularly in the case of amorphous glasses. Case-II type of rclaxation controlled processes havc bcen observed when relaxation times were considcrably smaller than diffusion time scalcs. Further, the notion of diffcrcnt timc scalcs for stress effects and transport respcctively, reconciles thc various expcrimentally observed "anomalous" recovery phenomena that have bcen discussed in section 4.4.

When stress relaxation time scales were larger than diffusional times, permcant sorption was found to cquilibrate at the prevailing stress, cven whilc the internal stresses varied with time. Hence, depending on the influcncc of stress, equilibrium solubility may vary quasi-statically from one equilibrium statc to another during a series of applied stress. It may be inferrcd that a change in the stress or strain states, due to internal relaxations for instance, alters the solubility of permeants in a material when thc time scales of transport processes are relatively large. In the instance when the diffusion time scale is smaller than the relaxation time, the material acts as an elastic medium and is in a state of mechanical equilibrium relativc to the diffusion processes. Howcver, because of local stresses and strains and the

relative slowness of diffusion processes, the material passes through a series of "instantaneous" mcchanical equilibrium states.

The balance between osmotic pressure and internal and external stress is believed to determine the instantaneous value of internal stress. A selective change in the activity, concentration, or size of permeant, exerts an influence on the mechanical equilibrium by changing local concentrations and consequently the internal stress distribution. This argument was applied by Baird et al. (1971) to explain the overshoots observed during sorption of organic solvents in glassy polymers. The higher initial sorption was attributed to the formation of microvoids, resulting from high permeant activity. Subsequently, sorption declined due to the healing of the "excess voids" via a relaxation process. In view of the above discussion, overshoots are likely to occur when the time scales of diffusion and relaxation are of approximately equal orders of magnitude.

The discussion so far mainly addressed the concurrent effects of stress and transport and the time dependent behavior associated with them. Yet another important consideration is the relative domination of the applied stress over history effects. On examining the pertinent literature related to sub-T_g glasses it becomes clear that the physical aging mechanism is analogous to annealing as it also involves volumetric relaxation processes (Adams 1987, Haward et al. 1980, Smith et al. 1986, Struik 1978). However, stresses sufficiently large relative to the yield stress actually counter history effects and quench the glassy material. Consequently, such stresses may in fact nullify the effect of a polymer's history and render it relatively immune from history dependence. This principle further suggests that history effects

are thermo-reversible in the same way that stresses generated by quenching a material can be relaxed by unconstrained annealing. The ability to contain history dependence, by the application of stress, gives rise to a variety of potential applications. In particular, it suggests an approach for the enhancement of consistency and reliability of polymeric components under cyclic environmental conditions.

4.3 Experiments

This chapter deals with the history dependent effects observed during constant stress and constant strain experiments. Sorption-desorption cycles were carried out cyclically on individual samples in one of the two modes. Constant stress or constant strain experiments, as described in Chapter 3 and Chapter 4, are performed on the materials listed earlier. The solubility of moisture was monitored during sets of direct and indirect sequential stress or strain experiments, for a number of sample tensions or elongations. These experiments thus examined the consequences of alternately saturating and drying samples under constant tension (or constant elongation). The qualitative changes that were observed in the stress(strain)-solubility envelope for each stress(strain) sequence, demonstrate the influence of the mechanical history of the material on subsequent hygro-mechanical equilibrium states. The thermo-reversibility of history effects was also examined in samples conditioned by prior exposure to multiple cycles of sorption and drying. Heat-treatment was performed by annealing the materials at temperatures below their respective glass transition

temperatures. The experimental sequence prior to heat-treatment was repeated, in order to determine its effect on transport characteristics. The main emphasis of this chapter is therefore on the effect of the hygrothermal history on stress-coupled transport in polymers.

4.4 Results and Discussion

4.4.1 Stress Coupled Sorption

The moisture content at equilibrium, for individual ribbons of PI during direct constant stress experiments was examined over three cycles. The results are plotted in Figure 4.1. It was observed that for the first cycle, the solubility was essentially the same at all three stresses, though it was higher by approximately one percent at 30 MPa. During the second sorption, the solubility at 20 MPa was significantly lower, suggesting that the previous exposure to moisture resulted in a lower free or excess volume. On examining the behavior of diffusion and swelling coefficients for similar experiments (Figures 4.2 and 4.3), it was seen that the diffusion coefficient increased noticeably while the swelling coefficient decreased at 30 MPa. Remarkably, the diffusion coefficients during desorption remained relatively unaffected by the state of stress, as seen for the three independent samples of Figure 4.2. It is apparent that the desorption was neither affected by history nor by the state of stress forth sample held at constant tension throughout. As stated earlier, this may be because the sample was saturated at the start of desorption and

internal relaxations may have been rapid enough to minimize the effect of the applied stress.

The dimensional change that accompanied every percent gain or loss in moisture (during sorption and desorption as seen in Figure 4.3) at the three stresses, also suggests that swelling increased with stress during the initial stages of sorption. Since the material was under stress at all times the swelling was not unconstrained. Also, it was not feasible to totally eliminate sample creep, particularly because internal mobility increased with each cycle. As discussed before, a numerically smaller "swelling coefficient" was evident again during desorption, since creep was superimposed on sample shrinkage. In the final stage of sorption, the swelling coefficient appeared to have reached a limit that was independent of the applied stress. Thus, in the case of the sample at 20 MPa the swelling coefficients remained essentially constant, while at 30 MPa the swelling coefficient decreased to the same value as at 20 MPa.

The effect of mechanical history was investigated by traversing the stress-solubility envelope during a set of direct constant stress experiments. For instance a sample of PI, dried under very low tension, was subjected to an applied stress of 50 MPa and exposed to moisture. On equilibration of the linear density, the applied stress was reduced to 25 MPa, while linear density determinations were continued. The stress was similarly reduced once again on attaining equilibrium while monitoring the linear density continually. In all cases, the change in the linear density due to sample swelling or shrinkage was duly compensated for and the change in sample length during reductions in tension was recorded for each stage.

Figure 4.4 illustrates the variation in equilibrium moisture with each cycle, including one following heat treatment (250 °C, 1 hour in nitrogen). The diffusion coefficients and swelling coefficients that were determined are similarly presented in Figures 4.5 and 4.6 respectively.

The moisture solubilities all increased, particularly at the higher stresses. This solubility enhancement was reversed on heat treatment, albeit well below the glass transition temperature (reported in the range of 300-400 °C, based on dynamic mechanical analysis). Broutman and Wong (1985) rationalized similar observations made on epoxy polymers, by considering that the applied stress increased internal "voids". They suggested the possibility that this occurred via microcrack formation and thus altered the equilibrium solubility by enabling additional sorption. Sample drying evidently did not reverse this enhancement, which in turn was found to be thermo-reversible, presumably via thermal healing of the previous internal "damage".

The fluctuation observed in diffusion coefficients (Figure 4.5) suggests that the first two cycles plasticized the material and raised the diffusion coefficients. The coefficients ultimately reverted to their values to their original values on heat treatment. The variation in the apparent diffusion coefficients demonstrates the influence of stress-coupled diffusion that took place in the sample. In the case of the apparent swelling coefficients, the effect of earlier cycles was less marked, and a drastic change resulted on heat treatment, in all cases. The changes were most prominent when smaller stresses were applied. However, for the sample at 50 MPa, the effect of history as well as annealing was almost completely masked.

The masking effect of sufficiently large stresses on history dependence had been reported for analogous situations (Struik 1978, Adams 1987) and was also referred to earlier. While swelling was greater at the highest stress during the first three cycles, the swelling coefficients dropped marginally throughout. An increase in the mobility of polymer chain segments on heat treatment, may have resulted in the large swelling coefficients observed. However, the exception was the sample at 50 MPa when this mobility was apparently overwhelmed by the constraining effect of the applied stress. Here, under the larger stress, no change in the swelling coefficient was observed since polymer mobility was constrained and the material performed like a quenched glass. This is clear from the fact that the highest swelling coefficient was observed at the lowest value of applied stress.

The results of sequential stress-coupled experiments on PI, PC and PPTA samples are summarized once again in Figures 4.7 - 4.9. The equilibrium weight percent of moisture is plotted as a function of the applied stress, for a sequence of cycles as described earlier. The result of heat-treatment, observed during such experiments on PI and PC samples, is also shown. The filaments of PPTA consistently broke on heating under tension after multiple sequences of sorption and drying. Such failure after many cycles was consistent with similar results reported in the literature and was attributed to stress-induced long term aging of the fiber. An additional factor was the weakening of the fiber as result of the repeated strikes for pulse initiation. An attempt was made to minimize localized damage by varying the position of the striker between cycles.

A steady increase in the moisture solubility at a particular stress was observed in the case of the PI with each succeeding cycle. At the lower stresses, this enhancement was relatively small but became more prominent at the largest value of stress applied. By contrast, the solubility of PC ribbons decreased at all stresses during the subsequent cycle. Also, history dependence was prominent at the low stress end rather than at the higher stresses applied. Presumably, the orientation induced by large stresses served to nullify any potential increase in solubility. This conjecture is also supported by the observation made that on annealing the sample at 100°C for an hour (glass transition temperature ≈145°C), the low stress solubility reverted to its original value.

The equilibrium sorption of moisture, plotted as a function of applied stress on a PPTA filament (Kevlar 49®), is presented in Figure 4.9. It is seen that the solubility depended linearly on the stress applied during each cycle. The experiments were conducted in the manner described earlier for PI and PC. The lines represent traces of the stress-solubility envelope for a number of cycles. With each succeeding cycle, there is an increase in the solubility was observed though the increment became smaller each time. The proportionality between the solubility and the applied stress lends credence to the hypothesis that the dilatational contribution of the stress served to create additional free volume for moisture sorption. Morgan et al. (1984) experimentally demonstrated that "microvoid" formation in Kevlar 49 ® by the action of applied stress. It is proposed here that a similar mechanism may have resulted in progressively higher solubilities with each cycle.

4.4.2 Stress Recovery During Sorption and Heat Treatment

The heat-treatment of samples with histories of exposure to multiple cycles of sorption-desorption was often found to induce a stress-recovery type of phenomenon in samples held at constant elongation. The recovery of stored energy of deformation in thermoplastics was extensively reviewed by Adams (1987). Similar stress recovery was also observed during the course of this study, in materials such as PC, Nylon 6,6 and Nylon 6,12. It was observed that such events occurred in samples with a recent history of hygro-mechanical fluctuations. Samples that underwent cycles of sorption and drying under externally applied axial stress or strain experienced this recovery phenomenon on prolonged exposure to moisture. Some of these observations are discussed below.

Remarkably, an increase in sample tension sometimes accompanied a rise in temperature during constant strain heat-treatment. Such a rise in tension was unusual as thermal expansion was expected to lower the tension. In fact, the stress increases were evident even above the decrease in tension resulting from thermal expansion. In Figure 4.10, the sample tension (a) and the temperature (b) for a sample of Nylon 6,6 are plotted as a function of time. The sample was previously exposed to moisture till saturation and then dried as usual, with the entire cycle lasting about 190 minutes. It was then held in a stream of dry nitrogen and heated as shown. It is clear that between 60 and 80 minutes after heating started, the tension in the sample actually increased even though the temperature continued to rise. Hence, the increase in tension dominated the counter effect of thermal expansion.

Morton and Hearle (1975) reported similar increases in tension in fiber samples typically resulting from the removal of the hydrogen-bonded water not removed during desorption at room temperature. However, it is particularly significant that the phenomenon usually occurred at about 100 °C corresponding to the boiling point of water. Also, the sample which had previously been dried under nitrogen at room temperature, suffered a net loss of weight as a result of the heat treatment The force-temperature data of Figure 4.11 clearly shows that a sample shrinkage was also observed to start at 100 °C corresponding to the boiling point of water.

The analogy between thermal and hygroscopic effects on polymers is considered to be a significant issue particularly in view of the phenomenological similarity between the two transport processes (McGregor 1974, Sih et al. 1986). The analogy between swelling and thermal expansion is related in a similar fashion. The plasticizing effects of moisture and organic molecules are believed to be similar in effect to the increase in internal mobility resulting from a temperature rise. In Figure 4.12 the tension (a) measured in in a Nylon 6,6 ribbon and the moisture gain (b) are plotted as functions of the exposure time. During a substantial period, the sample tension decreased monotonically as expected. However, a brief increase in sample tension was observed as the sample approached equilibrium. Similar observations were made with numerous samples of Nylon 6,6 and Nylon 6,12 which had orientations introduced during fiber spinning and PC which was a cold-rolled film. The link between the initiation of stress-recovery phenomena by thermal and hygroscopic means is provided by some of the experiments conducted on PC samples (Figures 4.13a and b are representative of the results).

In a recent report, Adams (1987) demonstrated the recovery of stored deformation energy by heating drawn PC samples. He argued that a fraction of the energy of deformation was stored within the material as a form of latent energy and was partially recovered on heating the material at a temperature below its glass transition. It is further proposed on the basis of this work that the moisture-activated recovery process is also attributable to an increase in chain mobility, in this case due to the absorbed water molecules. Clearly, this phenomenon of delayed recovery of stored energy and the analogy between thermal and hygroscopic effects, are areas of fundamental importance.

4.5 Conclusions

Equilibrium moisture and diffusion coefficients were found to be dependent on both the prevalent and historical stress as well as environmental conditions. While the equilibrium properties increased with applied stress, they also typically rose over repeated cycles, probably due to changes in internal chain mobility. The diffusion coefficient (transient characteristic) was observed to increase with applied stress but decreased with time through repeated cycles. It was also established that the hysteresis and the effect of repeated cycles was largely thermo-reversible in the materials studied. In some cases, the effect of history was even be nullified by the application of sufficiently large stresses.

The anomalous recovery of stress during sorption in samples under constant strain (Nylon 6,6 and PC) represented a remarkable aspect of history dependence in stress-coupled sorption. The phenomena was partly attributed to the preferential absorption of moisture into sites within the inter-chain regions of fiber samples, resulting in radial swelling and longitudinal shrinkage. This manifested itself as a brief maxima in sample tension, in the tension versus time data (Nylon 6,6). An alternative conjecture analogous to that applied to the PC samples was also considered. In this context, the brief increase in sample tension was attributed to the recovery of stored deformation energy. The recovery became possible only when the externally applied stress became either comparable or smaller than residual stresses, as the material became increasingly plasticized.

Based on the study of history dependence in stress-coupled sorption we conclude that, in addition to the effects of environmental humidity and applied stress, history dependence has to be taken into account. Such a study is important, in cases where the effect of stress alters the effect of history, for the determination of a stress-window in which history dependence may be controlled. Such control is obviously desirable in most industrial applications of polymeric materials.

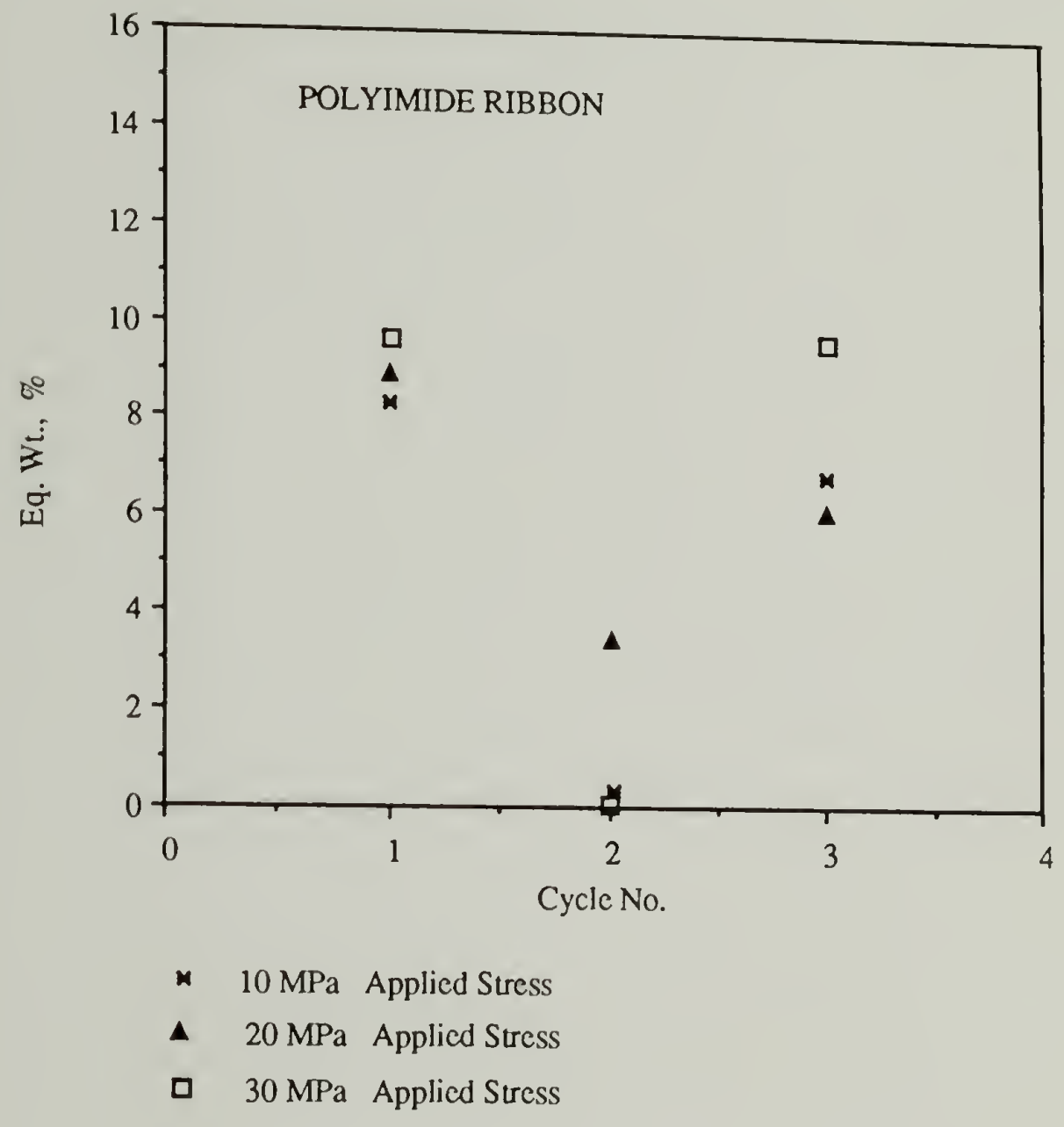

Figure 4.1 History dependence demonstrated by the changes in equilibrium sorption of PI. Three cycles were conducted: cycle 1 = sorption; cycle 2 = desorption; cycle 3 = sorption, performed on samples at 10, 20 and 30 MPa respectively.

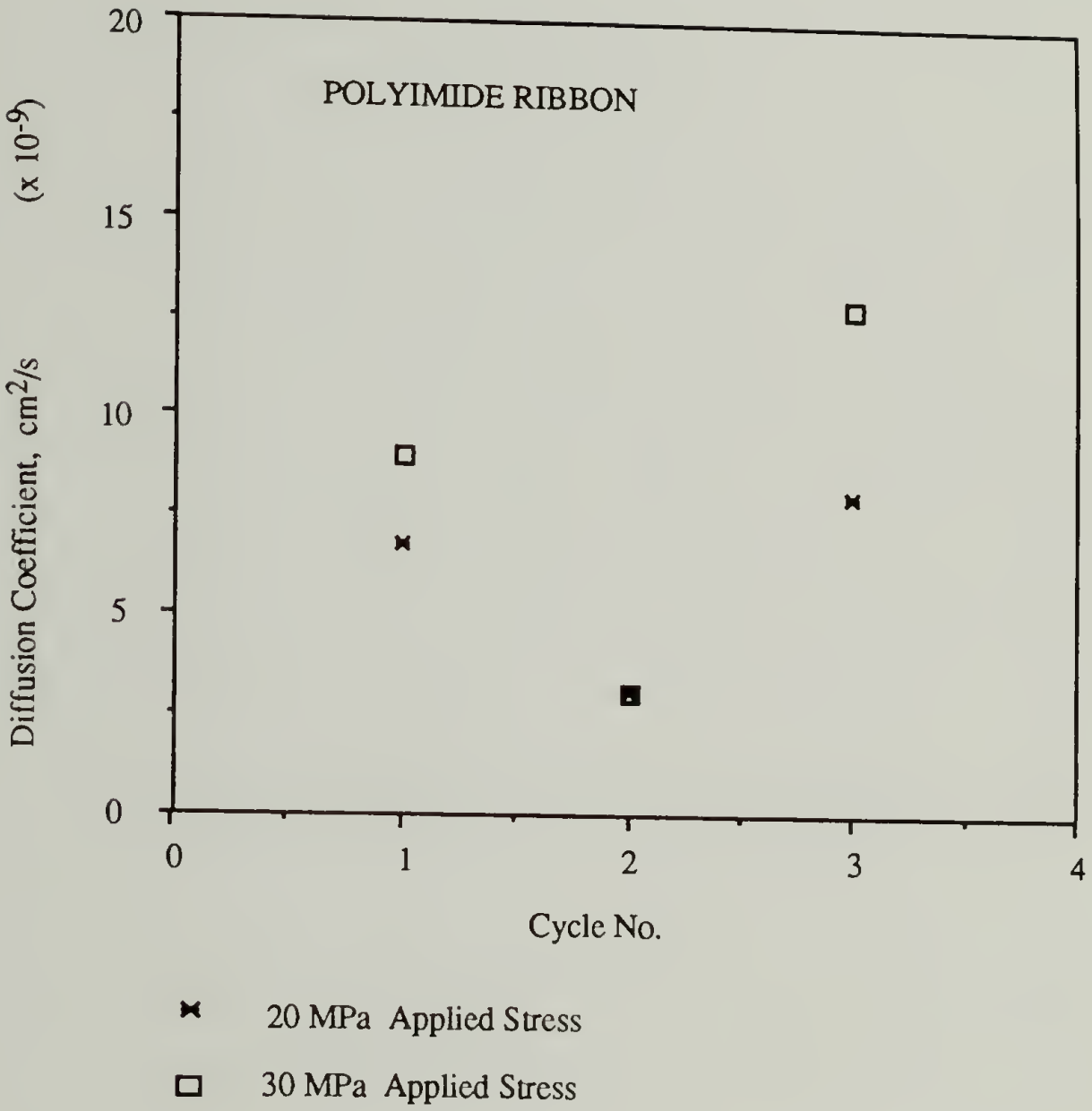

Figure 4.2 History dependence observed in the apparent diffusion coefficients for moisture transport in PI, during: cycle 1 = sorption; cycle 2 = desorption; cycle 3 = sorption, performed on samples at 20 and 30 MPa respectively.

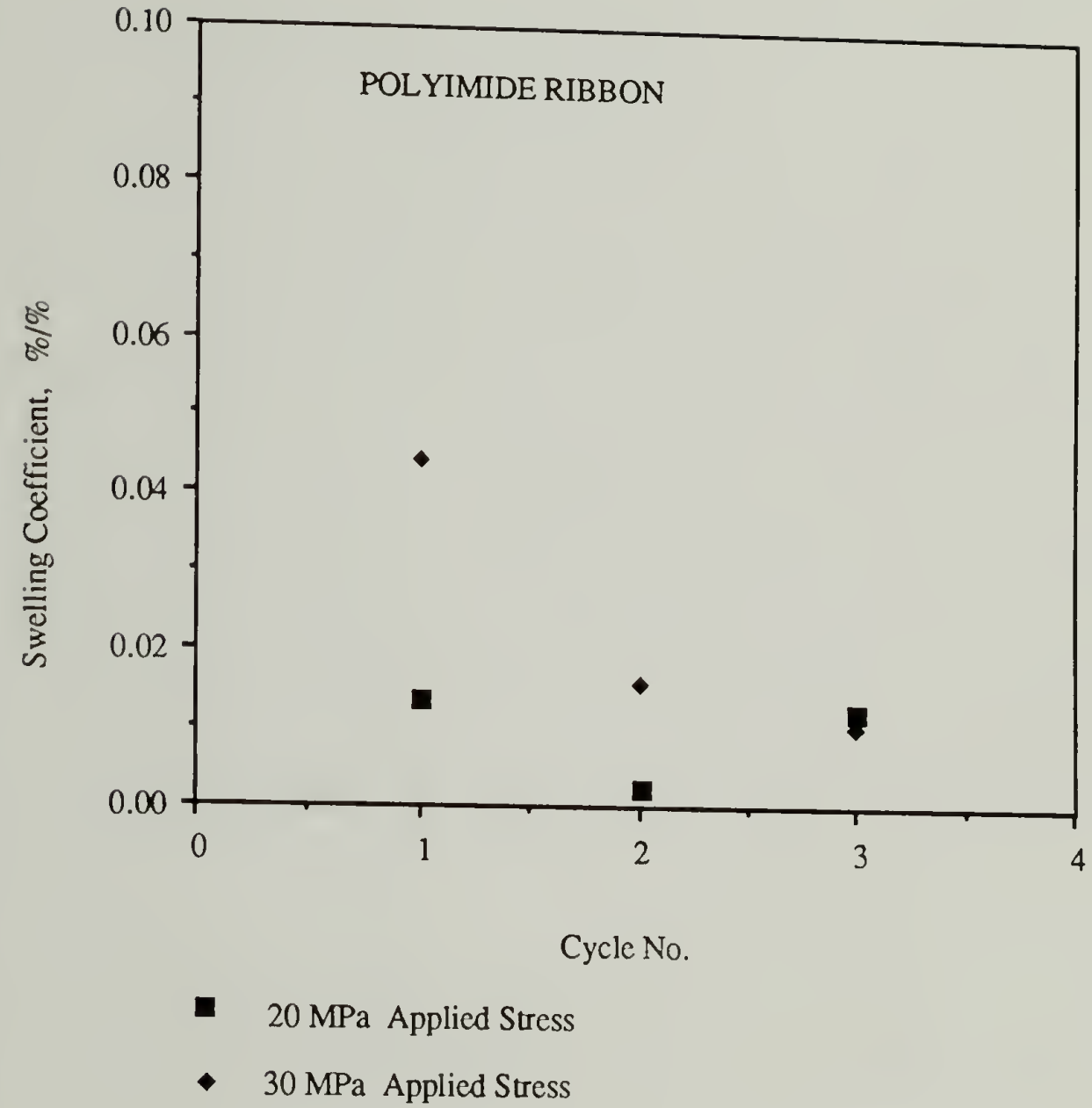

Figure 4.3 History dependence observed in the axial "swelling coefficients" of PI during: cycle 1 = sorption; cycle 2 = desorption; cycle 3 = sorption, performed on samples at 20 and 30 MPa respectively. The contribution from sample creep was not compensated for.

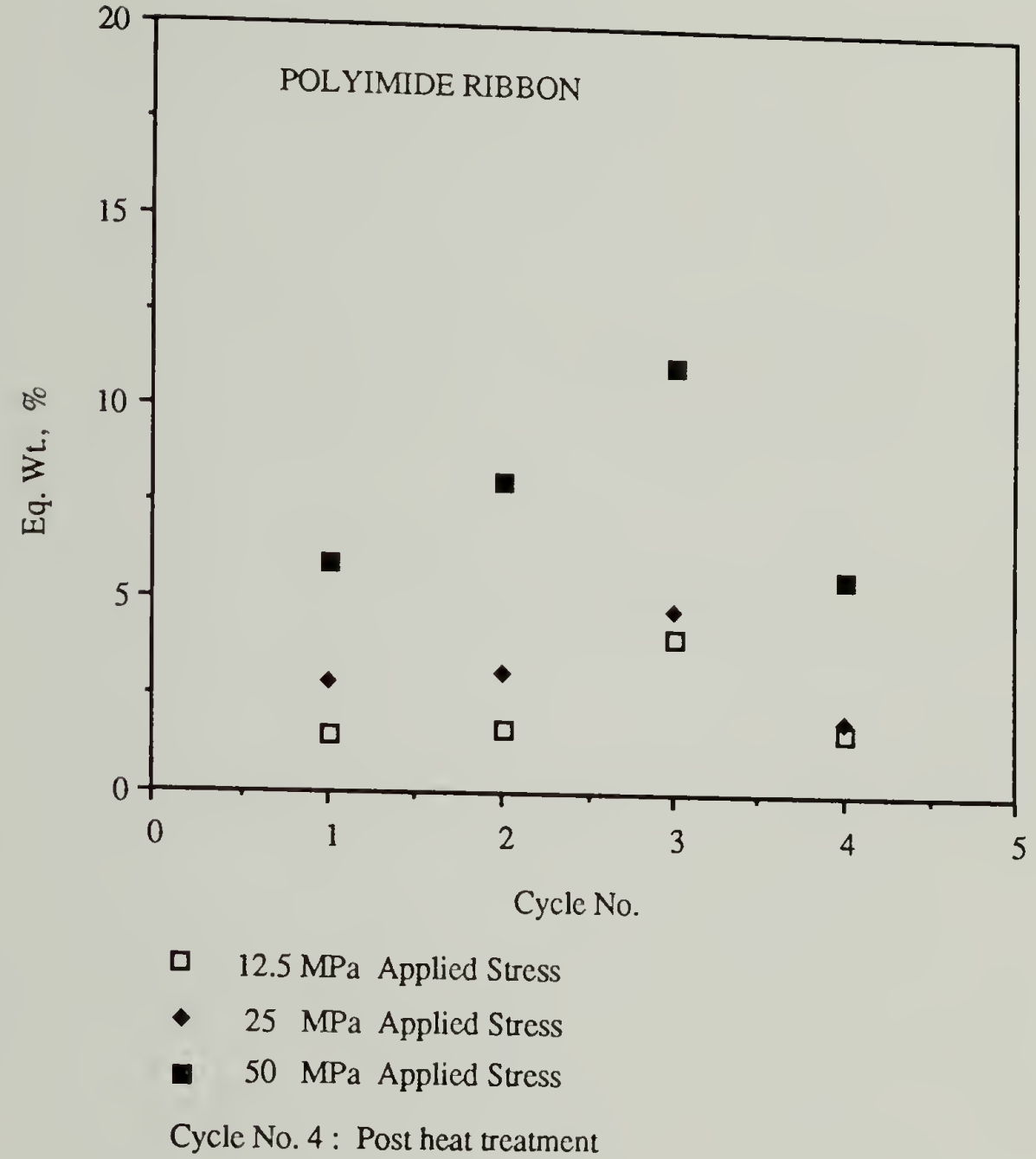

Figure 4.4 The variation of equilibrium moisture solubilities observed in a PI ribbon during sequential stress-coupled diffusion cycles before and after heat treatment (250 °C, 1 hour, N_2 atmosphere). Data for three levels of applied stress are shown here.

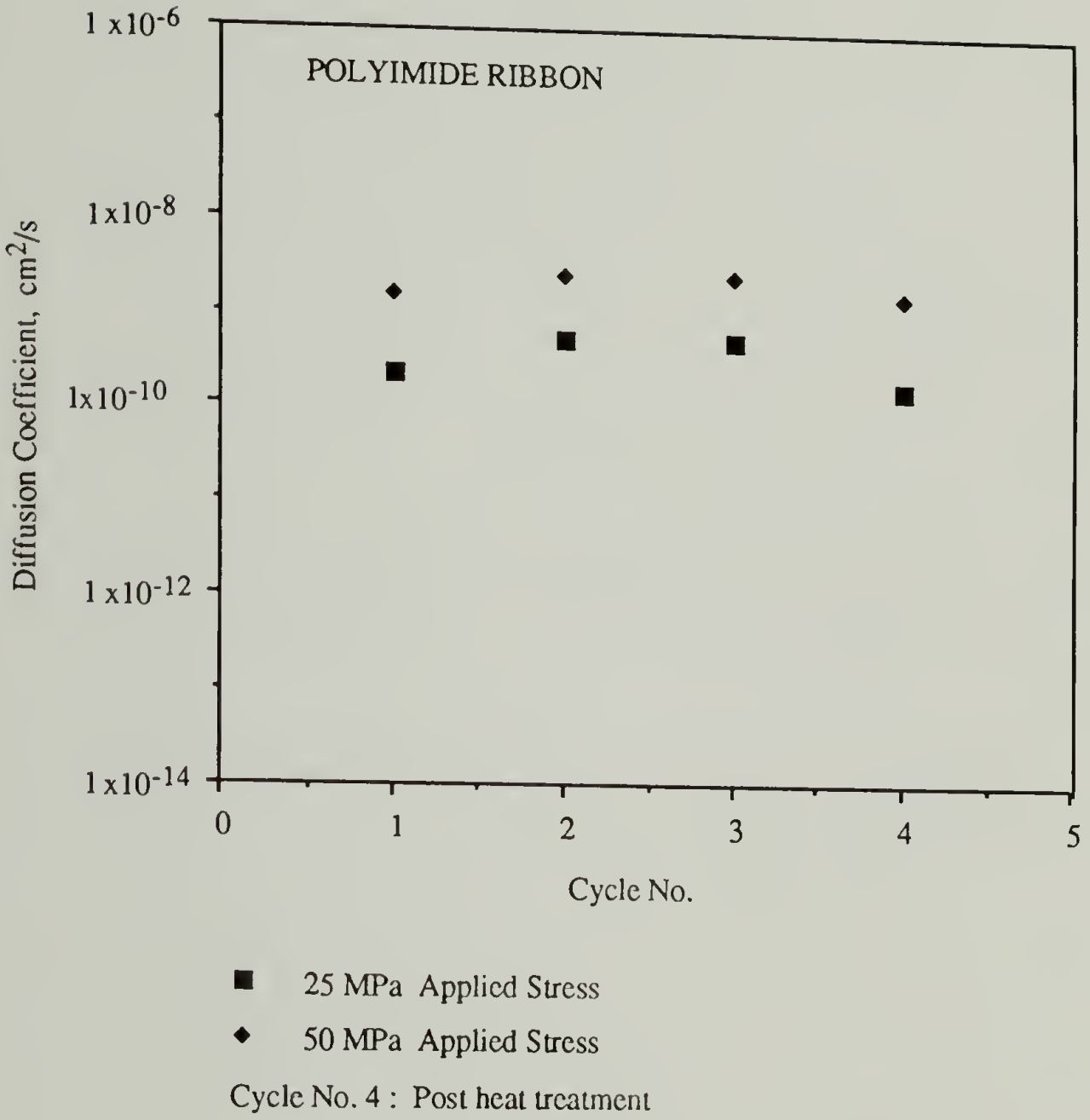

Figure 4.5 The variation of the apparent moisture diffusion coefficients observed in a PI ribbon during sequential stress-coupled diffusion cycles before and after heat treatment (250 °C, 1 hour, N_2 atmosphere). Data for two levels of applied stress are shown here.

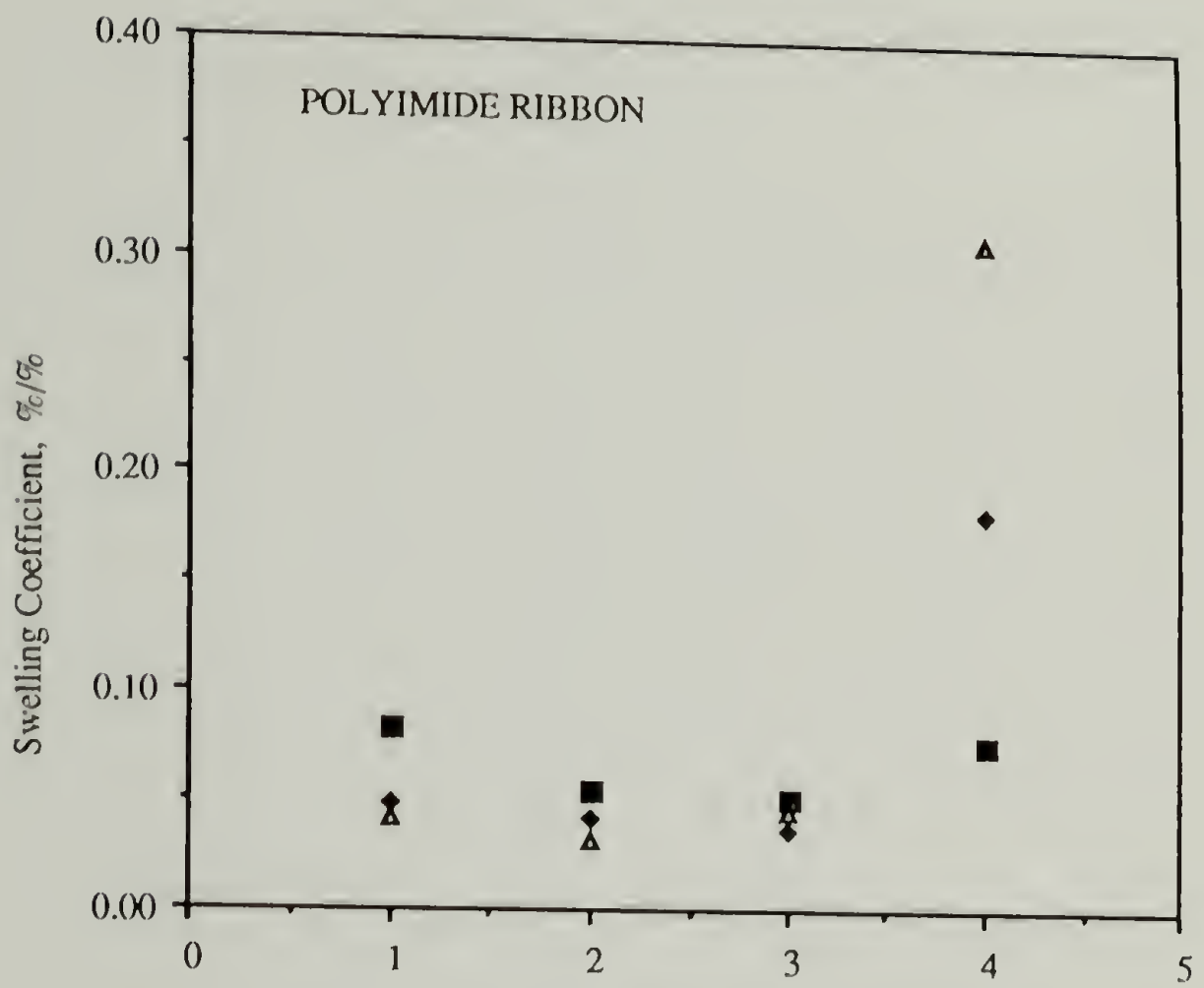

Figure 4.6 The variation of apparent swelling coefficients associated with moisture transport in a PI ribbon during sequential stress-coupled diffusion cycles before and after heat treatment (250 °C, 1 hour, N_2 atmosphere). Data for three levels of applied stress are shown here.

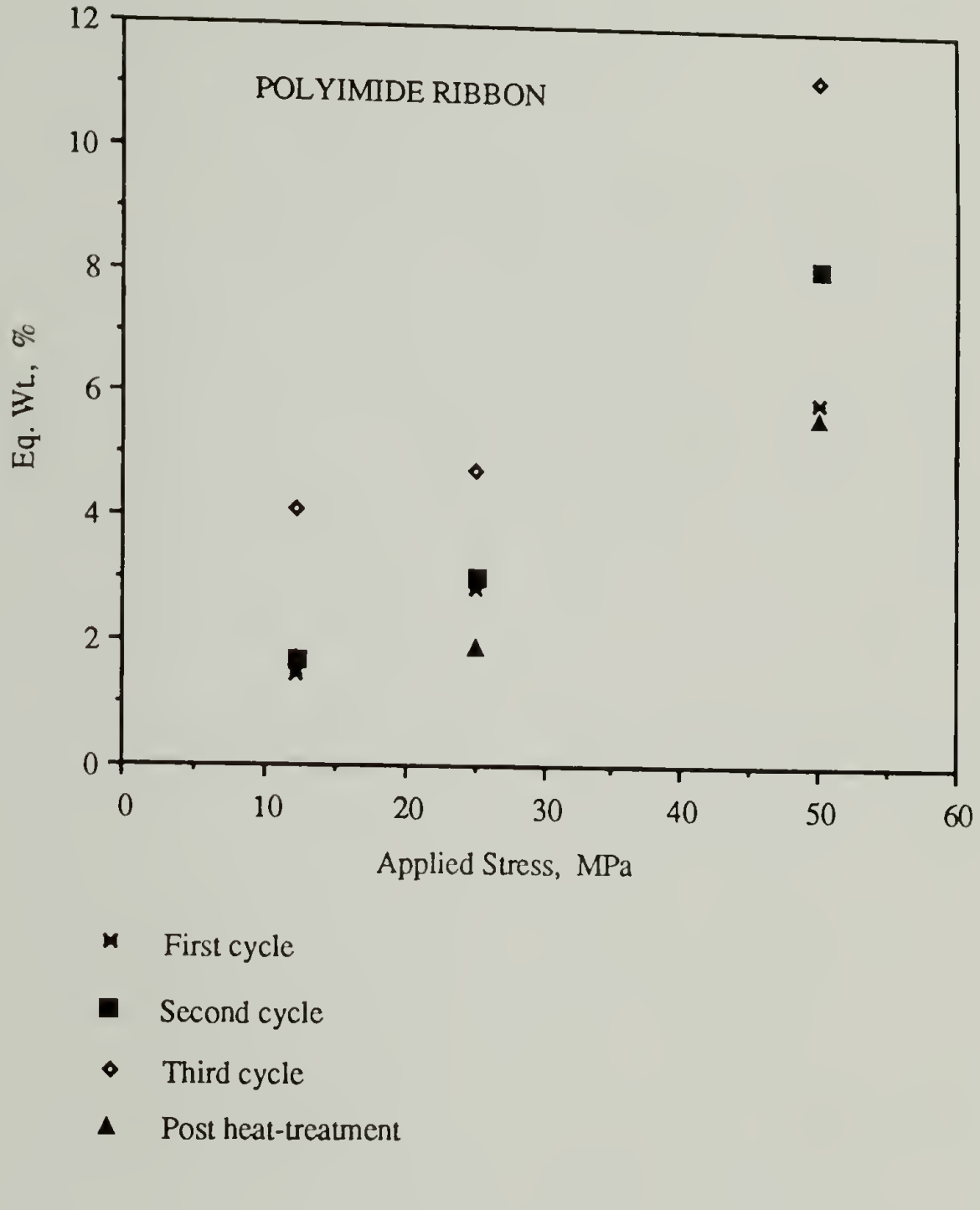

.Figure 4.7 The equilibrium solubility of a PI ribbon sample plotted as a function of the applied stress. Dry samples were exposed to moisture while held under constant tension (50 MPa). On saturation, the applied stress was reduced to new values progressively, with saturation at each stress. The experiments were repeated over four cycles including one after heat treatment (250 °C, 1 hour in nitrogen).

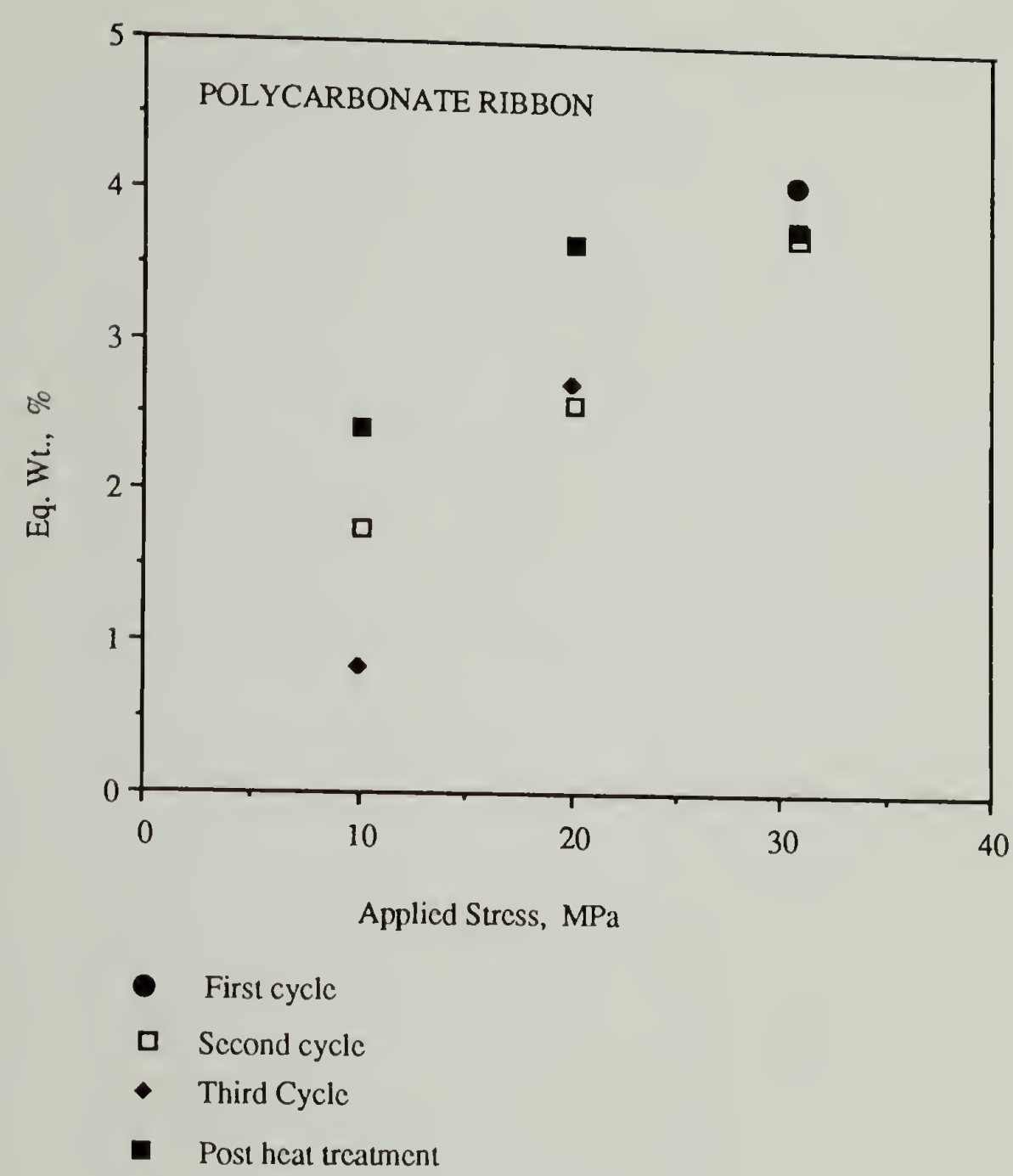

Figure 4.8 The equilibrium moisture solubility of a PC ribbon sample plotted as function of the applied stress. Dry samples were held under constant tension (33 MPa) and exposed to moisture. On saturation, the applied stress was reduced to new values progressively, as saturation was achieved at each stress. The experiments were repeated over four cycles including one after heat treatment (100 °C, 1 hour in nitrogen). Only one stress was used during the first cycle.

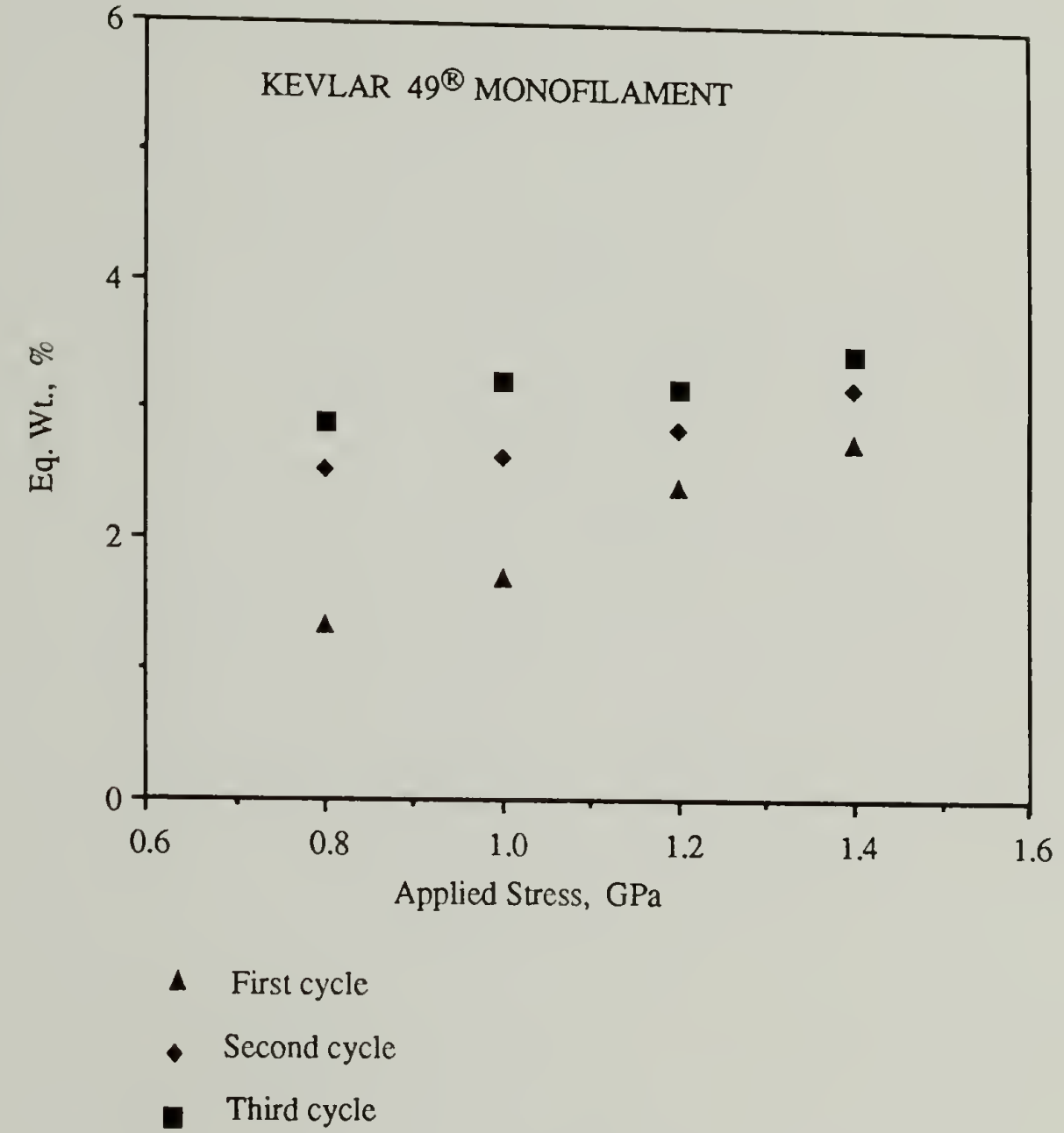

Figure 4.9 The equilibrium solubility of a PPTA sample plotted as a function of the applied stress. Dry samples were held under constant tension (1.5 GPa) and exposed to moisture. On saturation, the applied stress was reduced to new values progressively, as saturation was achieved at each stress. The experiments were repeated over three cycles.

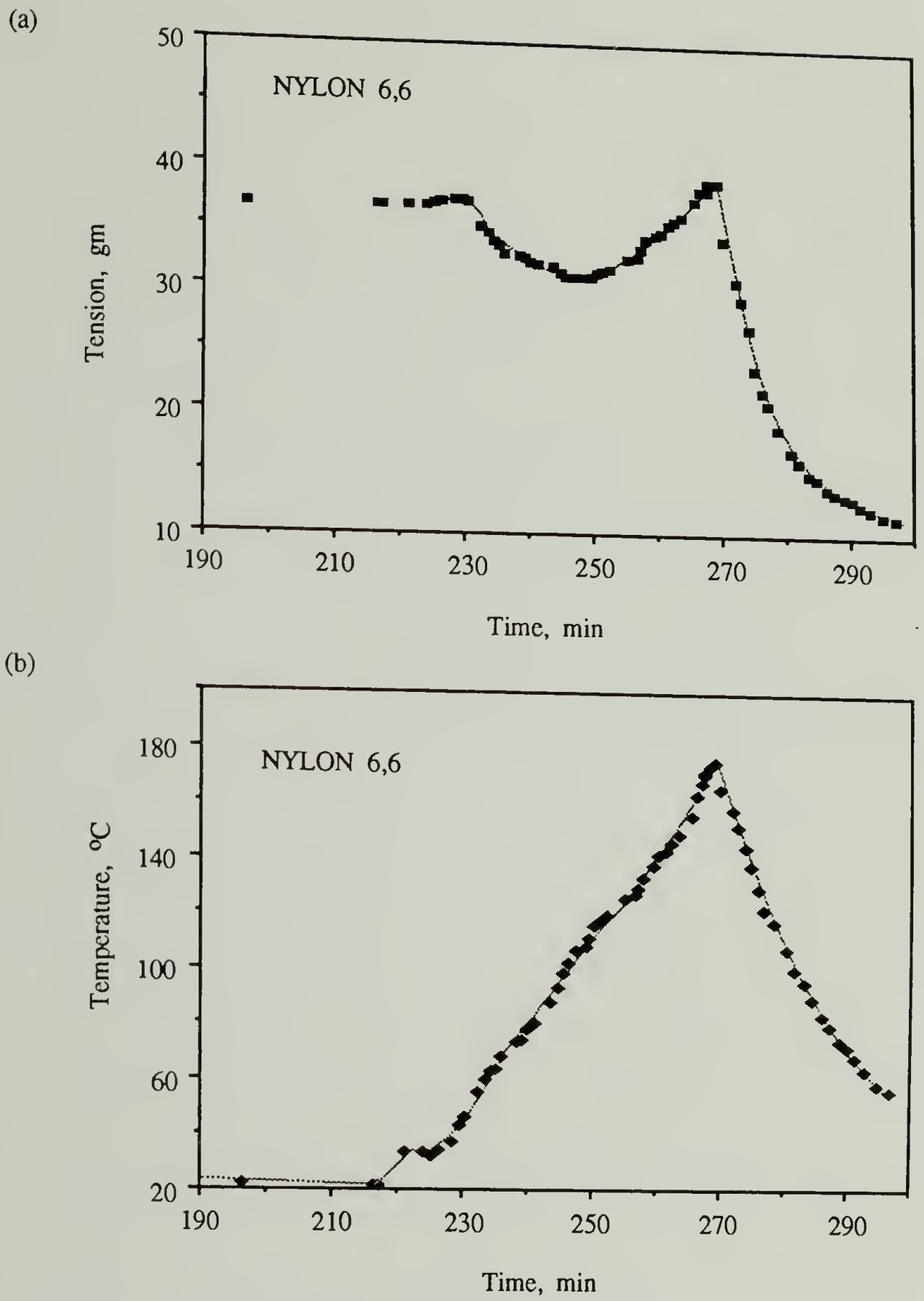

Figure 4.10 Heat-treatment data of a sample of Nylon 6,6 (under constant elongation) having a recent sorption-desorption history. The sample was previously exposed to moisture till saturation and then dried as usual, with the entire cycle lasting about 190 minutes. Variations of (a) sample tension (b) temperature are plotted as functions of the heating time for the subsequent heat treatment.

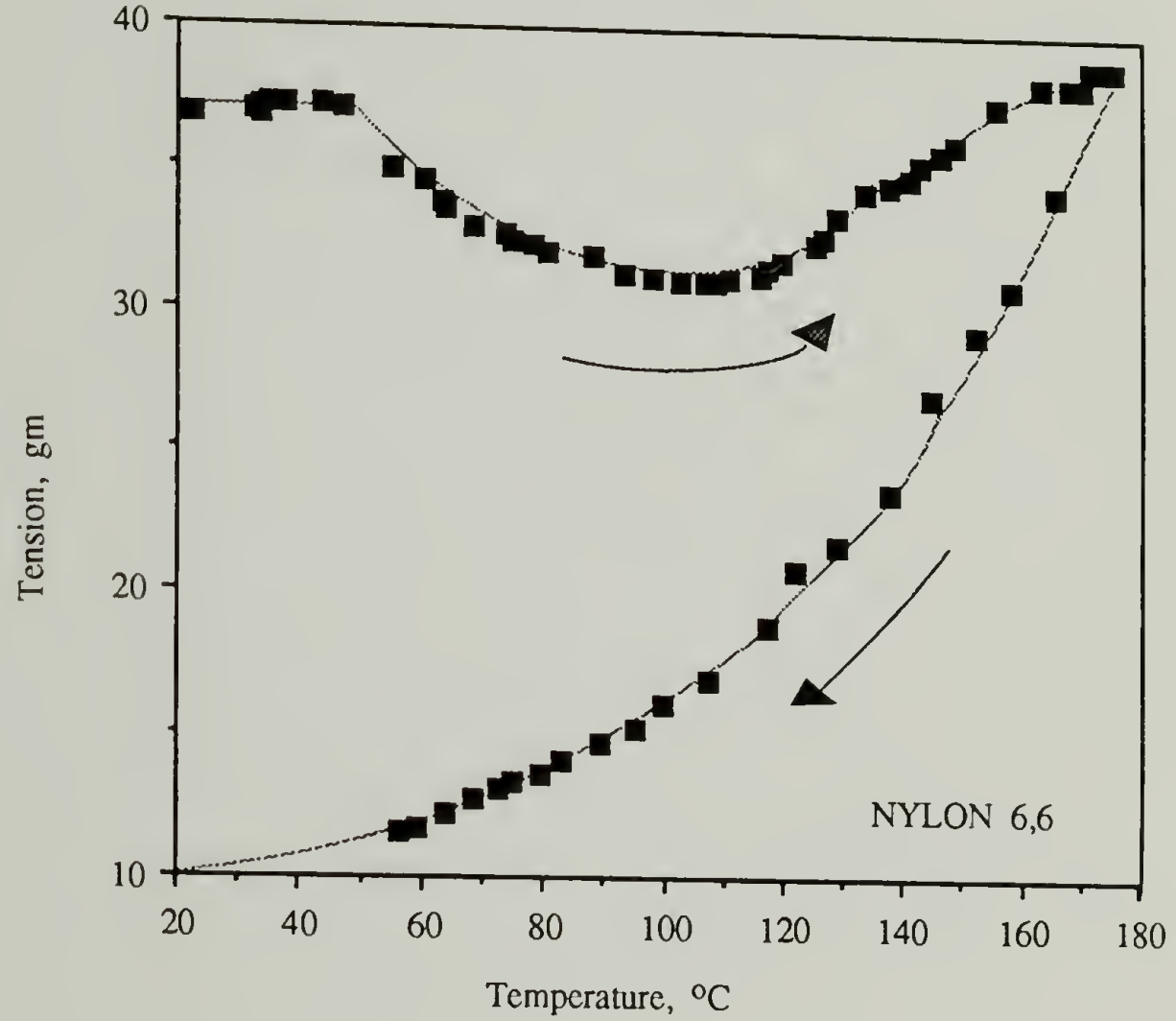

Figure 4.11 Force-temperature data for a sample of Nylon 6,6 with a recent history of sorption-drying cycles. The sample was previously exposed to moisture till saturation and then dried as usual, with the entire cycle lasting about 190 minutes. The sample tension is plotted as a function of the temperature.

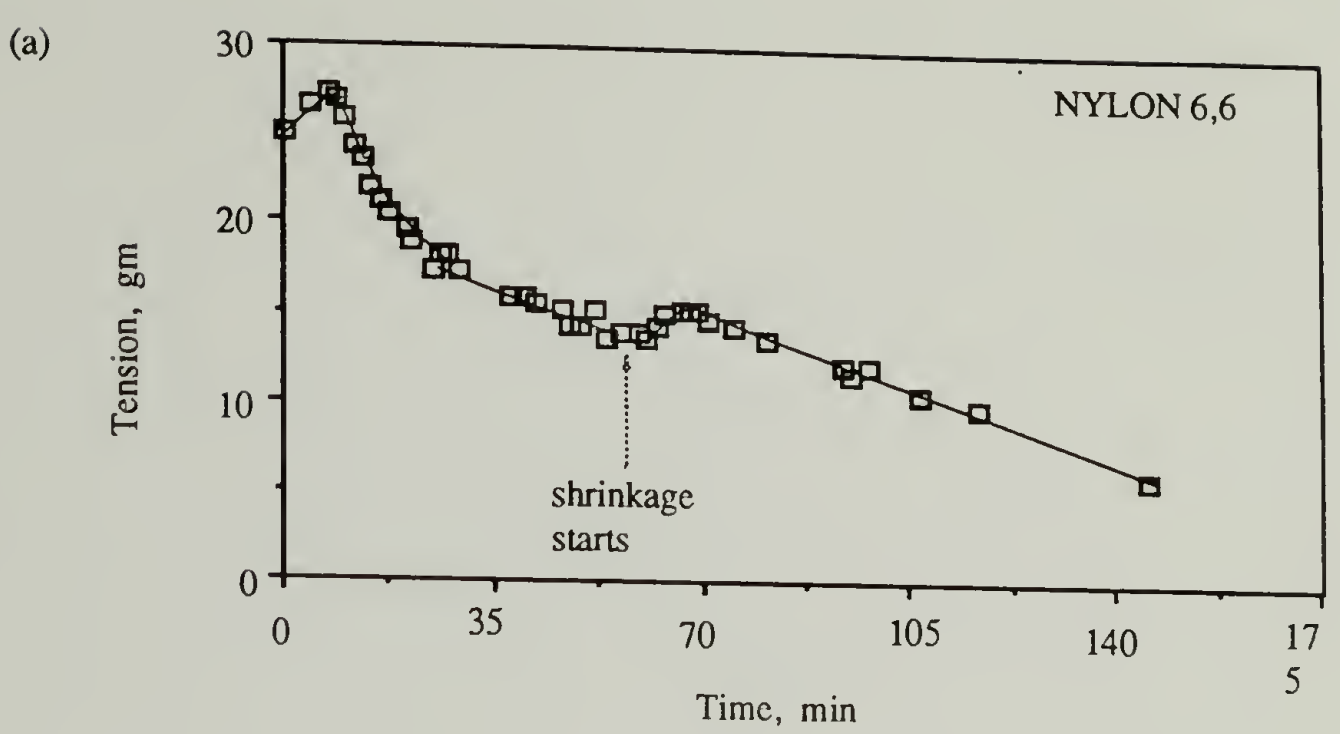

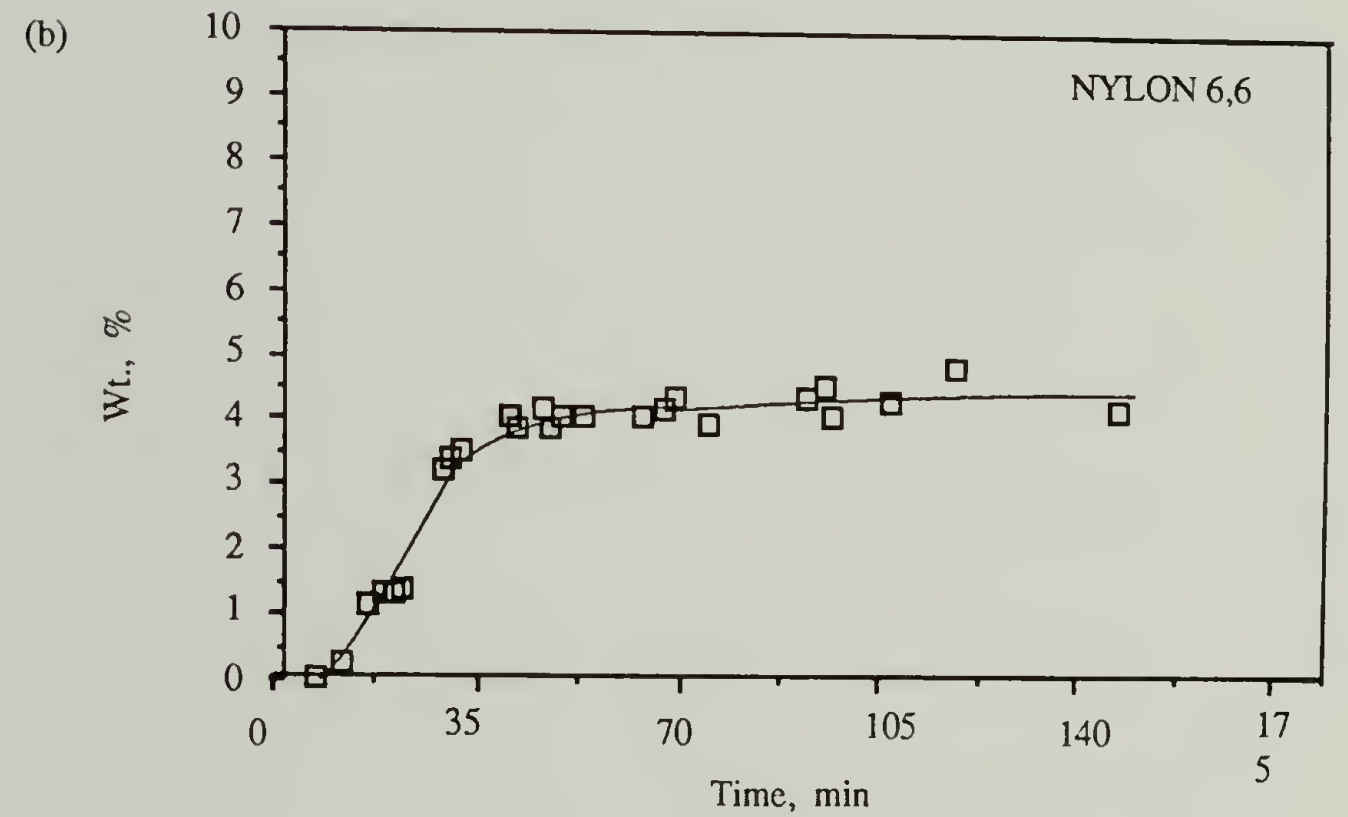

Figure 4.12 Variations in (a) tension; (b) weight gain are plotted as a function of the exposure time in a sample of Nylon 6,6 under constant elongation. An "anomalous" increase in the sample tension was briefly observed during sorption.

(a)

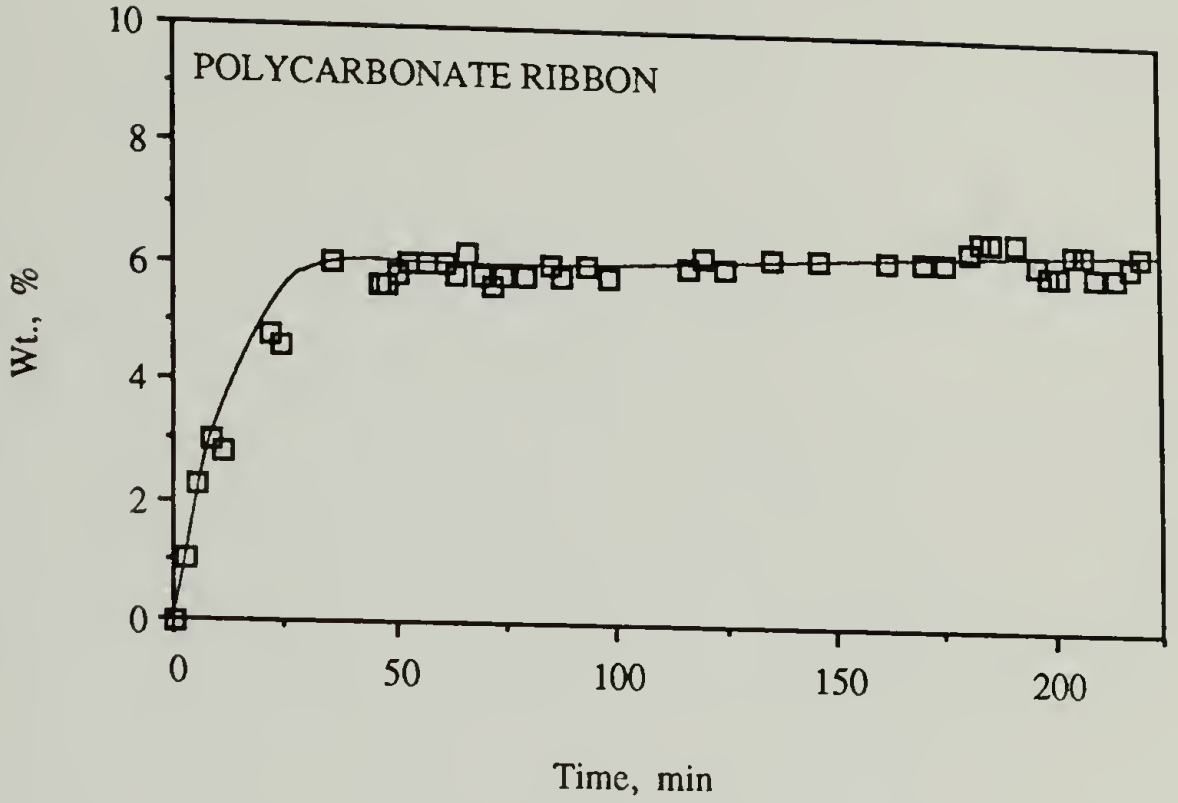

(b)

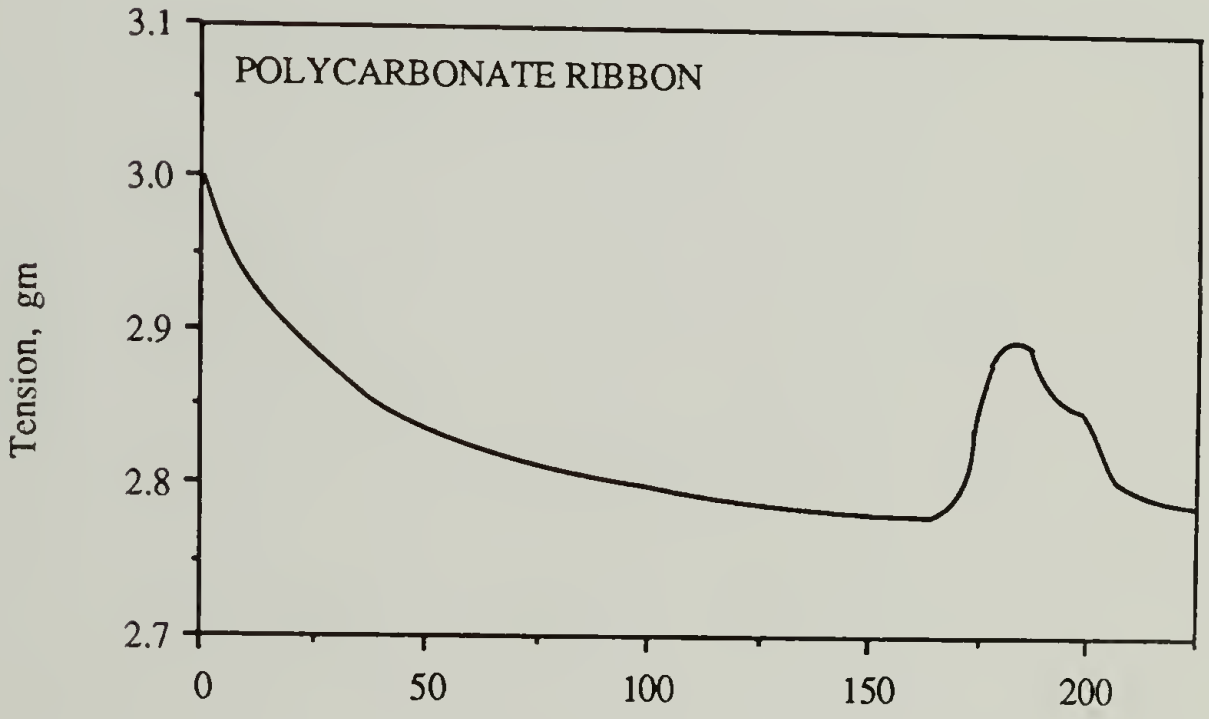

Figure 4.13 a) The weight gain plotted as function of time for a PC ribbon under constant strain. b) The corresponding change in sample tension during sorption. An anomalous "stress recovery" was observed 130 minutes after achieving equilibrium solubility (i.e. after 170 minutes).

CHAPTER 5

SUMMARY, CONCLUSIONS AND FUTURE WORK

5.1 Review of the Objectives and Background of the Dissertation

This dissertation focussed on the relationship between applied stresses, deformations and the diffusion of moisture within polymeric materials. The transport of moisture through a number of commercial materials was studied experimentally. Some of the specific objectives that were addressed during this investigation are recapitulated below.

- To develop an experimental technique that overcomes the limitation of traditional techniques used for studying transport in polymers. To enable systematic sorption and desorption experiments under constant stress or constant strain and to facilitate the study of the coupled phenomenon.
- To verify the coupling between sorption and applied stress. In particular, to examine the effects of applied stress or deformation in terms of the equilibrium solubilities, the diffusion coefficients and the swelling coefficients of the polymers studied.
- To examine of the influence of hygrothermal history on stress-coupled sorption and the effect of applied stress on history dependence in selected commercial polymers.

These objectives were motivated by the failure of prior investigators to adequately address the coupling of stress and diffusion. This was in part due to the lack of suitable experimental techniques and also because of the presumption that such effects are relatively insignificant. Most analyses of the properties of polymers exposed to weathering and solvent attack were therefore premised on "stress free" diffusion and sorption information and used a Fickian basis for transport. However, when the sorption characteristics of a matrix-penetrant system were indeed stress dependent or when large deformations of the matrix were involved, these analyses proved to be inadequate. This was established experimentally during the course of this dissertation. The discussion that follows is a summation of the main findings of this investigation as developed in earlier chapters and in the context of the the objectives of this dissertation.

The literature review of Chapter 1 identified the two main approaches adopted by previous investigators; both experimental as well as analytical. It was noted that the prevailing views on mechanisms and physical interpretations followed two approaches:

- The equilibrium thermodynamic approach considered the interaction of the stress and diffusion to depend on the balance between the osmotic driving force and the opposing elastic response of the swollen matrix. This premise then led to the conclusion that the equilibrium solubility would in fact increase with applied stress.
- The non-equilibrium analyses were based on the numerical solution of conservation equations for specific boundary conditions and polymer-permeant systems and were better suited for the prediction of

transient behavior. Some of the experimental approaches were also described in the review.

Typically, previous works did not refer to the coupled phenomenon, nor to a continuous measurement of stress and diffusion interactively with transport. This was pointed out to be a major limitation of prior techniques and was addressed by the development of the Vibrational Time Delay method. The simple basic principle of the Vibrational Time Delay technique and the associated apparatus were discussed. They were also demonstrated as being an effective means for the study of the coupled phenomenon, albeit within the limitations discussed in Chapter 2.

5.1.1 Summary of Conclusions: Experimental Technique

- The "Vibrational Time Delay" method was developed to measure the linear mass of fiber or ribbon samples. The technique relies on the measurement of the velocity of propagation of transverse wave pulses.
- The technique enables the continuous measurement of linear mass of fiber or ribbon samples and the stress or strain while they are exposed to permeants.
- The technique, in its present version, offers a relative means of mass measurement with an accuracy of 0.3% and a precision of 0.2% in samples of linear mass as low as 1.6×10^{-7} kg/m.
- The technique can be further extended to the measurement of the elastic modulus of the samples. It can also function as an extensiometric device.

• The main limitation of the technique is that the material must behave like a flexible "string" under tension, without involving stiffness and bending considerations. Hence, samples need to be sufficiently long and the tension high enough such that the material's elasticity does not come into play. Thus, travelling pulses involving only small segments of the sample length at a time, are generated between the sensors.

5.1.2 Summary of Conclusions: Experimental Results

• It was observed that the state of stress of a polymer included a contribution solely attributable to the diffusion of moisture into or out of the material. (PI; PC; PPTA; N 6,6; N 6,12; PBI).

• Conversely, moisture sorption and desorption were found to contribute to the net elongation of a sample held under constant applied stress. (PI; PC; PPTA; N 6,6; N 6,12; PBI)

• It was established that the equilibrium solubility within materials depended not only on the relative humidity of the environment but also on the state of stress of the sample. The moisture solubility at equilibrium was observed to increase with incremental sample tension beyond the equilibrium value at the previous value of tension (PI; PC; PPTA; N 6,6; N 6,12; PBI).

• The solubility in samples under constant strain was observed to depend on the elongation of the sample even though the humidity remained constant. (PBI; PC; N 6,6). The solubility was seen to increase with incremental strain within the linear elastic region of deformation (PBI).

• The diffusion and swelling coefficients under constant stress were

found to depend on the externally applied stress (PI; PC; PPTA; N 6,6; N 6,12) or strain (N 6,6; N 6,12; PBI) indicating that the mechanism of transport and the accompanying dimensional change was also affected by the stress.

- It was shown that the solubilities, diffusion coefficients and swelling coefficients exhibited history dependence as a result of repeated sorption-desorption cycles under constant humidity and applied stress (PI; PC; PPTA; N 6,6; N 6,12; PBI).

- It was also seen that the history dependence of equilibrium moisture content, swelling coefficients and diffusion coefficients could be reversed by heat-treatment below the glass transition temperature and subsequent quenching (PI; PC; N 6,12; N 6,6). Sufficiently large applied stresses seemed to suppress history effects by causing the material to act like a quenched glass (PI).

- Samples under constant tension or elongation were found to undergo strain or stress recovery respectively, when exposed to moisture for extended durations. The presence of moisture, like a rise in temperature, then triggered the recovery of internal energy stored during the extended period of the experiment or as a result of prior deformations (PC; N 6,6; N 6,12).

5.2 Recommendations for Future Work

There is considerable potential for the fruitful use of the Vibrational Time Delay technique in newer applications. Some suggestions for further utilization and modification of the apparatus as well as, potential sequels to the experiments discussed, are presented in this section.

At present, the apparatus is only suited for one-dimensional sample geometries, although the working principle can also be applied to two dimensional geometries. Thus the measurement of the change in velocity of transverse wave pulses as a function of material density, can be extended to membrane-like sample geometries by measuring the passage of wave pulses along the radial direction. This aspect is of particular significance in relation to coatings on rigid and non-rigid substrates. The technique in its present form is well suited to the study of solvent evaporation in cast films, or films cured from a liquid precursor.

Plasma polymerization of polymeric and organic materials has increasingly become an important and economically viable technology. In these applications, measurement of the rate of deposition as well as quantity of material deposited, is critical. The deposits may be achieved via vapor deposition of metals or plasma polymerization of surface polymers. In these applications the deposited film is often only a few Angstroms thick and can be monitored by depositing it on a rigid film substrates or a flexible surface. The Vibrational Time Delay technique can be suitably modified and enclosed to measure the material deposited and its rate of deposition, as well as monitor stress or strain during the cure of plasma polymerized materials. The same principle as before, is applicable to vacuum deposition of metals on rigid (silicon wafers) or non rigid substrates (Langmuir Blodgett films).

The experimental technique was demonstrated to be an accurate extensiometric instrument. The extension of a linear or planar sample resulted in a change in the linear density, which was determined accurately

from its effect on the pulse velocity. In the present application, the linear mass of the sample was calculated by compensating for a measured change in sample length. The proposed extensiometer would conversely provide a sensitive means of measuring very small values of shrinkage by its effect on the linear density. Such measurements may be made by first calibrating the instrument by using a material of known density such as a very fine steel fiber. This adaptation of the technique can also be suitably fitted for use as a process control component in a spinning-rig and used to monitor the denier of fibers. This application would of course, require high quality vibration free sensors so as to minimize noisy signals from extraneous sources. Furthermore, the velocity of the moving fiber would have to be compensated for in determining the velocity of the transverse wave pulse.

The study of polymeric optical fibers is an area of interest where the technique developed may be used to considerable advantage. Optical fibers are now increasingly used in communication lines. Most optical fibers in use today are made of glass are typically very brittle, unless they are made from very fine filaments of about 10-100 μm diameter. In that dimensional range the fibers, like the samples discussed here, act as strings. Hence, the problems associated with bending and elastic properties do not hinder their use as much. The relatively small dimensions of these fibers create alignment problems in addition to difficulties in handling. Polymeric optical fibers are viewed as an increasingly attractive alternative. They offer ease of manufacture in larger fiber diameters and more options for fiber-cladding waveguide systems. Their main disadvantage, in addition to relatively narrow bandwidths, is their sensitivity to the environment. Also an issue associated with their efficient utilization is the effect of local stresses on the optical properties of

transmission lines. Such stresses also assist the diffusion of aggressive environmental species into the fiber and thus erode its useful life. The vibrational time delay method can be adapted to study small sections of the fiber. A study of the stress-enhanced diffusion and its impact on fiber properties, particularly optical properties, is not only relevant but essential for the development of suitable polymeric materials and technologies for optical fiber applications.

An additional enhancement of the technique is in progress in our laboratory and involves the simultaneous measurement of the elastic modulus and linear density during diffusion. Since the principle of the technique in its present state is independent of the sample's elasticity, no indications of the effect of the permeants on the material are available. Hence, proposed enhancement is intended for the study of the effect of permeants on a polymer's mechanical properties. Further, the measurement of elastic modulii is expected to provide a means of monitoring the degree of cure of coatings since their mechanical properties are indicative of the progress of the polymerization reaction. A simple approach has been proposed to enable the determination of fiber modulus by the measurement of the stress response to a short displacement pulse to the sample length. A more sophisticated approach is based on "impulse viscoelastic" methods (Farris 1979).

An issue of considerable fundamental interest that has arisen from this research relates to the energy changes within a polymer because of diffusion and the applied stress or deformation. An understanding of the mechanism of stress-coupled diffusion lies in an understanding of the energy

transfers that take place during transport. Some parameters of interest are the heat of mixing, the energy of deformation and the energy stored during repeated cycles of stress-coupled diffusion. The deformation calorimetric method (Adams 1987) is recommended as a complementary technique for the purpose of such a study. Thus, the strain energy stored in a set of drawn samples can be measured and another such set examined for diffusion and solubility in samples with comparable strain. The phenomenon of sorption induced stress-recovery can then be investigated further in terms of its dependence on the stored energy. Such an investigation will provide critical insights into the effect of aggressive permeants on polymers with residual stresses. It would also offer a diagnostic technique for a post-molding analysis of the stresses induced in various molded parts, for instance, by solvents used during manufacturing operations.

The experimental evidence reported here, as well as current phenomenological interpretations of heat and mass transfer, underscore the analogy between the effect of heat and permeant sorption. It is felt that the combined use of deformation calorimetry along with diffusion experiments on samples under constant strain, will provide a deeper knowledge of these phenomena. Coupled with theoretical analyses based on non-equilibrium thermodynamics, such experiments will yield both quantitative and qualitative information about the coupling interactions of stress and transport in polymers.

BIBLIOGRAPHY

Adams, G.W., The Thermodynamics of Deformation for Thermoplastic Polymers, Ph.D. Dissertation, Polymer Science and Engineering, University of Massachusetts (1987).

Adkins, J.E., "Diffusion of Fluids through Aleotropic Highly Elastic Solids", *Arch. Ration. Mech. Analysis*, **15**, 222 (1964).

Aifantis, E.C., The Mechanics of Diffusion, Theor. and Applied Mech. Report No 440, University of Illinois, Urbana-Champaign (1980).

Akay, G., "Stress-Induced Diffusion and Chemical Reaction in Nonhomogeneous Velocity Gradient Fields", *Polym. Eng. Sci.*, **22**, No. 13, 798 (1982).

Alfrey, T. Jr.; Gurnee, E.F.; Lloyd, W.G., "Diffusion in Glassy Polymers", *J. Polymer Sci., Part C*, No. **12**, 249 (1966).

Apicella, A.; Nicolais, L.; Astarita, G.; Drioli, E., "Hygrothermal History Dependence of the Moisture Sorption Kinetics in Epoxy Resins", *Polym. Eng. Sci.*, **21**, 1, 18 (1981).

Baird, B.R.; Hopfenberg, H.B.; Stannett, V.T., "Effect of Molecular Weight and Orientation on the Sorption of N-Pentane by Glassy Polystyrene", *Polym. Eng. Sci.*,**11**, 4, 274 (1971).

Barkas, W.W., Wood Water Relationships-V: "The Hydrostatic Compressibility of the Wood-Water Aggregate", *Trans. Faraday Soc.*, **36**, 824 (1940).

Barkas, W.W., "Wood Water Relationships-VII: Swelling Pressure and Sorption hysteresis in Gels", *Trans. Faraday Soc.*, **38**, 194 (1942).

Barkas, W.W., "Wood Water Relationships-VIII: Some Elastic Constants and Swelling Pressures of Natural Wood and of its Gel Material", *Trans. Faraday Soc.*, **38**, 447 (1942).

Bastioli, C.; Romano, G., "Water Sorption and Mechanical Properties of Acrylic Based Composites", *J. Materials Sci.*, **22**, 4207 (1987).

Berens, A.R.; Hopfenberg, H.B., "Diffusion and Relaxation in Glassy Polymer Powders: Separation of Diffusion and Relaxation Parameters", *Polymer*, **19**, 489 (1978).

Berry, B.S.; Pritchet, W.C., "Bending-Cantilever Method for the Study of Moisture Swelling in Polymers", *IBM J. Res. Develop.*, **28**, 6 (1984).

Bowen, R.M., Theory of Mixtures, Eringen, C. (Ed.), Continuum Physics III, Academic Press, New York (1970).

Browning, C.E., "The Mechanism of Elevated Temperature Property Losses in High Performance Structural Epoxy Resin Matrix Materials after Exposures to High Humidity Environments", Tech. Report AFML-Tr-76-153, Air Force Materials Laboratory, Wright-Patterson A.F.B. (March 1977).

Buckley, D.J.; Berger, M., "The Swelling of Polymer Systems in Solvents. II Mathematics of Diffusion", *J. Polymer Sci.* **36**, 175 (1962).

Chen, S.P., "Effect of Volume Relaxation, Temperature, and Chemical Structure on Diffusion of Gaseous Hydrocarbons through Glassy Polymers", *A.C.S. Polymer Preprints*, **77** (1974).

Chern, R.T.; Koros, W.J.; Sanders, E.S.; Chen S.H.; Hopfenberg, H.B., "Implications of Thermal Mode Sorption and Transport Models for Mixed Gas Permeation", *A.C.S. Symposium Series 4223* (Industrial Gas Separations, 48 (1983).

Chipalkatti, H.R.; Chipalkatti, V.B.; Giles, C.H., *J. Soc. Dyers Colour.*, **70**, 652 (1955) as cited by Crank, J.; Park, G.S.,: Diffusion in Polymers: Methods of Measurement , Academic Press, New York, 262 (1968).

Chipalkatti, M.H.; Farris, R.J.; Hutchinson, J.M., "The Development of the Vibrational Time Delay Technique for the Study of Stress/Strain Coupled Diffusion in Polymers", *Rev. Scient. Instr.*, **58**, No. 1, 112 (1987).

Chipalkatti, M.H.; Farris, R.J.; Ottino, J.M., "History Dependence of Stress Coupled Transport in Polymer Fibers and Ribbons", *Proc. A.C.S. Fall Mtg.*, Anaheim, 831 (1986a).

Chipalkatti, M.H.; Farris, R.J.; Ottino, J.M., "Stress Coupled Transport in Polymer Fibers and Ribbons", A.I.Ch.E.Summer Natl. Meeting, Boston (1986b).

Crank, J., "A Theoretical Investigation of the Influence of Molecular Relaxation and Internal Stress on Diffusion in Polymers", *J. Polymer Sci.*, **11**, No. 2, 151 (1953).

Crank, J., The Mathematics of Diffusion, Clarendon, Oxford, (1975).

Crank, J.; Park, G.S., Diffusion in Polymers: Methods of Measurement (Ch. 1), Academic Press, New York (1968).

Crochet, M.J.; Naghdi, P.M., "On Constitutive Equations for Flow of Fluid through an Elastic Solid", *Int. J. Eng. Sci.*, **4**, 383 (1966).

Downes, J.G.; Mackay, B.H., Proc. 1st Int. Wool Text. Res. Conf., Australia, Paper D, 203 (1955), as cited by Crank and Park (1968).

Edelenyi, A.; Kethely, L.; Hegedius, S.; Boros, S., "Measurement of Closed Spatial Equilibrium Pressure Resulting from Oil-swelling of Various Rubber Types", International Rubber Conference, Moscow (1984).

Fahmy, A.A.; Hurt J.C., "Stress Dependence of Water Diffusion in Epoxy Resin", *Polymer Composites*, **1**, 2 (1980).

Farris, R.J., "A New Approach to Impulse Viscoelasticity", *J. of Rheol.*, **28**, 4 (1984).

Flory, P.J., Principles of Polymer Chemistry, Cornell University Press, Ithaca, New York (1953).

Fung, Y.C., Foundations of Solid Mechanics, Prentice Hall, Englewood Cliffs (1965).

Gonzalves, V.E., *Text. Res. J.*, **17**, 369 (1947) as cited by Crank and Park (1968).

Haward, R.N., The Physics of Glassy Polymers, Wiley, New York (1973)

Hearle, I.W.S., *Text. Res. J.*, **27**, 940, as cited by Morton and Hearle (1975).

Hopfenberg, H.B.; Stannett, V., The Diffusion of Gases and Vapors in Glassy Polymers, Chap. 9, Haward, R.N. (Ed.): The Physics of Glassy Polymers, Wiley, New York, 504 (1973).

Howsmon, G.J.; Peas, N. A., "Mathematical Analysis of Transport Properties of Polymer Films for Food Packaging. VI. Coupling of Moisture and Oxygen Transport Using Langmuir Isotherms", *J. Appd. Polym. Sci.*, **31**, 2071 (1986).

Kim, M.; Neogi, P., "Concentration-Induced Stress Effects in Diffusion of Vapors through Polymer Membranes", *J. Appd. Polym. Sci.*, **29**, 731 (1984).

Koros, W.J.; Paul, D.R., Rocha, A.A., "Carbon Dioxide Sorption and Transport in Polycarbonate", *J. Polymer Sci., Polymer Phys. Ed.*, **14**, 687-702 (1976).

Kovalenko, A.D., Thermoelasticity: Basic Theory and Applications, Wolters Noordhoff, Groningen, Netherlands (1969).

Larche, F.C.; Cahn, J.W., "The Effect of Self Stress on Diffusion in Solids", *Acta Metall.*, **30**, 1835 (1982).

Marom, G.; Broutman, J., "Moisture Penetration into Composites under External Stress", *Polymer Composites*, **2**, 31 (1981).

Marshall, J.M.; Marshall, G.P.; Pinzelli, R.F., "Diffusion of Liquids into Resins and Composites", *Chemtech*, July, 426 (1983).

Mashelkar, R.A.; Kulkarni, M.G., "Unified Altered Free Volume State Model for Transport Phenomena in Polymeric Media", *Pure and Applied Chem.*, 55, No. 5, 737 (1983).

McGregor, R., Diffusion and Sorption in Fibers and Films, Volume 1, Academic Press, London (1974).

Mijovic, J.; Weinstein, S.A., "Moisture Diffusion into a Graphite Epoxy Composite", **26**, 237 (1985).

Morgan, R.J.; Pruneda, C.O.; Butler, N.; Kong, F-M.; Caley, L.; Moore, R.L., "Hydrolytic Degradation of Kevlar 49® Fibers", *Proc. S.A.M.P.E. 29th Annual Mtg*, Reno, Nevada, 1 (1984).

Morton, W.E.; Hearle, J.W.S., Physical Properties of Textile Fibres, Heinmann, London, (1975).

Paul, D.R.; Ebra-Lima, O.M., "Pressure Induced Diffusion of Organic Liquids through Highly Swollen Polymer Membranes", *J. Applied. Polymer Sci.*, **14**, 2201 (1970).

Peas, N.A.; Sinclair, J.L., "Anomalous Transport of Penetrants in Glassy Polymers", *Colloid & Polymer Science*, **261**, 404 (1983).

Peterlin, A., Mechanical and Transport Properties of Drawn Semicrystalline Polymers, Chap. 3, The Strength and Stiffness of Polymers, Edited by A.E. Zachariades and R.S. Porter, Marcel Dekker Inc., New York, 97 (1983).

Petropoulos, J.H.; Roussis, P.P., "The Influence of Transverse Differential Swelling Stresses on the Kinetics of Sorption of Penetrants by Polymer Membranes", *J. Membrane Science*, **3**, 343 (1978).

Rosen, B., "Some Mechanical Aspects of the Swelling and Shrinkage of Polymeric Solids-I. External and Internal Restraints", *J. Polymer Sci.*, **58**, 821 (1962).

Rosen, B., "Time Dependent Tensile Properties-II: Porosity of Deformed Glasses", *J. Polymer Sci.*, **47**, 19 (1960).

Sackinger, S., Personal Communication (1987).

Sakuma, Y.; Rebenfeld, L., "Properties and Structure of Nylon Fibers in Relation to Drawing and Aqueous Phenol Treatments", *J. Appd. Polym. Sci.*, **10**, 637 (1966).

Shankar, V., "Calculation of Diffusion Coefficients of Organic Vapors from Short and Longtime Sorption Data", *Polymer*, **20**, 254 (1979).

Shi, J. J-J; Rajagopal, K.R.; Wineman, A.S., "Applications of the Theory of Interacting Continua to the Diffusion of a Fluid through Non-Linear Elastic Media", *Int. J. Eng. Sci.*, **19**, 871 (1981).

Sih, G.C.; Michopoulos, J.G.; Chou, S.C. (Eds.): Hygrothermoelasticity, Martinus Nijhoff, Dordrecht (1986).

Smith, T.; Adam, R., "Effect of Tensile Deformations on Gas Transport in Glassy Polymer Films", *Polymer*, **22**, 301 (1981).

Sternstein, S.S., "Inhomogeneous Swelling in Filled Elastomers", *J. Macromol. Sci.-Phys.*, **B6(1)**, 243-262 (1972).

Struik, L.C.E., Physical Aging of Amorphous Polymers and Other Materials, Elsevier, Amsterdam (1978).

Thomas, A.G., Muniandy, K., "Absorption and Desorption of Water in Rubbers", *Polymer*, **28**, 408-415 (1987).

Thomas, N.L.; Windle, A.H., "A Deformation Model for Case II Diffusion", *Polymer*, **21**, 613 (1980).

Timoshenko, S.P.; Goodier, J.P., Theory of Elasticity, 3rd ed., McGraw Hill, N.Y., 458 (1970).

Treloar, L.R.G., "The Absorption of Water by Hair, and its Dependence on Applied Stress", *Trans. Faraday Society*, **48**, 567 (1952).

Treloar, L.R.G., The Physics of Rubber Elasticity, 2nd Ed., Oxford Clarendon Press, (1958).

Treloar. L.R.G., "The Absorption of Water by Cellulose, and its Dependence on the Applied Stress", *Trans. Faraday Soc.*, **49**, 816 (1953).

Weitsman, Y., "Diffusion with Time-Varying Diffusivity, with Application to Moisture-Sorption in Composites", *J. Composite Materials*, **10**, 193 (1976).

Wolf, C.J.; Fanter, D.L., Solomon, R.L., "Environmental Degradation of Aromatic Polyimide-Insulated Electrical Wire", direct communication (1984).

Wolf, C.J.; Solomon, R.S., "Aging of Aromatic Polyimide Insulated Electrical Wire", S.A.M.P.E. J., Jan/Feb, 16 (1984).

Wong, T.C.; Broutman, L.J., "Moisture Diffusion in Epoxy Resins: Part I. Non-Fickian Sorption Processes", *Polym. Sci. Eng.*, **25**, 9, 521 (1985).

Yang, D.K.; Koros, W.J., Hopfenberg, H.B., Stannett, V.T., "Sorption and Transport Studies of Water in Kapton Polyimide I", *J. Appd. Polym. Sci.*, **30**, 1035 (1985).

Yang, D.K.; Koros, W.J.; Hopfenberg, H.B.; Stannett, V.T., "The Effects of Morphology and Hygrothermal Aging on Water Sorption and Transport in Kapton Polyimide", *J. Appd. Polym. Sci.*, **31**, 1619 (1986).

Yano, S.; Hatakeyama, H., "Dynamic Viscoelasticity and Structural Changes of Regenerated Cellulose during Water Sorption", *Polymer*, **29**, 566-570, (1988).

Yasuda, H.; Peterlin, A., "Gas Permeability of Deformed Polyethylene Films", *J. Appd. Polym. Sci.*, **18**, 531 (1974).

Yasuda, H.; Stannett, V.; Frisch, H.L.; Peterlin, A., "The Permeability of Strained Polymer Films", *Makromol. Chem.*, **73**, 188 (1964).

Zhurkov, S.N., Tomashevskii, E.E., "An Investigation of Fracture Process of Polymers by the E.S.R. Method", Proc. Physical Basis of Yield and Fracture, Oxford University Press, Oxford, 200 (1966); as cited by Wolf and Solomon (1984)